AD-A069 059 STANFORD TELECOMMUNICATIONS INC MCLEAN VA F/G 17/7
INVESTIGATION OF A PRELIMINARY GPS RECEIVER DESIGN FOR GENERAL --ETC(U)
JUL 78 B D ELROD, F D NATALI F04701-75-C-0239
UNCLASSIFIED STI/E-TR-8022 SAMSO-TR-79-34 NL

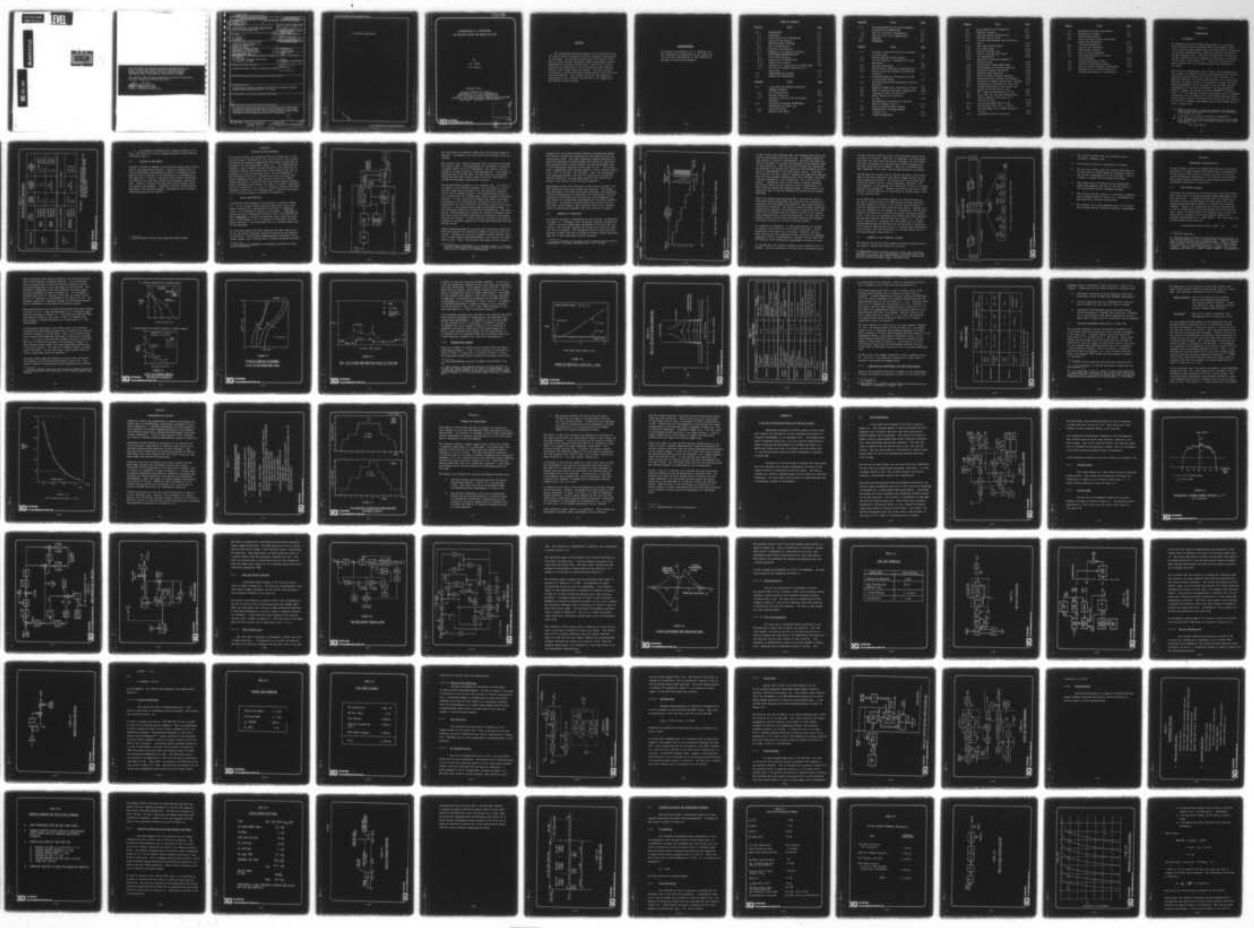

Unclassified

SECURITY CLASSIFICATION OF THIS PAGE (When Data Entered)

REPORT DOCUMENTATION PAGE	READ INSTRUCTIONS BEFORE COMPLETING FORM
1. REPORT NUMBER: SAMSO TR-79-34	2. GOVT ACCESSION NO.
3. RECIPIENT'S CATALOG NUMBER	
4. TITLE (and Subtitle): INVESTIGATION OF A PRELIMINARY GPS RECEIVER DESIGN FOR GENERAL AVIATION •	5. TYPE OF REPORT & PERIOD COVERED: Final, Sept. 7
6. PERFORMING ORG. REPORT NUMBER: STI/E-TR-8022	
7. AUTHOR(s): B.D. Elrod, F.D. Natali	8. CONTRACT OR GRANT NUMBER(s): F04701-75-C-0239, DOT-FA77WAI-37
9. PERFORMING ORGANIZATION NAME AND ADDRESS: Stanford Telecommunications Inc. 1307 Dolley Madison Blvd. McLean, VA 22101	10. PROGRAM ELEMENT, PROJECT, TASK AREA & WORK UNIT NUMBERS
11. CONTROLLING OFFICE NAME AND ADDRESS: Department of Transportation Federal Aviation Administration 800 Independence Ave., S.W. Washington, D.C. 20591	12. REPORT DATE: 14 July 1978
	13. NUMBER OF PAGES: 128
14. MONITORING AGENCY NAME & ADDRESS (if different from Controlling Office): HQ SAMSO/YEO P.O. Box 92960, Worldway Postal Center Los Angeles, CA 90009	15. SECURITY CLASS. (of this report): Unclas
	15a. DECLASSIFICATION/DOWNGRADING SCHEDULE

16. DISTRIBUTION STATEMENT (of this Report)

Approved for public release; distribution unlimited. 131 p.

17. DISTRIBUTION STATEMENT (of the abstract entered in Block 20, if different from Report)

18. SUPPLEMENTARY NOTES

Prepared under Interagency Agreement DOT-FA77WAI-37 between the Federal Aviation Administration and the U. S. Air Force.

19. KEY WORDS (Continue on reverse side if necessary and identify by block number)

20. ABSTRACT (Continue on reverse side if necessary and identify by block number)

The preliminary design and analysis of a potentially low cost GPS receiver for general aviation navigation applications is presented. The results indicate that the receiver could meet or exceed 2D area navigation (RNAV) requirements without dependence on external altitude data.

DD FORM 1 JAN 73 1473 EDITION OF 1 NOV 65 IS OBSOLETE

410 444

Unclassified

SECURITY CLASSIFICATION OF THIS PAGE (When Data Entered)

(Left Blank Intentionally)

STI/E-TR-8022
14 July 1978

INVESTIGATION OF A PRELIMINARY GPS RECEIVER DESIGN FOR GENERAL AVIATION

By:

B.D. Elrod

F.D. Natali

Prepared under:

Contract #F04701-75-C-0239 to
Department of Air Force Headquarters
Space and Missile System Organization
Funded by the Federal Aviation Administration through
Interagency Agreement # DOT-FA77WAI-737

STANFORD TELECOMMUNICATIONS INC.

ABSTRACT

The preliminary design and analysis of a potentially low cost GPS receiver for general aviation navigation applications is presented. The results indicate that the receiver could meet or exceed 2D area navigation (RNAV) requirements without dependence on external altitude data. Effects of aircraft maneuvers and variations in carrier power-to-noise spectral density ratio (C/N_o) have been studied. Possible receiver re-designs to achieve additional margin against C/N_o variations are also reported. Test options to verify the design and performance of the receiver are presented, and suggestions for further study are given.

ACKNOWLEDGEMENT

The authors are grateful to T. L. Savarino for his assistance in preparation of the report and his technical contributions to the sensitivity analysis of receiver performance.

Table of Contents

SECTION 1

INTRODUCTION

1.1 BACKGROUND

The NAVSTAR Global Positioning System (GPS) is a satellite-based navigation system currently under development by DOD. It will provide radio signals from a constellation of satellites for accurate determination of position, velocity and time by suitably equipped users. When fully operational in Phase III, the GPS constellation will comprise 24 satellites in circular, 12-hour orbits (see Figure 1-1).* This will provide world-wide coverage with 6-11 satellites above 5° in elevation at all times.

GPS satellite transmissions will include a coarse/acquisition (C/A) signal for moderate accuracy applications which could be employed by non-military users such as civil aviation, the maritime community, law enforcement agencies, etc. One of the important technical issues to be resolved is whether FAA navigation requirements can be met with a low cost GPS receiver. A summary of the accuracy requirements for area navigation (RNAV),[1] which also embody those for VOR/DME,** is given in Table 1-1.*** The maximum accuracy requirements which a candidate system must meet for RNAV apply in the landing approach phase. In particular, 1800 ft (2σ)-along track and 200 ft (2σ)-vertical are the most stringent requirements for 2D and 3D RNAV applications, respectively.

---

* Present plans have 8 satellites uniformly arranged in three orbital planes, each inclined 63°, with ascending nodes spaced 120° apart.

** A glossary of acronyms is provided in Appendix D.

*** User equipment error (UE) requirements were derived from total system error (TE) and flight technical error (FTE) according to: [1]

$$UE = (TE^2 - FTE^2)^{\frac{1}{2}}$$

FIGURE 1-1
GPS ORBIT TRACKS AND SATELLITE LOCATIONS AT EPOCH (T=0)

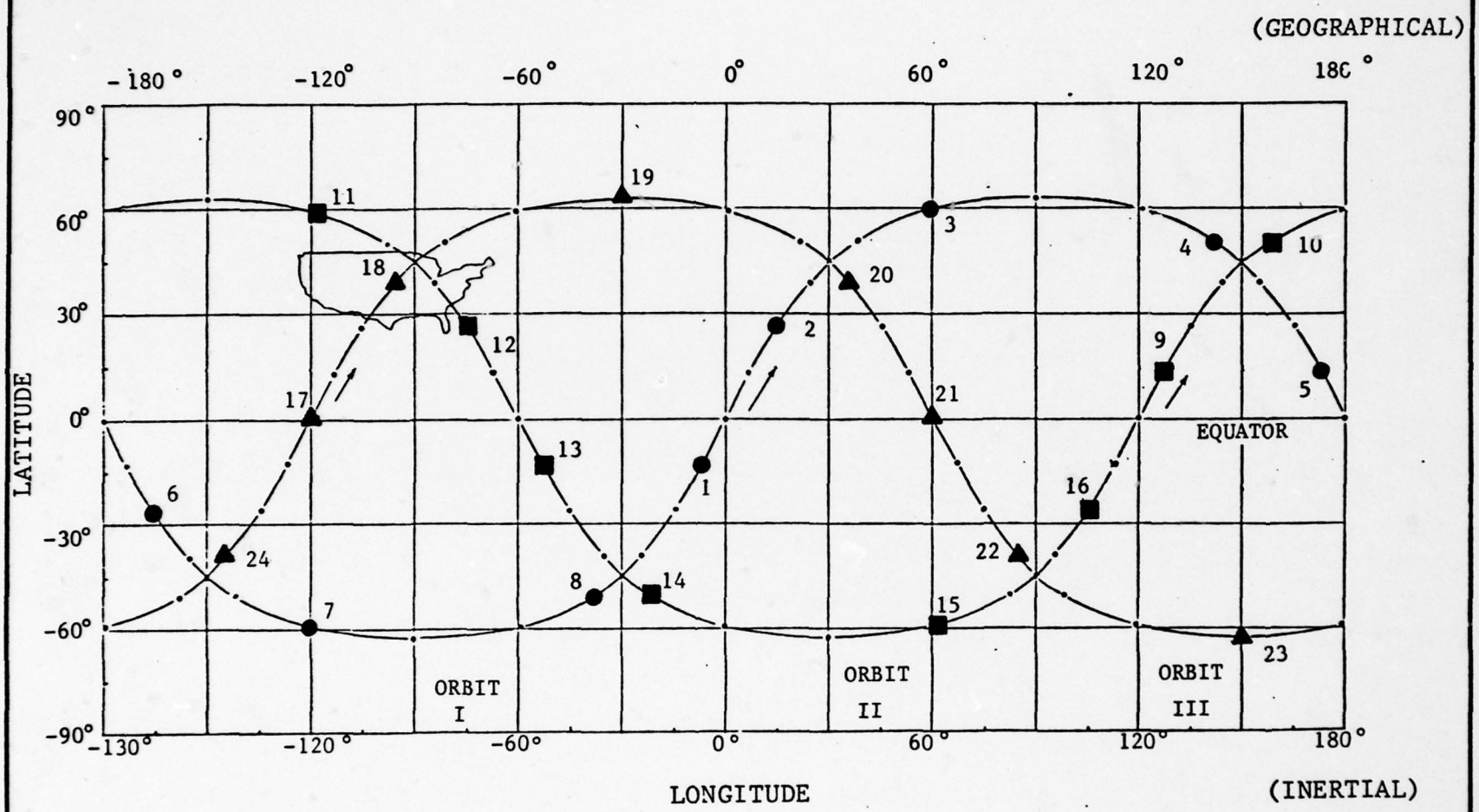

STANFORD TELECOMMUNICATIONS INC.

1.2 STUDY OBJECTIVES AND ASSUMPTIONS

This study addresses the design and performance analysis of a minimum configuration GPS receiver which is aimed at meeting the needs of low budget GA users. Specific objectives of the report are:

- to analyze the C/A signal detection performance of a low cost GPS receiver design,
- to evaluate the potential position determination capability of the receiver design with respect to both 2D and 3D navigational accuracy requirements for VOR/DME and RNAV (see Table 1-1),
- to identify experiments for validating the performance characteristics of the receiver design during the development phases (I and II) of the GPS program.

In pursuing these objectives, the following assumptions were made:

- the minimum received power available with the GPS C/A signal is -160 dBw,
- the radio frequency environment in the National Airspace System is non-hostile in nature, that is, no consideration is given to intentional electronic jamming of the receiver,
- the noise present in the receiver front end consists of the ambient background noise and, possibly, other sources of unintentional radio frequency interference (RFI) in the frequency range of the GPS C/A signal (1575.42 $\pm$ 1 MHz),

Table 1-1

NAVIGATION ACCURACY REQUIREMENTS

APPLICATION	ERROR CATEGORY		TOTAL SYSTEM ERROR*	FLIGHT TECHNICAL ERROR*	USER EQUIPMENT ERROR
2D RNAV (2σ)	CROSS TRACK	EN ROUTE	2.5 NM	2.0	1.5 NM (9000')
		TERMINAL	1.5	1.0	1.2 (7200')
		APPROACH	0.6	0.5	0.5 (3000')
	ALONG TRACK	EN ROUTE	1.5	NOT SPECIFIED	1.5 (9000')
		TERMINAL	1.1		1.1 (6600')
		APPROACH	0.3		0.3 (1800')
3D RNAV (2σ)	HORIZONTAL ELEMENTS			SAME AS 2D RNAV	
	VERTICAL GUIDANCE	ENROUTE	350 FT	NOT SPECIFIED	350 FT
		TERMINAL	350		350 FT
		APPROACH	200		200 FT

*REFERENCE: FAA ADVISORY CIRCULAR 90-45A
"APPROVAL OF AREA NAVIGATION SYSTEMS FOR USE IN THE NATIONAL AIRSPACE SYSTEM"
21 FEBRUARY 1975

- the dynamic environment for a typical GA user is low (e.g., 200 knots and 0.5g for maximum aircraft velocity and acceleration, resp.).

1.3 OUTLINE OF THE REPORT

Section 2 contains a summary of the receiver design and a discussion of the operational sequence. Section 3 presents the receiver performance characteristics based on a navigation error analysis and an analysis of the sensitivity of performance to the input $\dot{C}/N_o$.* Section 4 presents some possible experimentation options to verify the design and performance characteristics. Section 5 presents the conclusions and indicates areas for further investigation. Appendix A provides a detailed description of the receiver design. Appendices B and C contain supporting analyses for Section 3.

---

* Carrier Power-to-Noise Power Spectral Density Ratio

SECTION 2

RECEIVER DESIGN OVERVIEW

The receiver design was approached from the standpoint of seeking the simplest configuration that could provide a fully satellite-based 2D navigation capability* which meets present FAA requirements for area navigation (Table 1-1). The underlying philosophy is that a simpler receiver should be less expensive to ultimately develop and produce than a more complex one, even if economies of scale are realized (e.g., via LSI techniques). A basic guideline then was to minimize the use of critical and costly components such as high accuracy oscillators, phase-locked multipliers, crystal filters and custom digital elements. Design techniques which reduce the number of receiver components were also considered, e.g., use of a single correlator and single bandwidth filters for all tracking loops. A detailed discussion of the resulting design is presented in Appendix A.

2.1 BASIC CONFIGURATION

A functional block diagram of the receiver is shown in Figure 2-1. It is a single channel receiver which must acquire and process signals from selected GPS satellites in sequential order. It is designed to operate in two modes: a NAV Mode to provide the basic navigation capability with a fast update rate and a DATA Mode to collect the necessary data (satellite ephemeris, clock updates, etc.) to support the NAV mode; the navigation function is still provided, but at a reduced update rate in the DATA Mode.

All received signals are first amplified and down converted to an IF; the latter requires a single RF multiplier and standard LC filtering. After further downconversion to baseband the incoming signals are correlated with a locally generated reference

---

* This implies no dependence on barometric altitude for horizontal positioning.

Figure 2-1

OVERALL RECEIVER BLOCK DIAGRAM

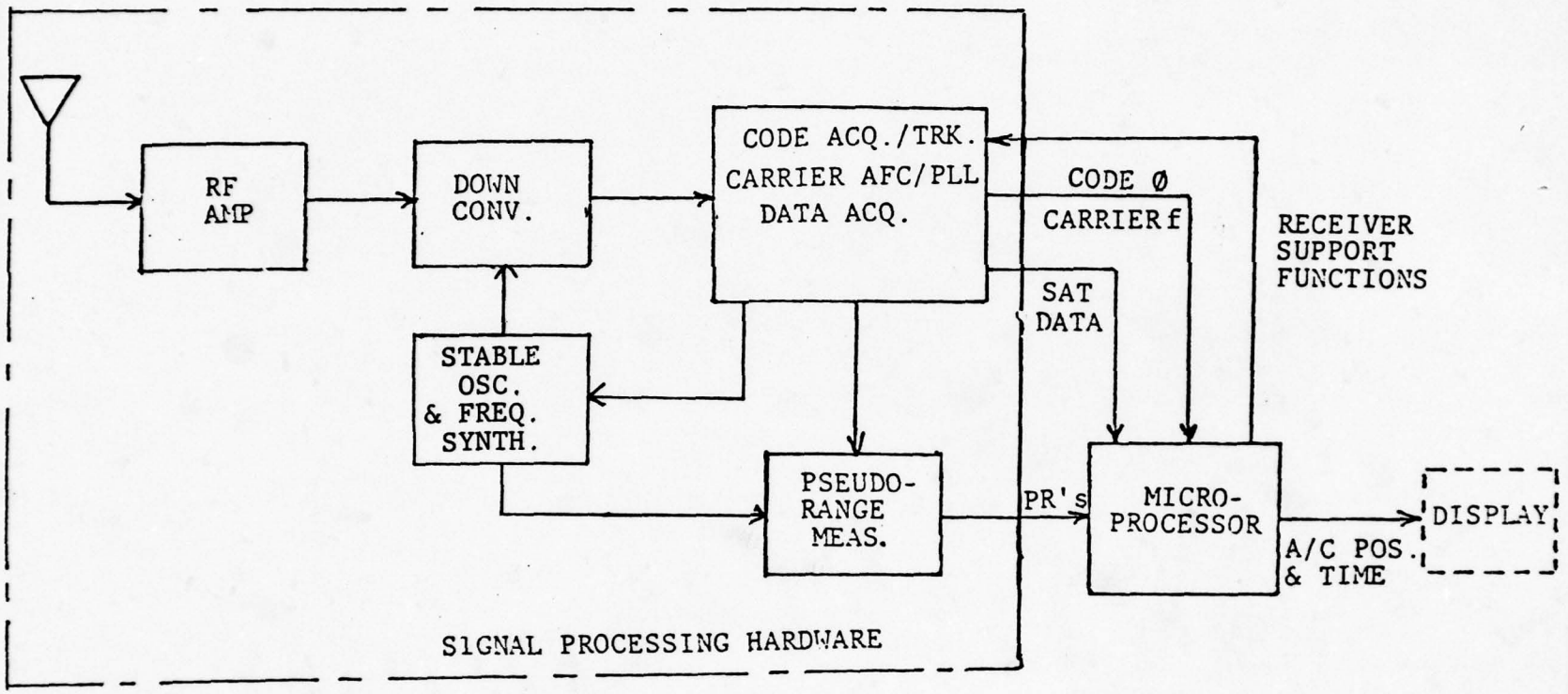

STANFORD TELECOMMUNICATIONS INC.

C/A code which is stepped in phase until the desired signal is acquired. Susequently both code and carrier tracking loops are enabled.

The receiver has a single correlator that is shared by the code and carrier loops. By implementing the correlator at baseband, a crystal filter for IF is eliminated. The carrier loop can operate in either an AFC or a PLL configuration. For signal acquisition and in the NAV mode, the AFC version is sufficient. During the DATA mode the PLL version would be implemented to provide the necessary code/carrier coherence.

The microprocessor operates in two separate ways: the first is in support of the receiver hardware, and the second is to perform the computations necessary for the navigation function. In the role of hardware support, the microprocessor selects a set of satellites for tracking which yield acceptable navigation accuracy. It also stores and estimates the signal code phase and carrier to aid reacquisition; performs bit and frame synchronization for data detection, and controls the receiver functions (e.g., the change between data and navigation modes, or the functional change for the AFC/PLL configuration). For navigation, the microprocessor updates the satellite ephemeris data, does the actual aircraft positioning and tracking, and formats the data for display. The data display could be in the form of distance to the next waypoint, and cross-track deviation from the desired course.

Pseudo-range measurements* are made after particular satellites have been selected and sufficient ephemeris data have been collected. Although, the receiver sequences rapidly between satellites to make pseudo-range measurements, two features are important to note. First, the previous code phase (ϕ) and carrier

---

* A pseudo-range measurement is an apparent range to a satellite which is offset from true geometric range by the user's clock bias which is common to all measurements.

frequency (f) are stored between satellite accesses and second, the receiver operates non-coherently in this mode and does not require phase lock. The rapid sequencing between satellites reduces the component of pseudo-range error caused by clock drift. The navigation goals of the receiver can thus be achieved with a clock oscillator stability on the order of 10^{-7}. This represents a substantial cost savings compared to more accurate clocks (e.g., 10^{-9} in the GPS Z set receiver). Also, the noncoherent fast sequencing enables the use of a noncritical voltage controlled oscillator, because exact memory of the carrier frequency is not crucial to the receiver operation.

Substantial efforts have been made in the receiver design to reduce complexity where cost savings are possible. The antenna and associated RF circuitry have been economized; the sequencing receiver configuration is simplified; the requirements for both oscillators and filters are non-critical; and an emphasis has been placed on microprocessor implementation of various receiver functions. In addition, further saving could result from the fact that several digital logic functions used by the receiver could be constructed primarily with non-custom LSI circuitry.

2.2 SEQUENCE OF OPERATIONS

The overall sequence of operations for the receiver is summarized in Figure 2-2. Although a full navigation solution (3D position + time)*, requires pseudo-range measurements from only four satellites, this receiver acquires and tracks five satellites whenever this is possible. The information from an extra satellite provides a margin that may be necessary during aircraft maneuvers when one or more satellites could be obscured.

---

* Vertical position is included in the solution process because availability of encoded altimeter data is not assumed.

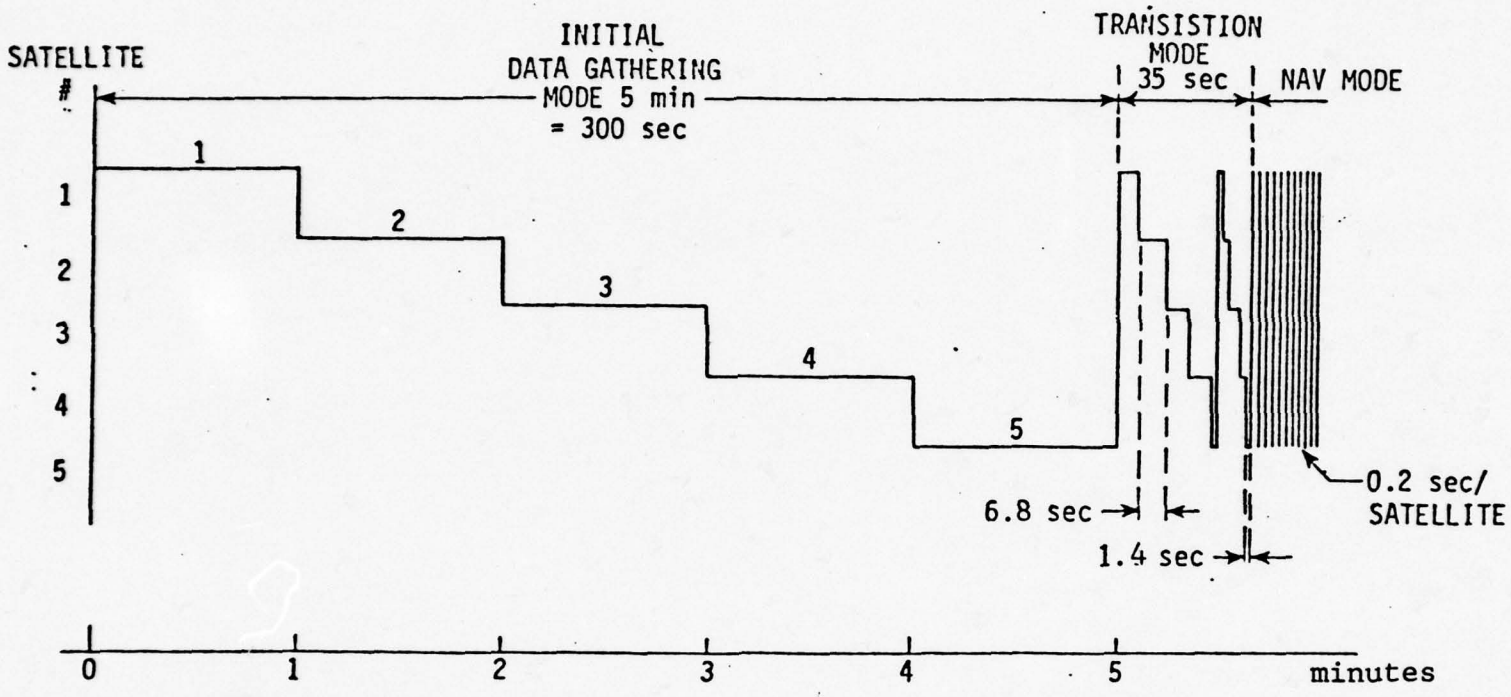

Figure 2-2

LOW COST RECEIVER - SEQUENCE OF INITIAL OPERATIONS

In the initial data gathering mode, the operator must first provide his approximate position and time. An almanac algorithm then selects a satellite configuration, supplies the proper satellite addresses (C/A codes) and estimates of the doppler shift for each satellite. Then the receiver performs the operations of sequentially acquiring each satellite, and obtaining the data which is superimposed on the code-spread carrier. Initially, the satellite C/A code, carrier frequency and phase are acquired. After bit and subframe synchronization are performed, the satellite data (ephemeris, clock corrections, etc.) are read and stored. Information such as code phase, received frequency and carrier phase are also stored to aid in reacquisition of each satellite during the navigation mode. This process is repeated for each of the five satellites selected by the almanac algorithm.

After this initial data gathering mode, the receiver enters a transition period during which the satellites are sequentially reacquired, and the window over which the code search occurs is progressively narrowed. The shorter interval between successive reacquisition decreases the uncertainty in code phase until the transition is complete and the receiver arrives at its steady-state sequencing rate (5 satellites/second). At this time, the receiver enters the NAV mode and begins updating the estimate of aircraft position at a rate of once per second.

As indicated in Appendix A, it takes approximately 63 seconds to sequence each satellite in the initial data mode, and the transition period lasts for 35 seconds. Together, the data mode interval and the transition period constitute the time-to-first-fix, which is approximately 6 minutes from the time that the operator first provides his approximate position and time.

In the NAV mode, the receiver dwells on each satellite for 0.2 seconds. For each satellite, the C/A code is reacquired using

the data from the previous access, and the pseudo-range to the satellite is measured. When this is completed, the microprocessor stores the code phase and carrier frequency for the current satellite and brings the code phase and carrier frequency for the next satellite out of memory. After five satellites have been sequenced in this mode, the aircraft position is updated.*

The NAV mode may continue for as long as two hours, after which some of the stored satellite data may no longer provide the desired navigation accuracy. This would occur in the event that either the current data no longer adequately represents the true ephemeris or the geometry for satellites in use is no longer favorable for navigation. Because the receiver has only a single channel, the NAV mode must be interrupted to refresh some or all of the satellite data.

In the DATA mode, the receiver updates the satellite data in use and/or acquires data for transitioning to other satellites. The same sequence of events as for initial data acquisition would be performed for each satellite data update. Between each data set (whether it be an update or a transition), the aircraft position is updated as in the NAV mode after reacquiring satellites. After all the necessary data updates have been completed, the receiver reenters the NAV mode (see Figure 2-3). This method of operation is continued for the duration of the flight, alternating between the NAV mode and the DATA mode as necessary. Since position updates would occur at a reduced rate (one/minute) in the latter, the pilot would have an override option for restricting automatic entry into it.

2.3 SUMMARY OF KEY TECHNICAL FEATURES

The receiver has the following signal processing characteristics that make it unique and potentially low cost:

---

* Batch updating of aircraft position rather than interative updating (i.e., after each measurement) is feasible with a fast satellite sequencing rate and/or availability of a sufficiently accurate velocity estimate from a tracking filter.

Figure 2-3

RECEIVER OPERATIONS

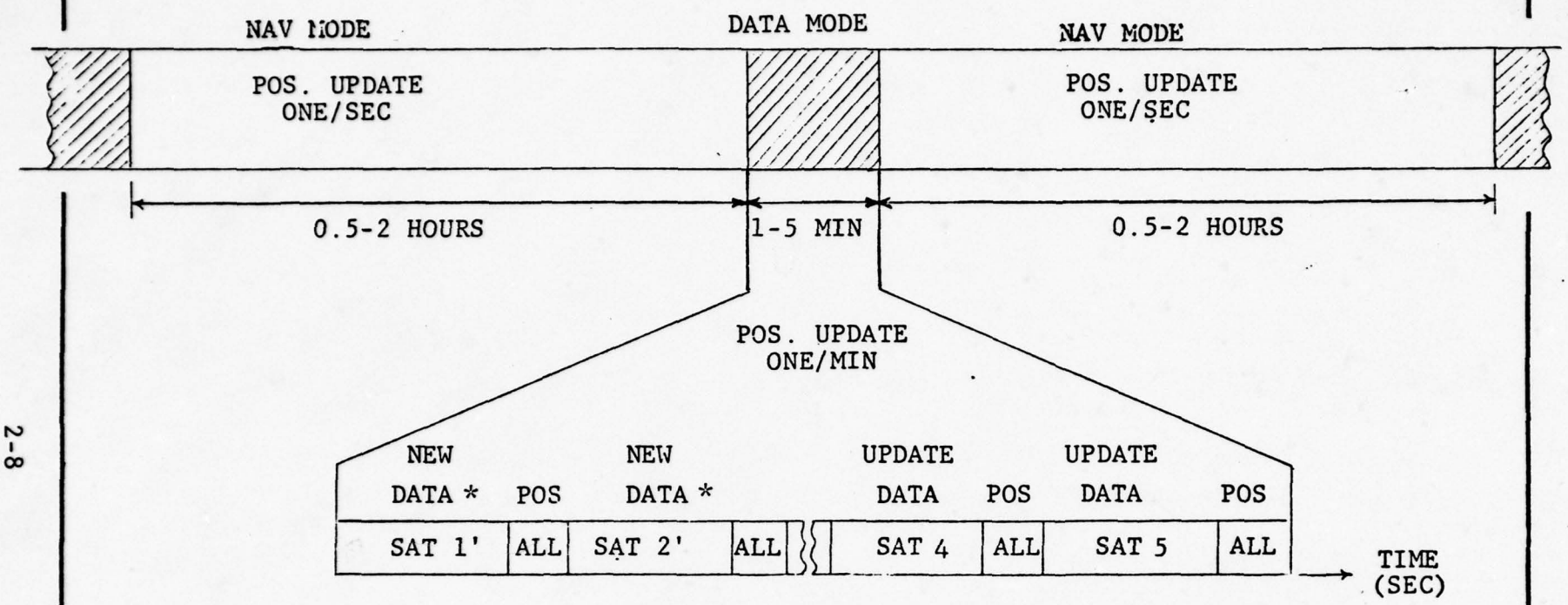

* Sat 1' and Sat 2' are replacements satellites.

- The receiver employs only one correlator with a "dithered" reference code.

- Correlation filtering is performed at baseband.

- The receiver contains only one voltage controlled oscillator which is either phase or frequency locked to the carrier, depending on the receiver mode. The oscillator is preset from the master oscillator.

- Code phase error is derived from the noncoherent τ-dither discriminator and used to vary the phase of the counted-down carrier frequency estimate.

- The receiver operates either in a continuous coherent mode to gather satellite data or in a noncoherent sequencing mode to measure pseudo-range.

- The receiver has a high sequencing rate (0.2 sec/sat) which reduces master oscillator stability requirements.

SECTION 3

PERFORMANCE CHARACTERISTICS

In the previous section* the design philosophy and operational functions of a single channel GPS receiver have been described. In this section the results of several analyses to assess potential performance capabilities of the receiver are presented. The specific aspects considered are positioning accuracy and performance sensitivity to input C/N_o.

3.1 POSITIONING ACCURACY

A GPS user can determine his 3D position and clock bias (offset from system time) by processing pseudo-range measurements from four satellites. If external altitude data is available or if the user's clock is synchronized with the system time, fewer pseudo-range measurements suffice to determine the remaining elements. However, no requirement for external altitude data or use of a high quality clock was assumed in the receiver design. Hence, it would usually be necessary that at least four satellites be available and provide adequate geometry for position determination (i.e., good GDOP**). For this study the accuracy analysis was based on:

$$2\sigma \text{ Horizontal Position Error} \equiv \text{HDOP} \cdot 2\sigma_R \qquad (3\text{-}1)$$

---

* Also see Appendix A.

** GDOP expresses the ratio of positioning error statistics to the standard deviation of the ranging errors, assuming these are equal and uncorrelated among the measurements. PDOP is commonly used to denote the position dilusion of precision when time is also evaluated in the solution process. (Note: $GDOP^2 = PDOP^2 + TDOP^2$). HDOP and VDOP represent the horizontal and vertical components of PDOP (i.e., $PDOP^2 = HDOP^2 + VDOP^2$). See Appendix C.

$$2\sigma \text{ Vertical Position Error} \equiv \text{VDOP} \cdot 2\sigma_R \qquad (3\text{-}2)$$

and

$$2\sigma \text{ User Clock Error} \equiv \text{TDOP} \cdot 2\sigma_R \qquad (3\text{-}3)$$

where σ_R is an equivalent ranging error related to the pseudo-range measurements and the solution process. Before presenting the results and comparing them with RNAV requirements, geometrical considerations (related to GDOP performance) and the ranging error budget (related to σ_R) are discussed.

3.1.1 Geometrical Considerations

Detailed studies have previously been made of the visibility characteristics of the 24 satellite GPS constellation [2,3,4]. The results indicate that at CONUS latitudes, 6-9 satellites with a minimum elevation angle of 5°, would be visible to an aircraft in level flight. Situations can arise, however, when fewer satellites are visible.

One of these situations can occur if a higher minimum elevation angle is necessary due to user antenna characteristics and/or physical obstructions. The number of visible satellites can be reduced at certain times and locations to only 4, and these also may have poor geometric deployment for accurate 3D positioning.* In the affected areas the duration of minimum visibility (i.e., 4 satellites) is highly sensitive to the user's elevation angle mask as shown in Figure 3-1b. For this analysis however, it is assumed that a 5° elevation mask is generally applicable based on the antenna gain characteristics in Figure A-2.**

---

* In Figure 3-1a the symmetrical deployment of satellites 4, 5, 22, and 23 relative to the indicated user location would produce a very large GDOP (>100).

** Experimental validation of this assumption is one of the test options suggested in Section 4.

A) ILLUSTRATION OF SATELLITE VISIBILITY CONSTRAINTS AT T=8.5 HRS FROM EPOCH

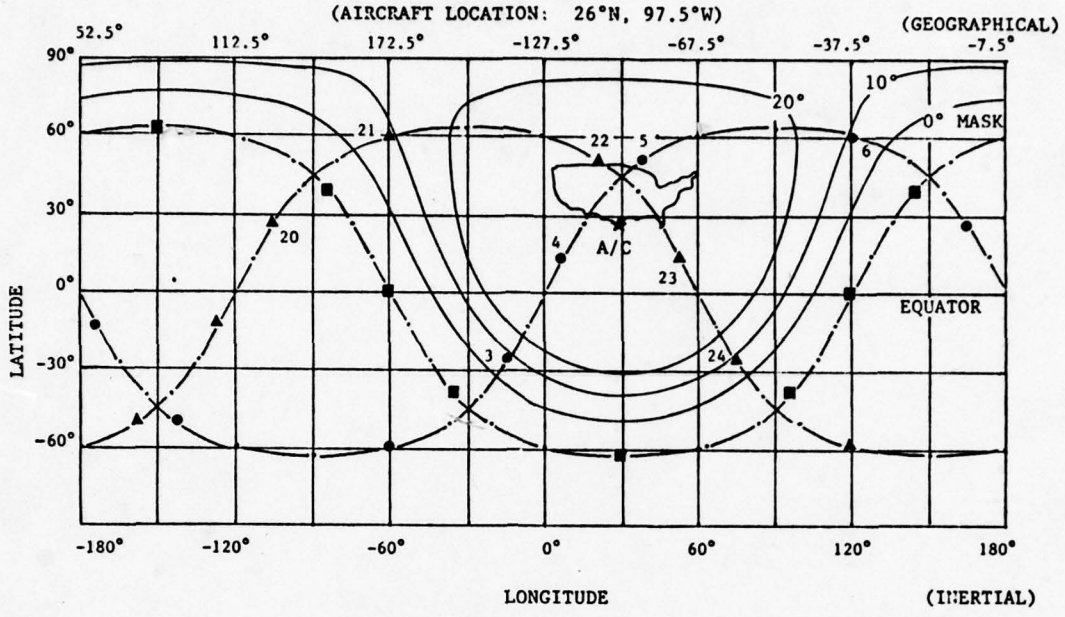

B) MINIMUM VISIBILITY DURATION VS MASK ANGLE

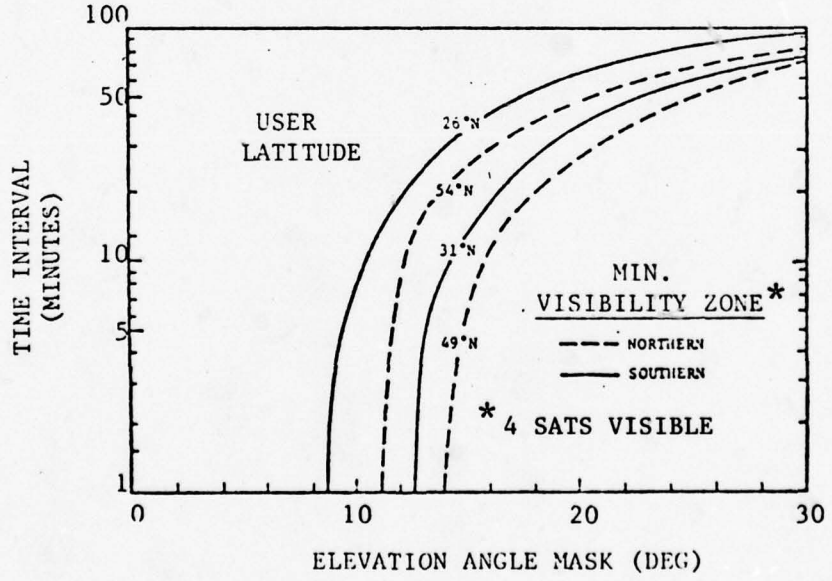

FIGURE 3-1

GPS SATELLITE VISIBILITY CHARACTERISTICS

STANFORD TELECOMMUNICATIONS INC.

Other situations with reduced visibility can arise when an aircraft is performing a sustained maneuver. In a coordinated turn a satellite may be obscured from the antenna by wing or airframe blockage due to the bank angle of the aircraft. The duration of shadowing varies with satellite elevation angle and turn parameters as shown in Figure 3-2. As an example, a standard rate turn of 3 deg/sec at 200 mph can cause a satellite at 5° elevation to be shadowed for as long as 60 sec. The potential impact of a temporary outage on positioning accuracy must be considered in the satellite selection process.

GDOP characteristics for the GPS constellation have been studied in detail [2,3,4]. Some corresponding to a 5° elevation angle mask are presented in Figure 3-3. They show that HDOP and VDOP would nearly always be less than 2.5 and 4.0, respectively. This assumes an optimal selection of 4 satellites, i.e., for minimum GDOP.

In the present application two primary goals are to achieve acceptable 2D postiioning accuracy and to maximize the time the receiver operates in the NAV mode. Hence, the satellite selection process would emphasize achieving a sufficiently low HDOP (e.g., < 2.5) and a long interval between satellite transitions. The type of trade-off involved is illustrated in Figure 3-4 which presents both optimal and suboptimal HDOP profiles over a four hour interval. The latter is somewhat higher, although still acceptable. On the other hand, significantly fewer satellite transitions would be required.*

Although pseudo-range measurements from only four satellites are required, the receiver would normally track five. This permits smoother transitioning during changeovers and provides

---

* Thusfar, analysis indicates that acceptable HDOP performance could be maintained with intervals of 0.5-2 hours between transitions.

A) SATELLITE SHADOWING DUE TO AIRCRAFT BANKING

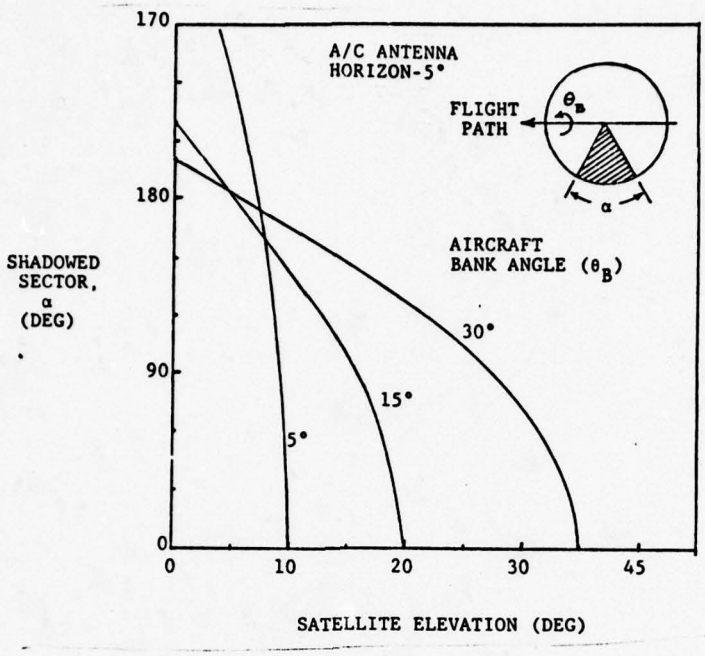

B) MAXIMUM DURATION OF SATELLITE SHADOWING IN TURNING MANEUVER

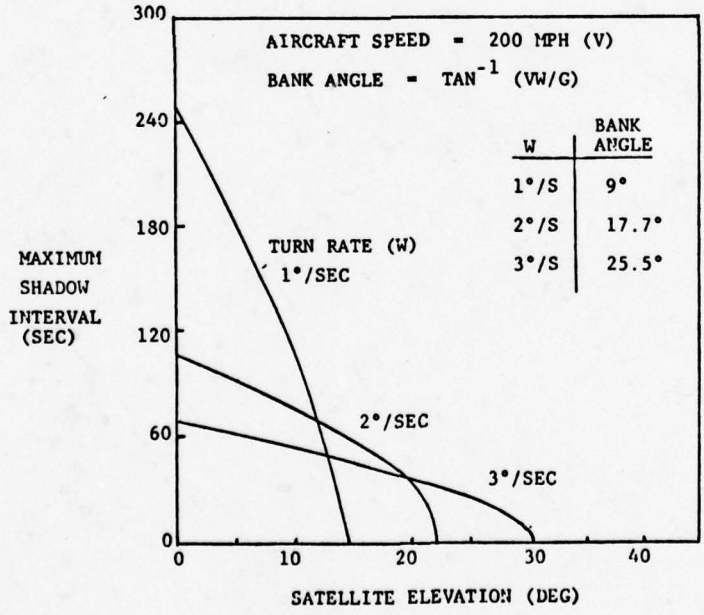

FIGURE 3-2

EFFECT OF AIRCRAFT BANKING ON SATELLITE VISIBILITY

STANFORD TELECOMMUNICATIONS INC.

(BOGEN [2])

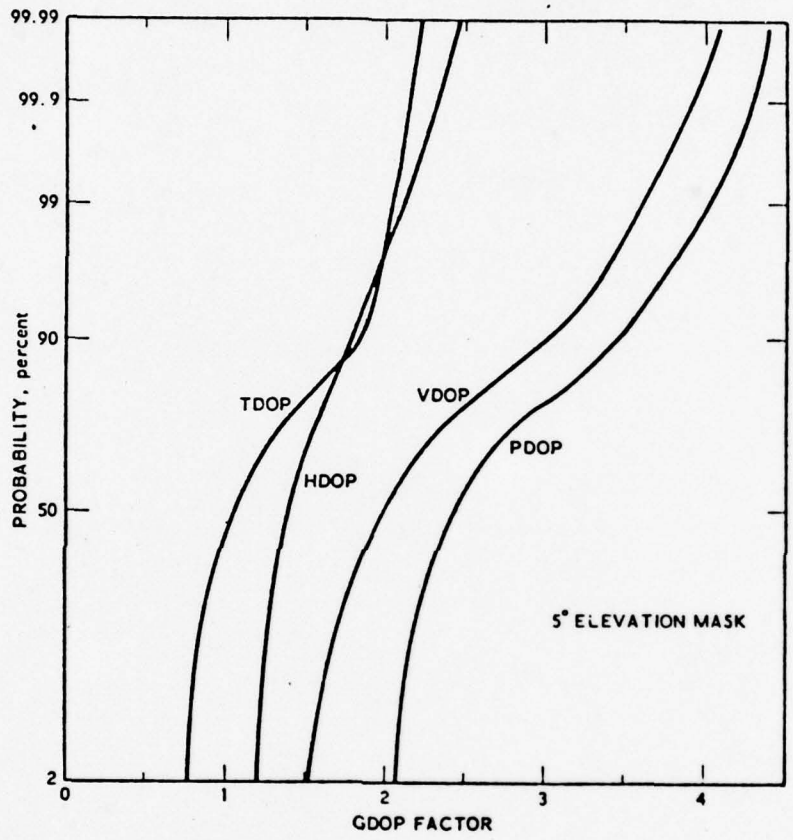

FIGURE 3-3

POTENTIAL GEOMETRIC PERFORMANCE
OF GPS IN THE OPERATIONAL PHASE

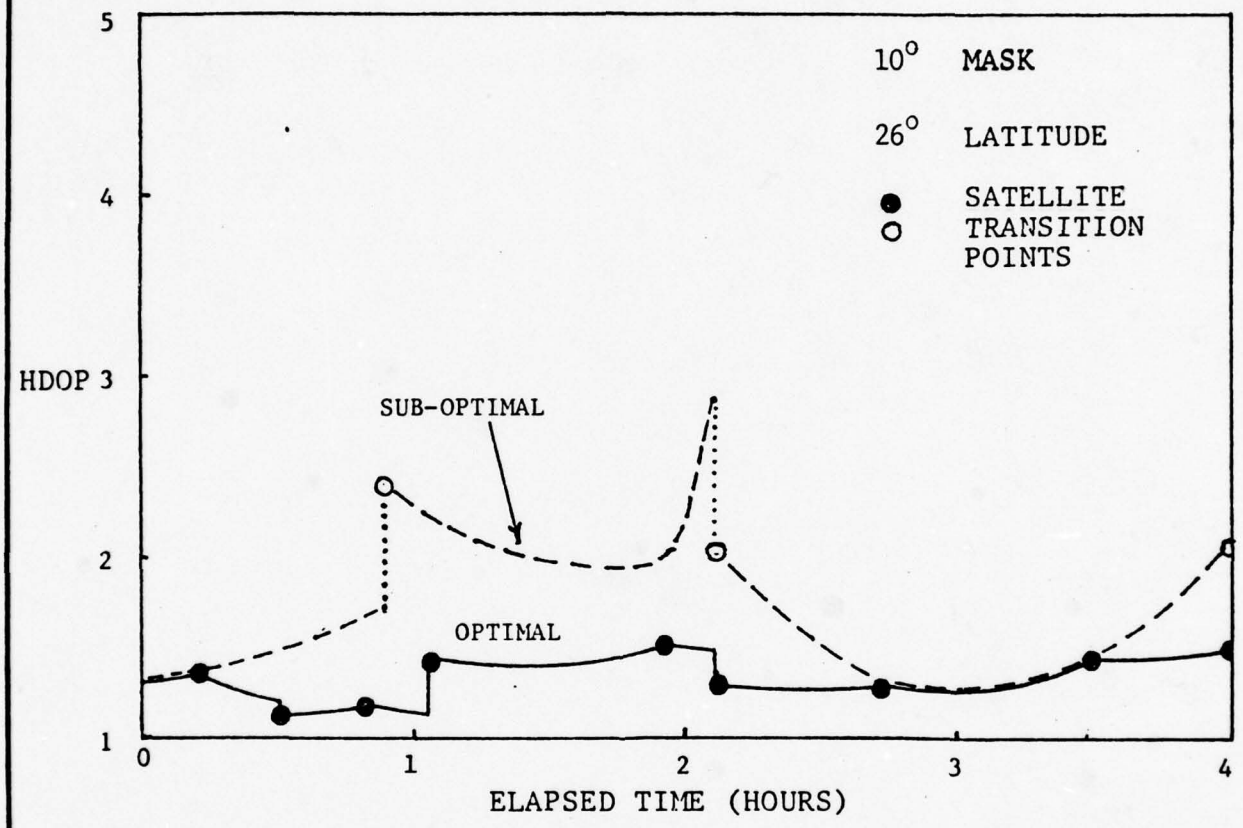

FIGURE 3-4

HDOP WITH OPTIMAL AND SUBOPTIMAL SATELLITE SELECTION

a backup in case one satellite becomes shadowed. If two satellites are temporarily shadowed so that only three are available, the usual 3D position + clock update is not possible. Over a limited interval however, the position elements can still be updated by assuming the clock to remain synchronized. The length of this interval will depend on the clock oscillator stability. In Appendix C a derivation is presented for the HDOP and VDOP corresponding to a "3 satellites + clock" solution. An example of the HDOP performance is shown in Figure 3-5 as a function of clock stability. For a 10^{-7} clock, HDOP increases in this case from about 2 to 7 over a 60 second interval.*

If an encoding altimeter were available, user position and clock bias could be determined by combining the altitude data with pseudo-range measurements. In Appendix C the equivalent HDOP is also derived for an "n satellites + altimeter" solution. An example with $n=4$ is shown in Figure 3-6 as a function of altimeter accuracy(μ) normalized to the pseudo-range error. Since μ would typically not exceed 5 in this application, it is apparent that an acceptable HDOP can be achieved where even a four satellite solution ($\mu=\infty$) would be indeterminate.**

3.1.2 Ranging Error Budget

There are a number of possible error sources which can affect positioning accuracy. A list of the principle contributors is given in Table 3-1 along with an estimate of their 1σ values. No distinction between purely random and systematic errors will

---

* The corresponding variation in VDOP is more severe (3 to 40)

** This arises if the ranging equations for the selected satellite set become singular or at least ill-conditioned. Such a situation would actually occur with the satellite deployment shown in Figure 3-1a if the elevation angle mask were to exceed 9°.

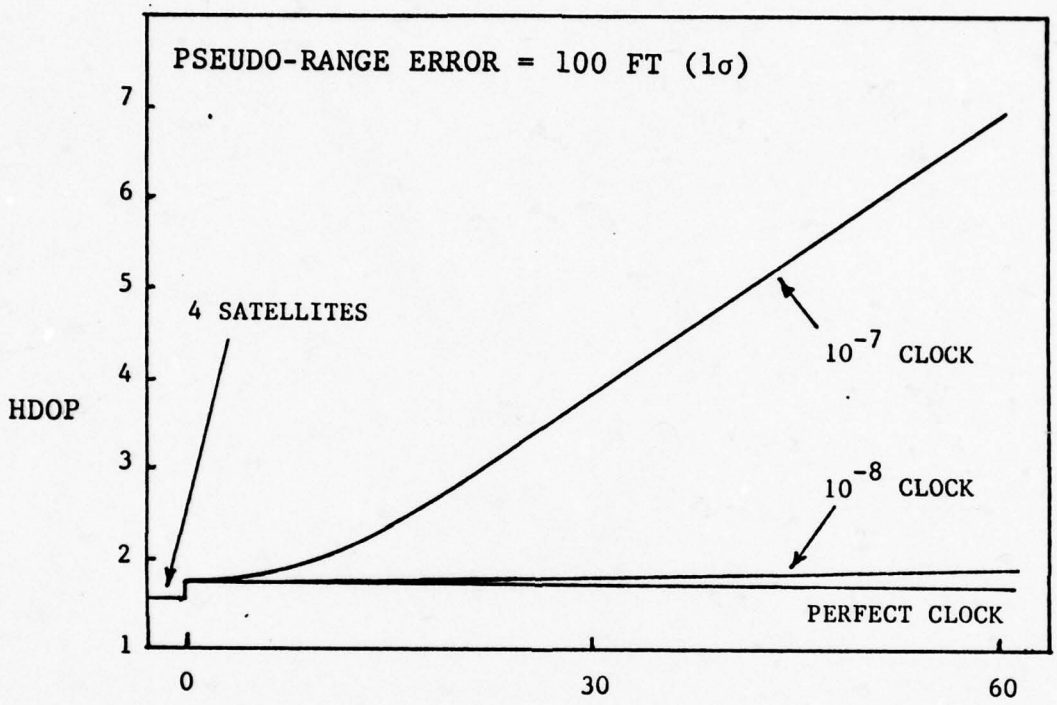

FIGURE 3-5

EXAMPLE OF HDOP WITH 3 SATELLITES + CLOCK

FIGURE 3-6

HDOP VS TIME WITH ALTIMETER AUGMENTATION

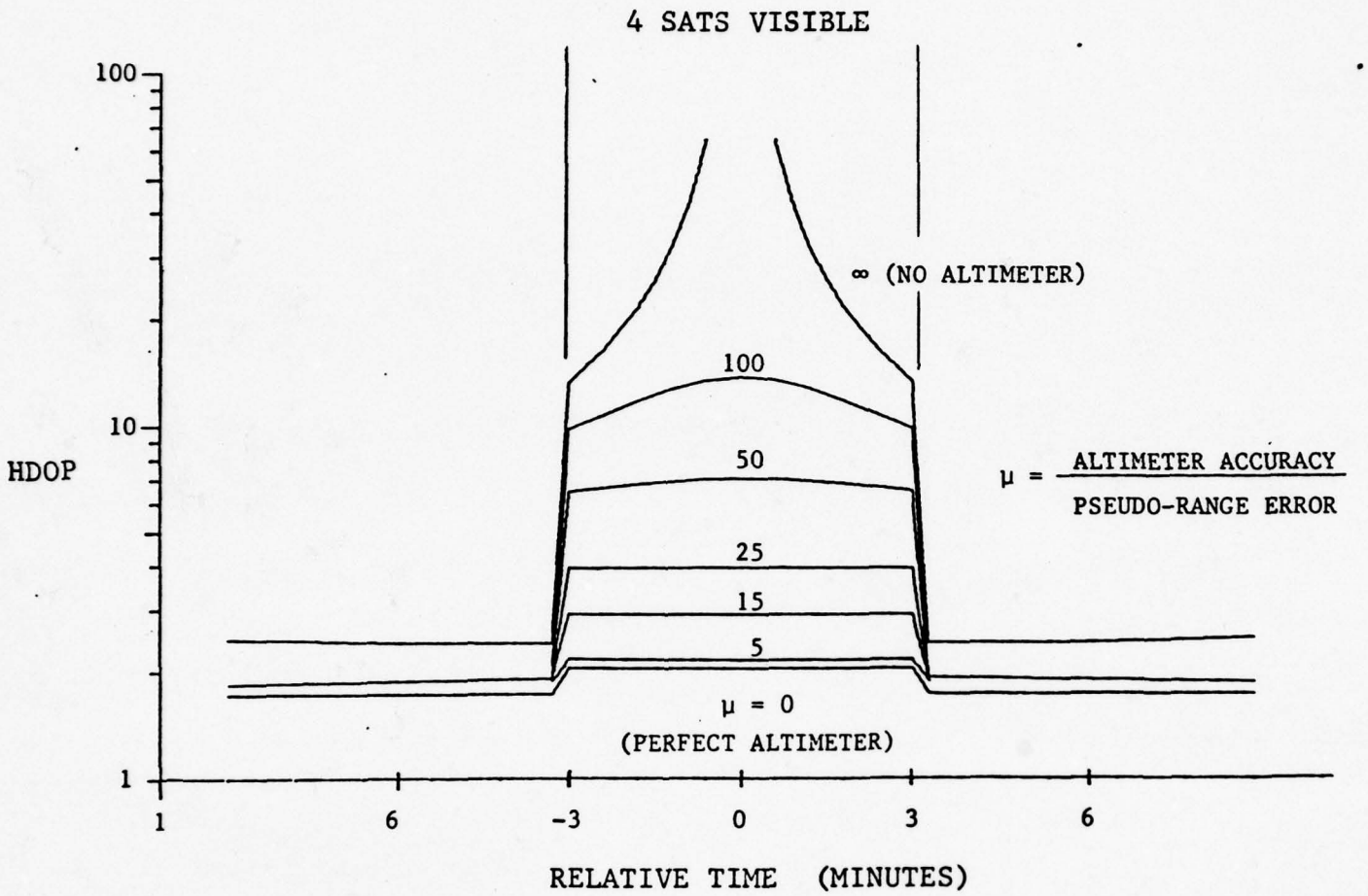

STANFORD TELECOMMUNICATIONS INC.

TABLE 3-1
RANGING ERROR BUDGET

ERROR CONTRIBUTORS		VALUE (1σ)	REMARKS
RECEIVER	PSEUDO-RANGE NOISE	50 FT	INPUT C/N_o = 40 dB-Hz DLL BANDWIDTH = 55 Hz
	PSEUDO-RANGE QUANTIZATION	15 FT	50 NS COUNTER QUANTIZATION
	CLOCK DRIFT	40 FT	OSC. $\Delta f/f = 10^{-7}$; 200 MS/SAT SEQUENCING
	COMPUTATIONAL	T B D	ACCURACY vs SPEED TRADEOFF
SPACE SEGMENT	EPHEMERIS UNCERTAINTY	5 - 20 FT	EQUIVALENT UERE (HIGHER FIGURE ONLY FOR UPDATES EVERY 2 - 3 HOURS)
	SAT. CLOCK BIAS & GROUP DELAY	5 FT	
PROPAGATION EFFECTS	IONOSPHERIC DELAY UNCERTAINTY	5 - 50 FT	WITH CRUDE MODEL
	TROPOSHERIC DELAY UNCERTAINTY	< 10 FT	WITH CRUDE MODEL
	MULTIPATH	0 - 50 FT	ENVIRONMENT DEPENDENT
MOTIONAL EFFECTS	AIRCRAFT	< 10 FT	1 SEC UPDATE RATE; 200 MPH A/C
	SATELLITES	< 3 FT	200 MS/SAT SEQ.; 5 Hz AFC LOOP
COMPOSITE		65 - 100 FT	(RSS)

be considered in this analysis, since an independent position fix is assumed to occur with each new measurement set.

The pseudo-range noise (50 ft.) due to timing jitter in the receiver code tracking loop is based on an input C/N_o of 40 dB-Hz.* Counter quantization (50 ns) produces an additional error but this is assumed to be uniformly distributed over the quantization range so the net effect is ~ 15 ft. Receiver clock drift of 10^{-7} produces an uncertainty of $\pm$ 40 ft. relative to the center satellite when sequencing over 5 satellites in 1 sec. The effects of computational errors on accuracy have yet to be addressed and thus were not included. However, based on the error budget entries in Table 3-1 it is clear that allowance for computational error could be as much as 50 ft without significant impact on accuracy**.

The lower figures for errors due to the space segment (ephemeris, etc.) are target values for GPS in Phase III. The higher figure of 20 ft. indicates the estimated degradation in ephemeris accuracy if 3 hours elapse between DATA mode updates. [13,14] Propagation effects, particularly ionospheric delay, can at times produce significant errors, which are reflected in the range of values given in Table 3-1. Errors due to aircraft and satellite motion over the measurement interval are relatively small, principally because of the 0.2 sec/sat sequencing rate.

An RSS of the error budget components yields a composite error of ~ 65-100 ft. For purposes of analysis the upper limit is chosen as the equivalent ranging error.

3.1.3 Comparison of Performance with RNAV Requirements

Based on the preceding discussion a summary of the positioning accuracy performance is presented in Table 3-2 for normal and

---

* See Appendix A.

** Development of a suitable microprocessor to provide such performance is reasonable to expect. [12]

TABLE 3-2

POSITIONING ACCURACY

DIMENSION		NORMAL MODE 4 SATS	AUGMENTED MODE 3 SATS + CLOCK+	AUGMENTED MODE 3 SATS + ALT.
HORIZONTAL	HDOP (typ)	1.5 - 2.5	2 - 7	2 - 3
	ACCURACY* (2σ)	300 - 500 FT	400 - 1400	400 - 600
VERTICAL	VDOP (typ)	3 - 4	3 - 40	N/A
	ACCURACY* (2σ)	600 - 800 FT	>1000 FT	ALTIMETER ACCURACY

* BASED ON 200 FT (2σ) RANGING ERROR

\+ BASED ON 10^{-7} CLOCK FOR $\leq$ 60 SEC

augmented modes of operation (4 sats and 3 sats + clock or altimeter). Comparison with the data in Table 1-1 indicates that:

- horizontal accuracies in level flight are more than sufficient to meet 2D RNAV (and VOR/DME) requirements,
- vertical accuracies are not sufficient for satellite-based 3D RNAV with this low cost receiver design*,
- acceptable 2D performance can be maintained during typical maneuvers by tracking five satellites, temporary use of the receiver clock and/or augmentation by altimeter data to offset loss of a satellite due to shadowing.

3.2 RECEIVER PERFORMANCE SENSITIVITY TO INPUT C/N_o

This section summarizes results (presented in Appendix B) of a preliminary sensitivity analysis of the receiver performance to the input C/N_o. A nominal design value of 40 dB-Hz was used based on C = -160 dBW and N_o = -200 dBW/Hz. While expectations are that higher satellite power will be available in Phase III**, there is always the possibility that in some cases it could degrade below specifications prior to the projected 7 year satellite lifetime. Even if it doesn't, situations may arise where N_o increases, e.g., due to higher radio frequency interference (RFI) during aircraft maneuvers (banking or pitching).***

---

* 3D RNAV could be achieved with encoding altimeter input.

** A received power of -158 dBW from Phase I satellites has been measured.[5]

*** If projections of RFI at L band [6] due to man-made noise in urban areas prove substantial, the antenna noise temperature (and thus N_o) could be several dB higher than that for pure sky background noise assumed here in calculating N_o = -200 dBW/Hz.

Two approaches to the sensitivity issue were studied, one based on the nominal receiver design and the other on a re-design. The questions considered in the two cases are:

Nominal Design: What is the margin in C/N_o between nominal and threshold operation for the various receiver functions - signal lock detection, code tracking (DLL) and carrier tracking (AFC and PLL)?

Re-design: What is the signal acquisition time and update rate as a function of C/N_o?

For the nominal receiver design it was determined that the threshold margin (relative to C/N_o = 40 dB-Hz) was 2 dB-Hz for the lock detector, 4 dB-Hz for the DLL, 13 dB-Hz for the AFC loop and 2 dB-Hz for the PLL. Thus, the lock detector and the PLL are the most sensitive elements. However, the PLL is only active in the DATA mode and therefore less susceptible to a drop in C/N_o due to RFI, since this mode would typically occur during level flight. The 2 dB-Hz margin for the lock detector is more of a problem in the NAV mode. It corresponds to a decrease in the probability of detection from 0.9 to 0.65 (assumed to be the minimum operational limit). Thus, in the NAV mode the receiver would have to cope with a higher missed alarm rate during satellite sequencing operations. A 2 dB-Hz drop in C/N_o would also cause the code loop timing jitter to increase about 40%; this changes the pseudo-range noise in Table 3-1 from 50 ft to 70 ft.

In the re-design case, the receiver parameters (loop bandwidths, integration time, etc.) were adjusted as a function of C/N_o to provide the same accuracies as in the 40 dB-Hz design. The resulting signal acquisition time and dwell interval in satellite sequencing are plotted in Figures 3-8 and 3-9 as a function of C/N_o. The result of a 3 dB-Hz drop in the C/N_o design

value would be to lengthen the dwell interval from 0.2 to 0.7 sec and increase the acquisition time from 63 to 82 sec. The increased dwell time changes the update rate from 1 sec to 3.5 sec when tracking 5 satellites. Acquisition time is less sensitive because most of it is consumed by satellite data detection (30 sec), sub-frame synch (20 sec) and data bit synch (5 sec), none of which are strongly C/N_o dependent.

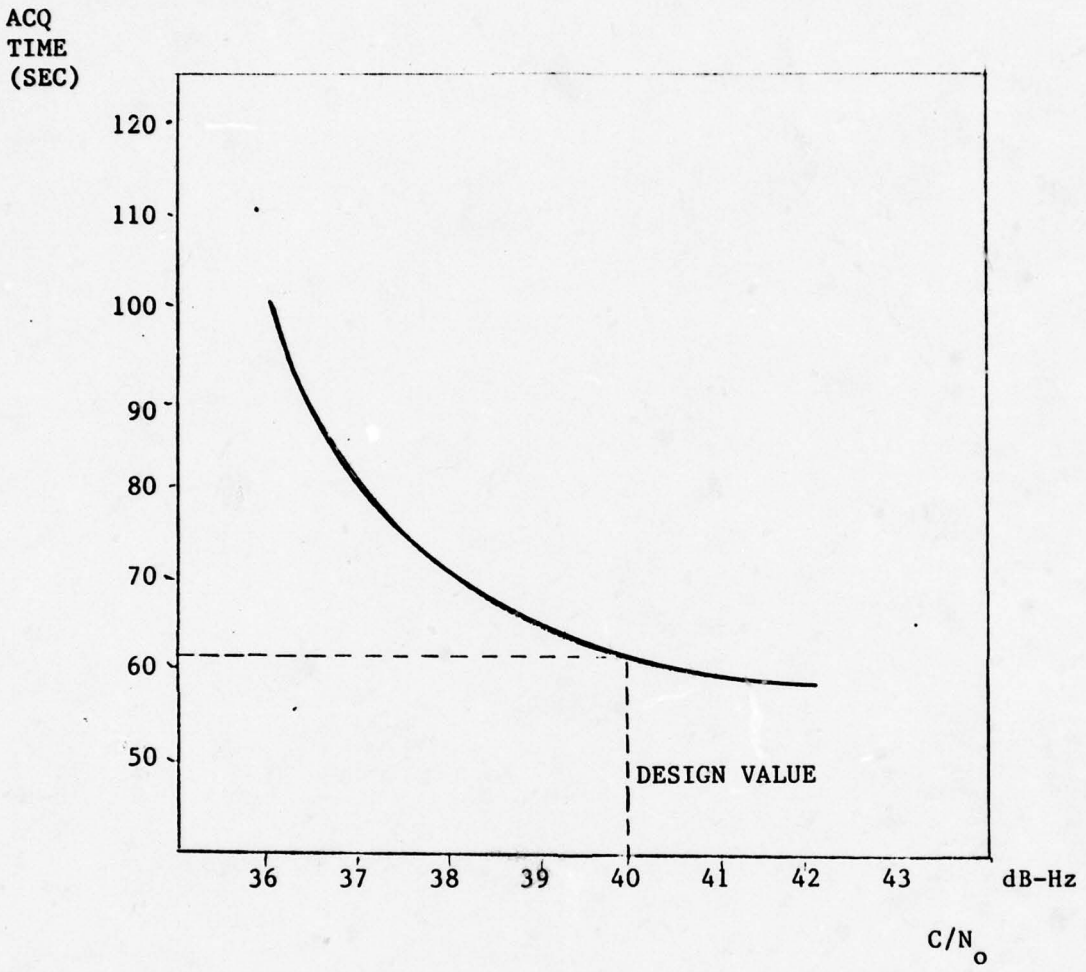

Figure 3-7

ACQUISITION TIME PER SATELLITE VS C/N$_o$

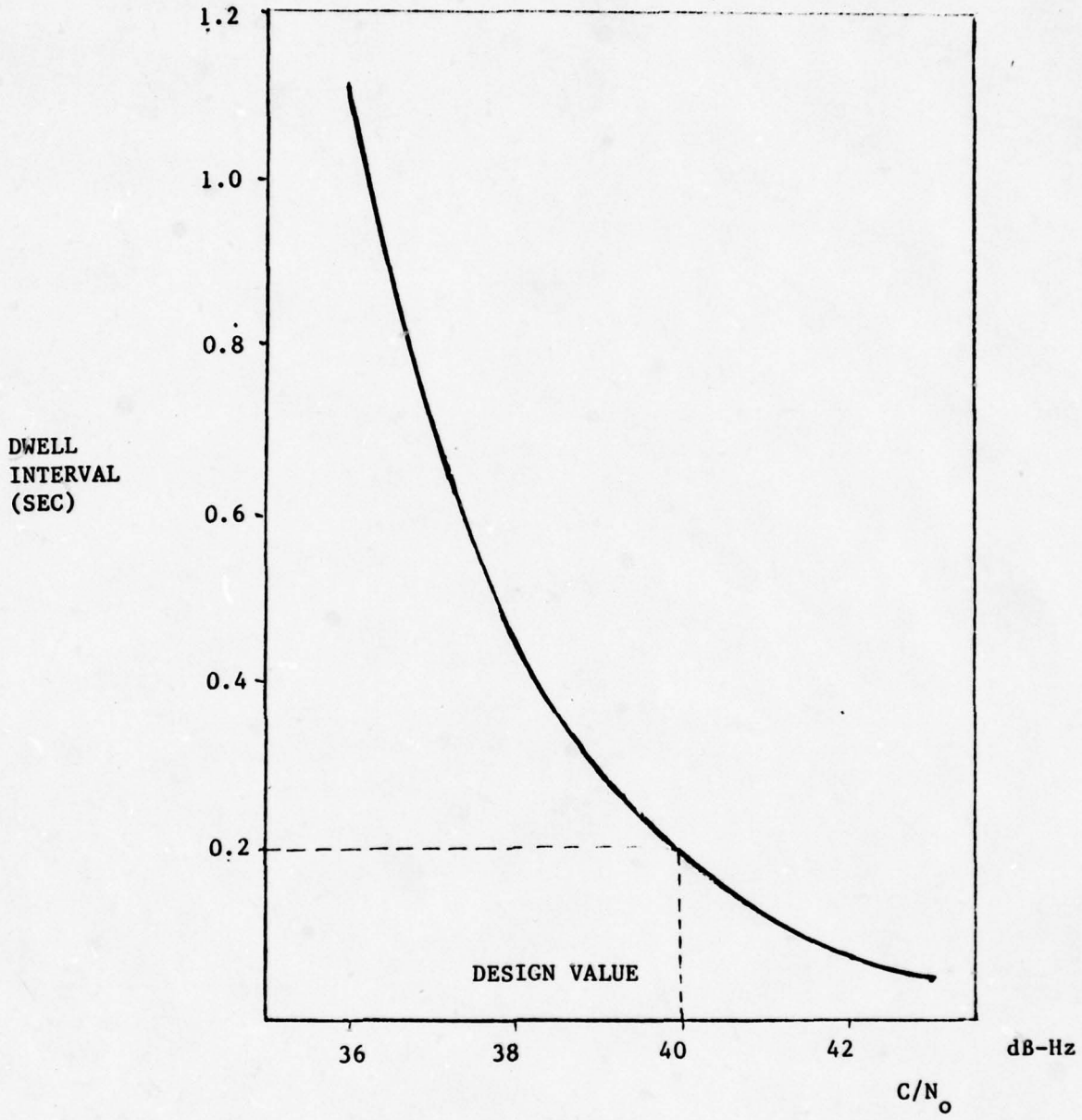

Figure 3-8

DWELL INTERVAL PER SATELLITE VS C/N$_o$

SECTION 4

EXPERIMENTATION OPTIONS

Analytical studies and simulations of receiver performance are useful tools in establishing a preliminary assessment of technical feasibility. A suitable measurement and test program is also necessary to evaluate engineering models of the hardware and software designs and to demonstrate performance under operational conditions. A list of some possible static and dynamic tests to evaluate receiver performance is given in Table 4-1.

Experiments should include an evaluation of the satellite selection process, particularly in terminal areas during a non-precision approach when maneuvers are more frequent. Also, any operational constraints on alternating between the NAV and DATA modes (with pilot override for the latter) should be evaluated under both IFR and VFR conditions.

Potential sites for the dynamic tests would include the Yuma test range (Arizona) and the NAFEC facility (New Jersey). Visibility of GPS satellites at both locations in Phases I and II (once 6 are launched) is shown in Figure 4-1. At Yuma there are ground transmitters available for satellite simulation that increase the testing capability and simplify the calibration requirements. Also, the range is already designed specifically for testing of the GPS. NAFEC has close proximity to an Air Traffic Control operational environment and in particular to multiple VOR/DME facilities for performance comparsion.

Detailed procedures for the test options identified in Table 4-1 are not addressed here. However, the development of a comprehensive test plan should consider relevant aspects of the current GPS test series [15] and previous satellite/aeronautical technology experimentation supported by the FAA [16, 17].

TABLE 4-1

TESTS FOR VERIFICATION OF RECEIVER DESIGN AND PERFORMANCE

- STATIC TESTS (LAB DEMOS/AIRPORT GROUND TESTS
  - VERIFY BASIC DESIGN PARAMETERS & SOFTWARE
  - EVALUATE SIGNAL ACQUISITION PERFORMANCE
  - DETERMINE STATIC POSITIONING ACCURACY

- DYNAMIC TESTS (FLIGHT DEMOS)
  - VERIFY DESIGN UNDER OPERATIONAL & ENVIRONMENT CONDITIONS
  - EVALUATE SIGNAL ACQUISITION PERFORMANCE (COLD START/RESTART)
  - EVALUATE SATELLITE SELECTION PROCESS
    - -- SATELLITE SHADOWING EFFECTS
    - -- CHOICE OF MASK ANGLE
    - -- DATA MODE REQUIREMENTS
  - DETERMINE DYNAMIC POSITIONING ACCURACY
    - -- TERMINAL AREAS
    - -- NON-PRECISION APPROACH APPLICATIONS
  - ASSESS POTENTIAL MODIFICATIONS IN APPROACH PATTERNS WITH GPS POSITIONING CAPABILITY

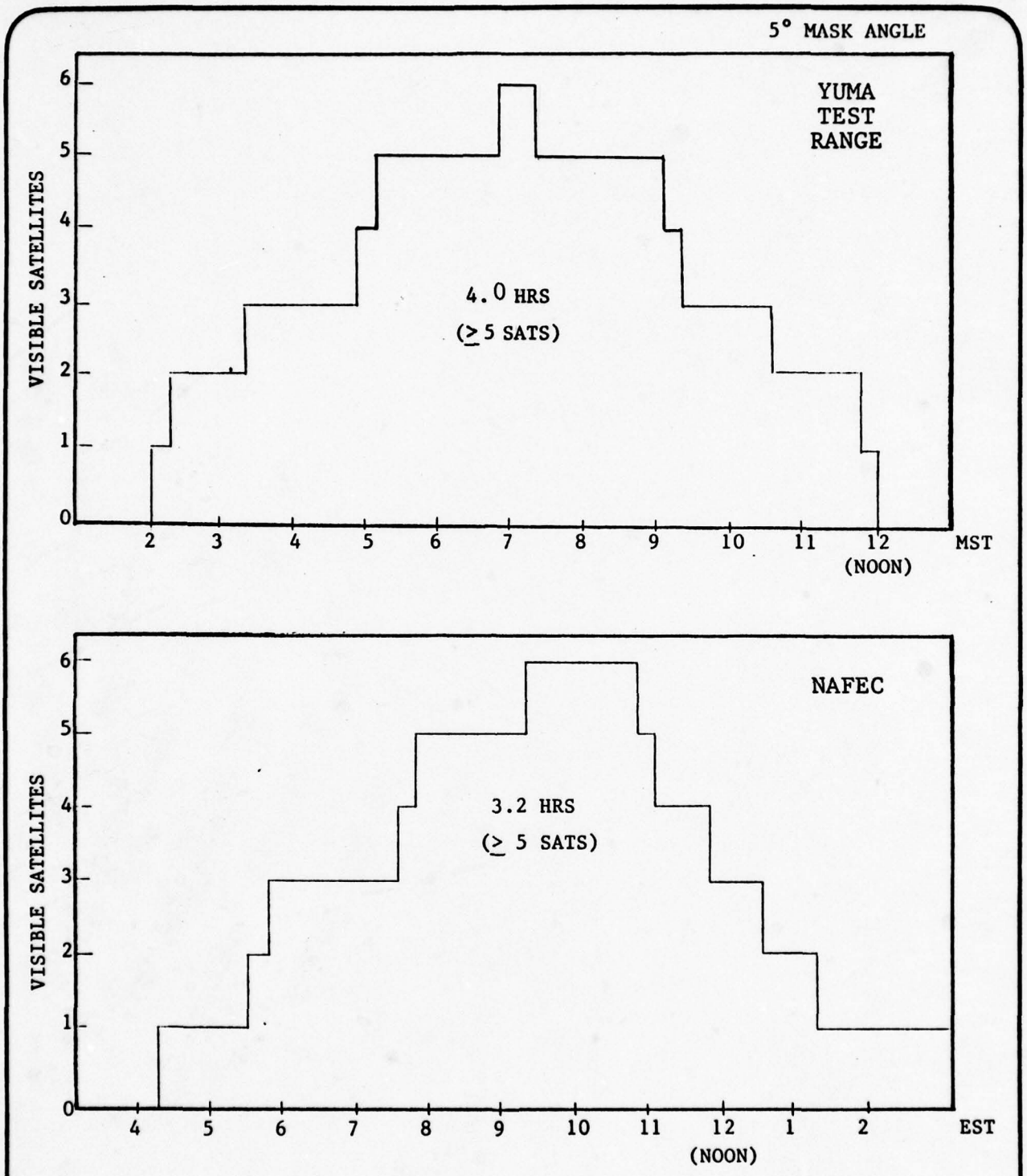

FIGURE 4-1

GPS SATELLITE VISIBILITY AT YUMA AND NAFEC IN PHASES I AND II

STANFORD TELECOMMUNICATIONS INC.

SECTION 5

SUMMARY AND CONCLUSIONS

The purpose of this report has been to present and analyze the basic design of a Low Cost GPS Receiver (LCR) for General Aviation applications. The receiver is intended to meet 2D RNAV requirements without dependence on external altitude data at a cost which would make it accessible to the GA community.

The receiver utilizes a single channel which functions in either a navigation (NAV) mode or in a DATA mode. In the NAV mode, the receiver tracks the GPS C/A signal code and provides position updates at a rate of one/sec. The DATA mode would be used for 1-5 minutes every 0.5-2 hours to acquire navigation data (satellite ephemeris, etc.) for transitioning to new satellites and/or updating the data for those satellites currently in use. Since position updates would then occur at a slower rate (one/min), a user would be provided with an override option for controlling entry into this mode.

The results of an analysis of receiver performance indicate that:

- The basic design could provide excellent horizontal positioning accuracy, $\leq$ 500 ft (2σ), during level flight. This more than meets the minimum 2D RNAV and VOR/DME accuracy requirements of 1800 ft (2σ).

- Satisfactory performance could also be maintained during typical aircraft maneuvers in terminal areas by tracking five satellites, temporary use of the receiver clock and/or augmentation by altimeter data to offset the effects of satellite shadowing caused by these maneuvers.

- The accuracy required for fully satellite-based 3D RNAV does not appear to be achievable with this low cost receiver design. 3D RNAV would be achievable in a hybrid configuration using independently derived altitude data, as is current practice with OMEGA, LORAN-C and inertial navigation systems.

The extent to which LCR functions are affected by variations in the input carrier power to noise spectral density ratio (C/N_o) has also been examined. A drop in the C/N_o can be caused by either a decrease in the satellite radiated power or an increase in noise level, for example from radio frequency interference. For a receiver design based on C/N_o = 40 dB-Hz, the margins between the nominal and threshold operation for the signal lock detector, the code tracking loop, the AFC loop, and the phase locked loop (PLL) would be 2, 4, 13, and 2 dB-Hz, respectively.

A re-design of the receiver based on a lower input value of C/N_o was investigated, with the aim of providing additional margin. The impact of a re-design is to increase the time necessary to acquire satellite data in the DATA mode, and decrease the position update rate in the NAV mode. In particular, a 3 dB drop in the design C/N_o increases the initial acquisition time from 5 minutes to 7 minutes; it changes the time between position updates from 1 sec to 3.5 sec.

It should be noted that a 6 kHz IF bandwidth was assumed throughout the analysis. However, the maximum anticipated carrier frequency uncertainty is about $\pm$ 1750 Hz, so a lower IF bandwidth appears possible. Since a faster update rate for the same C/N_o could result, additional analysis should be pursued to determine the feasibility of decreasing the IF bandwidth (e.g., to 4 KHz or even lower, if the doppler uncertainty can be reduced).

Other technical issues remain to be addressed. These include an assessment of dynamic range requirements for the receiver

and the related questions of multiple access interference effects from other GPS satellites. These could become more significant if the design value of C/N_o is decreased to offset susceptibility to RFI. Another area for investigation is the process for signal reacquisition in the NAV mode after a temporary outage (e.g., due to satellite shadowing). A moderate outage (e.g., < 60 sec) could be accommodated within the basic 1 sec update interval. However, longer outages would likely require a longer C/A code search interval and thus impact the overall update rate.

From a cost point of view, another area for investigation is the extent to which a digital implementation* would be preferable for certain receiver functions than the analog implementation considered in the present design. In the code loop (DLL) this would include the squaring and sum functions (at baseband), the τ-dither discriminator and the DLL filter. In the carrier loop (AFC/PLL) this would include the Q/I channel multiply function (at baseband) and the loop filters. Bit and frame synch functions for data detection are already assumed to be performed in the microprocessor.

Finally, there is a question as to whether the basic LCR design would be suitable for all GA operations in terminal areas. Indications are that the basic design would be suitable for VFR flight operations, but the slower position update rate while operating in the DATA mode is a potential concern for IFR operations. Modifications of the LCR design by the addition of a second channel to permit simultaneous NAV and DATA mode operations is an alternative which could be investigated in a subsequent study.

---

* i.e., implementation in the microprocessor.

APPENDIX A

A Low Cost GPS Receiver Design for General Aviation

Widespread utilization of GPS by general aviation (GA) will require the availability of user equipment which meets all technical requirements at an acceptable cost. This appendix presents a candidate design for a low cost receiver (LCR) which is aimed at meeting FAA requirements for 2D RNAV (see Table 1-1). Additional design goals were to provide a position update rate $\leq$ 1 sec and horizontal position without dependence on external altitude data.

Discussion of the LCR design is divided into three parts. The first describes the receiver configuration and each of the stages involved in processing the GPS C/A signal. The second concerns the receiver operating modes and the scheme for satellite sequencing. The third deals with selection of LCR parameters and a preliminary estimate of performance.

A.1 LCR Configuration

A functional block diagram of the LCR is shown in Figure A-1. The receiver employs a single correlator with the reference code "dithered" such that both code tracking and carrier recovery can be performed. The carrier is tracked in either an AFC or phase-locked mode using a long-loop configuration, thus preserving code-carrier coherence. The code loop clock is derived from the carrier loop so that only one VCO is used. The code clock phase is controlled by a digital phase shifter which is set by the noncoherently derived code loop error voltage.

The LCR has two basic modes, one for data collection (DATA mode), and the other for psuedo-range measurement (NAV mode). In order to gather satellite data, the receiver acquires the desired satellite, and performs coherent data demodulation.

Once data has been gathered from the designated satellites, the receiver begins sequencing over four or five satellites (depending on availability) to make psuedo-range measurements. Approximate code phase and carrier frequency are remembered between accesses of the same satellite. The receiver is noncoherent in this mode and does not require phase-lock. This allows rapid satellite sequencing ($\approx$ 200 ms/sat) which, in turn, reduces the psuedo-range error caused by receiver clock offset. As a result, the receiver navigation goals can be met with a clock accuracy on the order of 10^{-7}, which is relatively easy to achieve.

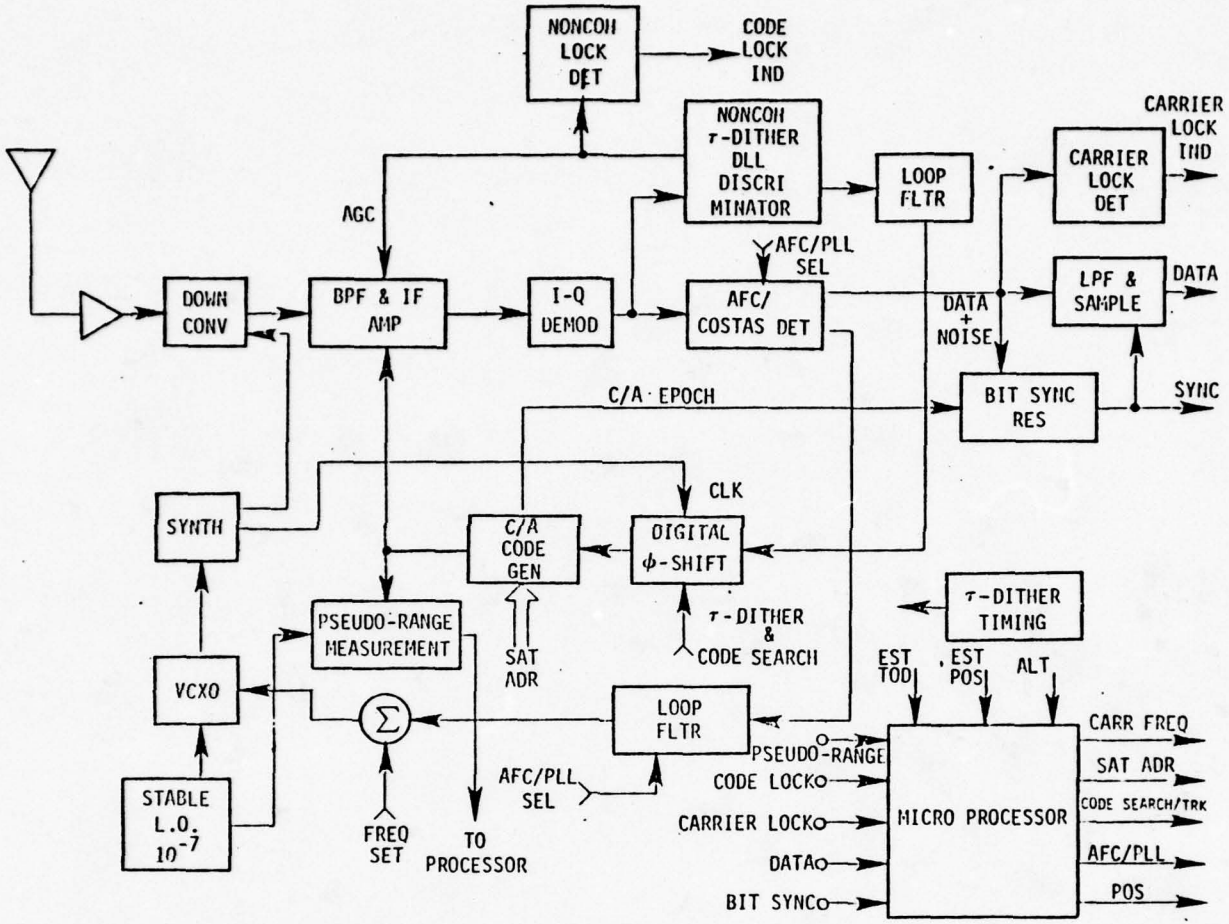

FIGURE A-1

OVERALL RECEIVER BLOCK DIAGRAM

The noncoherent rapid sequencing concept is key to employing a noncritical VCO, as well as a 10^{-7} clock oscillator, since accurate carrier frequency memory is not required.

The baseband data processing is handled by the microprocessor. This includes much of the bit sync function, frame sync, and data storage. Some of the code and carrier loop functions might also be performed in the processor; however these are considered to be analog functions pending further investigation.

A more detailed discussion of receiver elements is presented next.

A.1.1 L-band Antenna

The L-band antenna is a right hand circularly polarized conical spiral. The antenna has hemispherical coverage with 0 dBIC gain or higher at all elevation angles above 5°. A typical antenna pattern is shown in Figure A-2.

A.1.2 L-band Preamp

The LCR uses an inexpensive preamp with stripline bandpass filtering as shown in Figure A-3. The amplifier gives approximately 24 dB of gain with an overall noise figure of less than 4 dB.

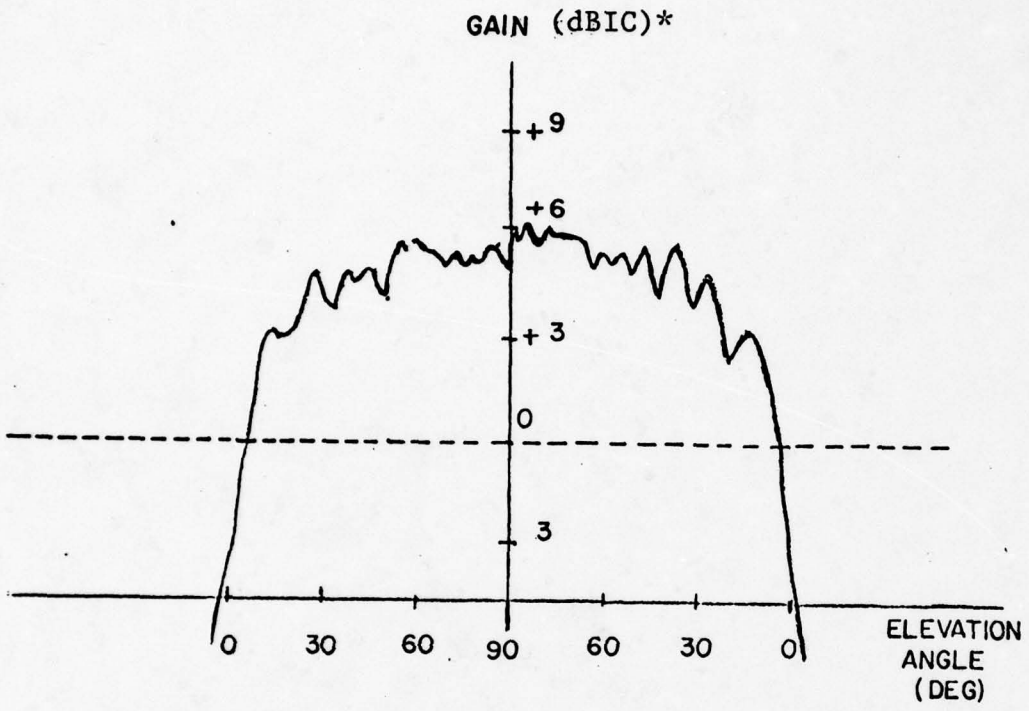

* 7 ft x 12 ft Ground Plane

L_1 = 1575.42 MHz

FIGURE A-2

HEMISPHERICAL COVERAGE ANTENNA PATTERN AT L_1 [7]
(ALL AZIMUTHS)

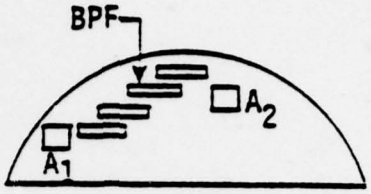

24 dB AMP/FILTER
NF ~ 3 TO 4 dB

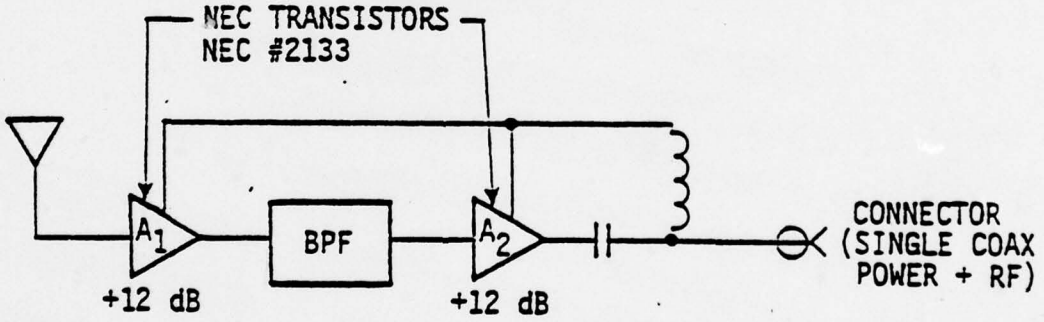

FIGURE A-3

L-BAND PREAMPLIFIER

A.1.3 Down Converter and IF Amplifier

The down converter and IF amplifier are configured with the following features:

- Only one rf multiplier
- Single conversion with 71.61 MHz IF
- No critical filters.

A block diagram of the down converter and IF amplifier is shown in Figure A-4.

The L_1 signal at 1540 F' (1575.42 MHz) is downconverted to 70F' using a reference at 1470 F' generated by a single X21 phase-locked multiplier (PLM). The carrier loop VCXO operates at 70F' and can be used to demodulate the IF signal without further conversions. Some leakage of the VCXO signal into the low-level IF amplifier may be experienced, however, multiplication of the IF signal by the C/A code will provide 20 to 25 dB of additional isolation. Details of the PLM are shown in Figure A-5. The 71.61 MHz spacing of the comb generator lines is sufficiently wide to permit the use of an inexpensive UHF oscillator with relatively poor stability (better than 4×10^{-2}).

Note that the bandpass filters are simple L-C elements with the primary function of eliminating undesired conversion products. The correlation filter is implemented at baseband, thus eliminating a critical crystal filter.

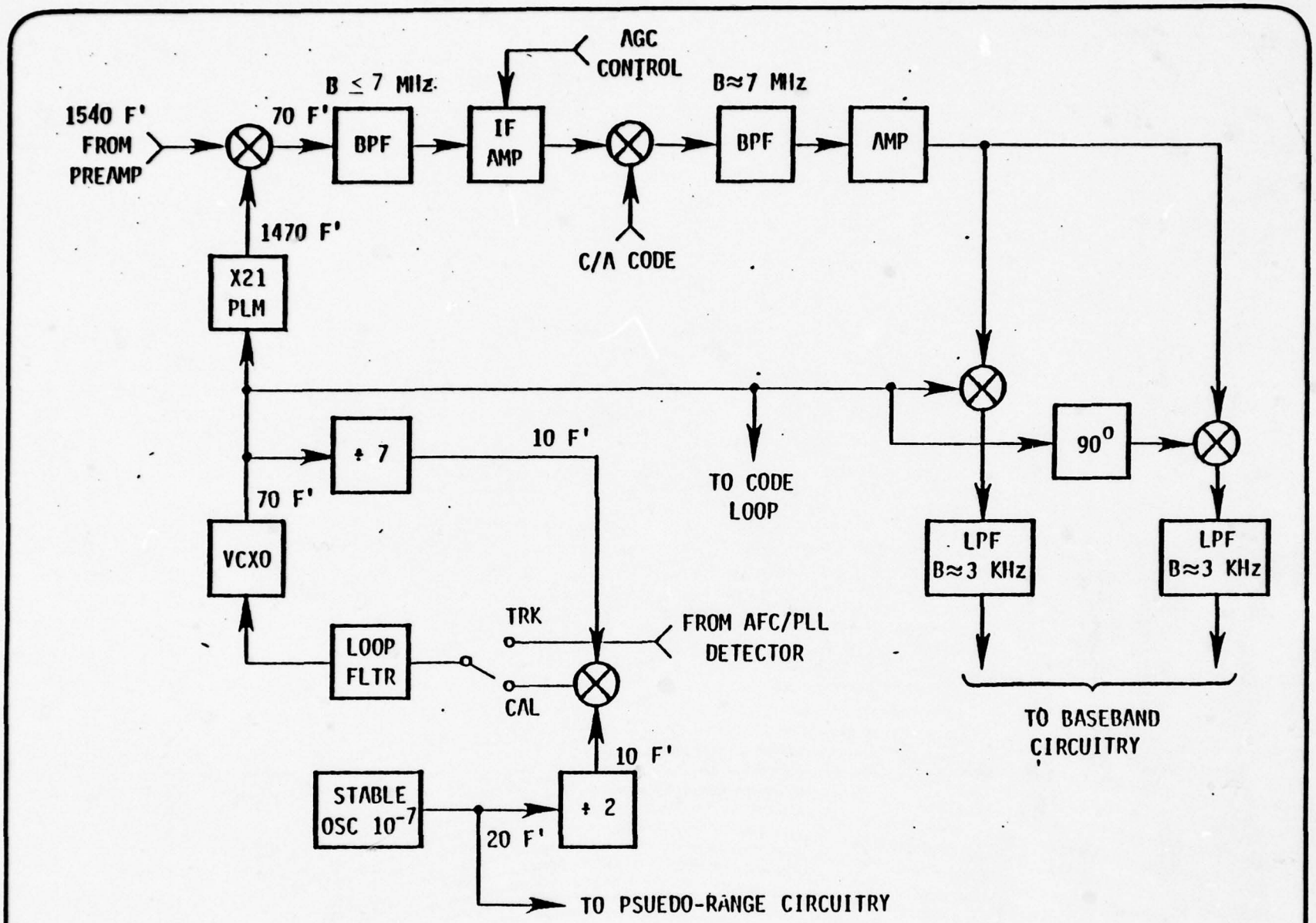

FIGURE A-4

DOWN CONVERTER AND IF AMPLIFIER

STANFORD TELECOMMUNICATIONS INC.

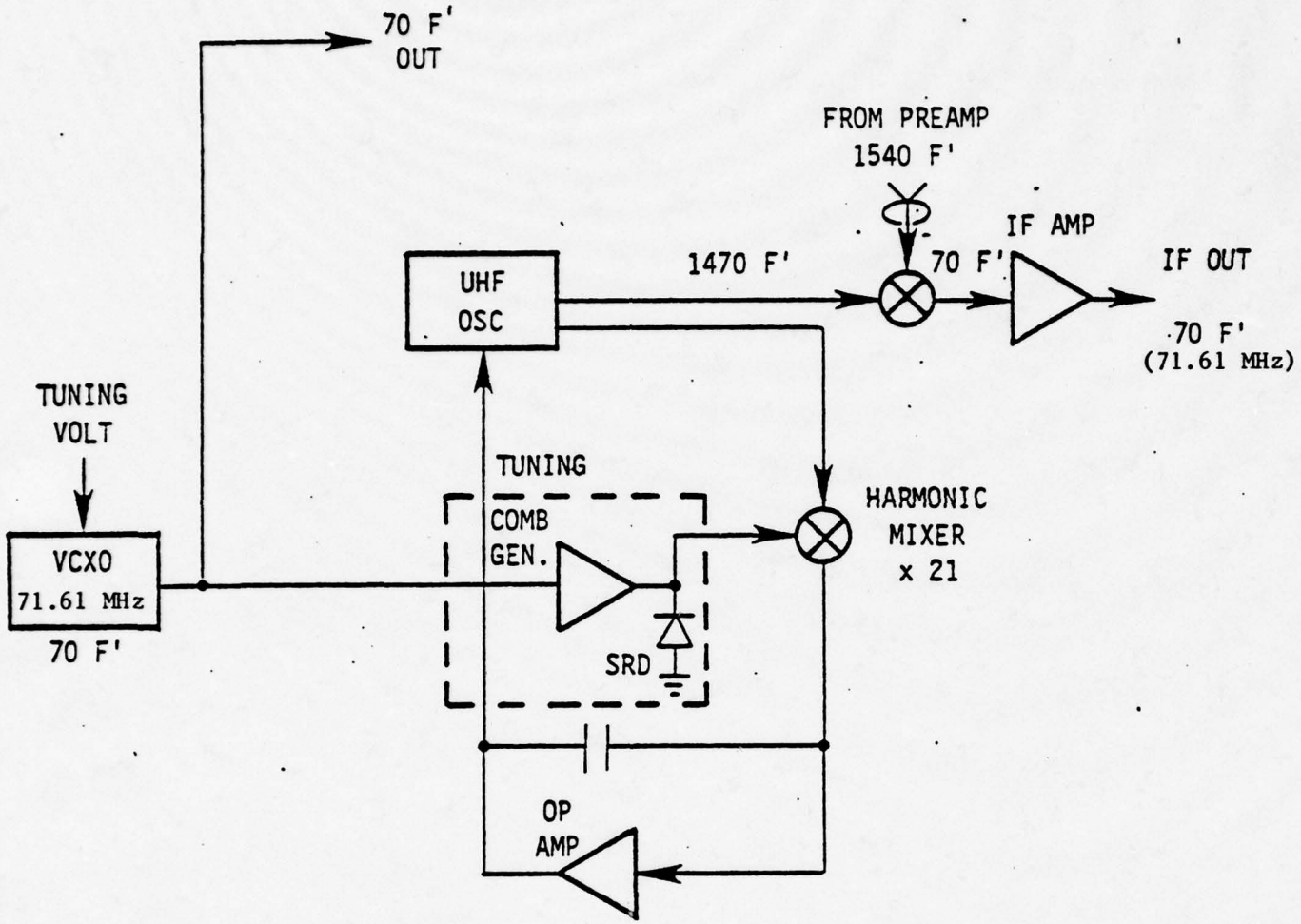

FIGURE A-5

PLM/MIXER ASSEMBLY

STANFORD TELECOMMUNICATIONS INC.

The VCXO is automatically calibrated from the stable oscillator before signal acquisition. The VCXO phase noise can be troublesome in this type of design, since the VCXO output is multiplied by twenty one. This phase noise can cause excessive jitter in a narrow carrier loop and represents a design risk area. However, the carrier loop is sufficiently wide in the proposed design that phase noise should not be a limiting factor even with a relatively inexpensive VCXO.

A.1.4 Code and Carrier Tracking

A functional block diagram of the code and carrier loops is shown in Figure A-6. The loops are interdependent since they share a common correlator and the carrier loop provides a code frequency estimate to the code loop.

The carrier loop operates in either an AFC or PLL configuration. The AFC is used for both initial acquisition and ranging (NAV mode) and can acquire over the full $\pm$ 3KHz correlation bandwidth. A long-loop configuration is used in order to preserve code/carrier coherence. A more detailed block diagram of the code and carrier loops is shown in Figure A-7. The code loop is described below and the carrier loop is described in Sec. A.1.4.2.

A.1.4.1 Code Tracking Loop

The code loop is basically a noncoherent τ-dither loop with a single correlator. Its function is to correct the phase of the code clock and thus eliminate the need for a VCO in the code

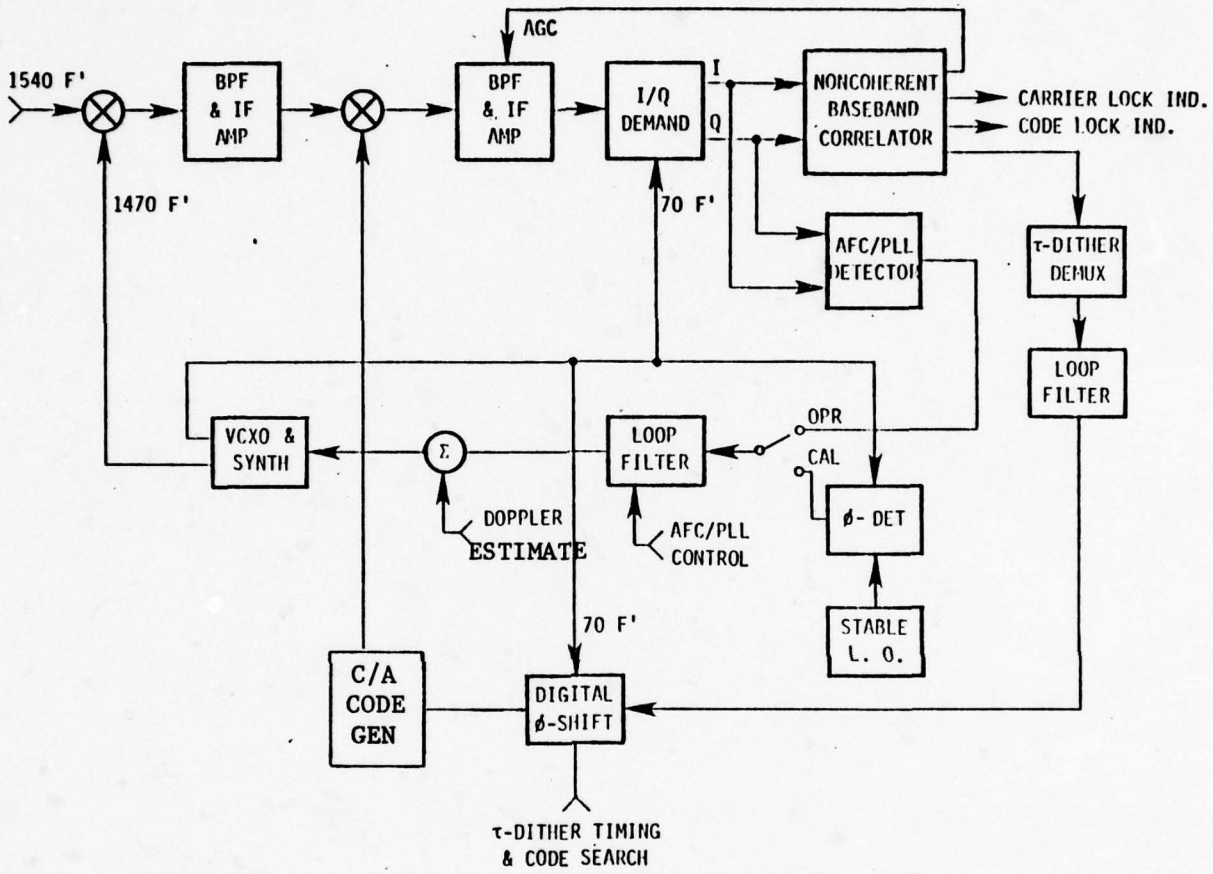

FIGURE A-6

CODE AND CARRIER TRACKING LOOPS

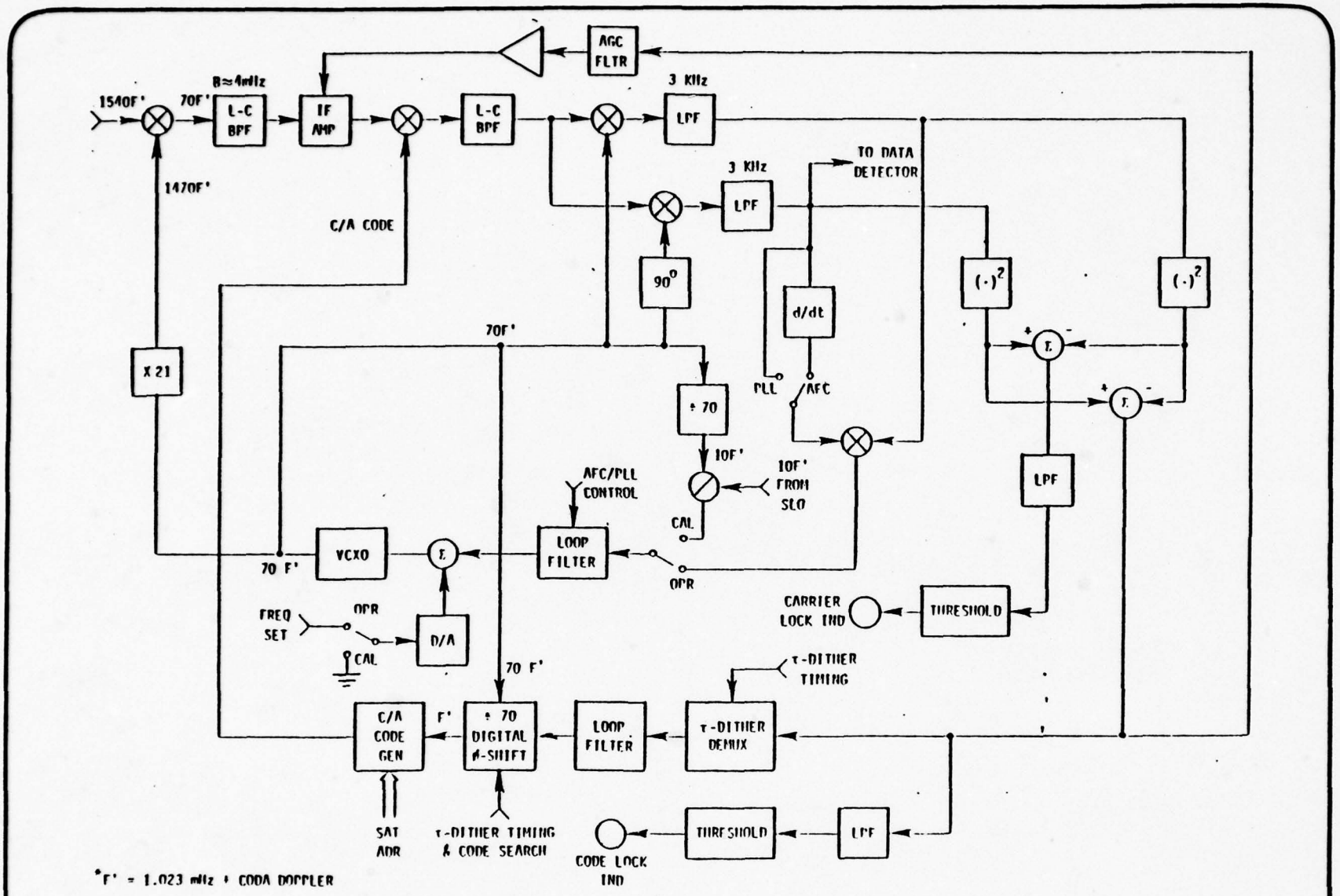

FIGURE A-7

CODE AND CARRIER LOOPS

STANFORD TELECOMMUNICATIONS INC.

loop. The correlator is implemented at baseband, thus eliminating a crystal filter at IF.

The correlated signal is held within the correlator band-pass by the carrier tracking loop. A carrier frequency estimate is derived from the carrier loop. The code clock, derived from this estimate is maintained in proper phase by the code loop. Its operation is described in conjunction with Figure A-7.

The incoming signal is mixed with the multiplied VCXO output to produce an IF signal at 71.61 MHz. The amplified IF signal is multiplied by the C/A code for despreading. The collapsed signal is then downconverted to baseband I-Q channels and passed through R-C low-pass correlation filters with a 3KHz low pass bandwidth. A voltage proportional to power in the correlation bandwidth is derived by summing the squares of the I and Q signals. The correlator reference code is dithered $\pm$ 0.3 chips in order to form a loop error signal. The resultant discriminator characteristic is shown in Figure A-8. The use of a single correlator causes some loss in recovered carrier power due to the reference code jitter.

The correlator carrier output power, normalized to total carrier power, is plotted in Figure A-8 versus code offset. The correlation curve is somewhat different than that usually observed. There is a 3dB loss for zero offset, however the recovered power actually increases for offsets up to 30% of a chip. Thus the despread signal power is not sensitive to code loop jitter as in the conventional implementation.

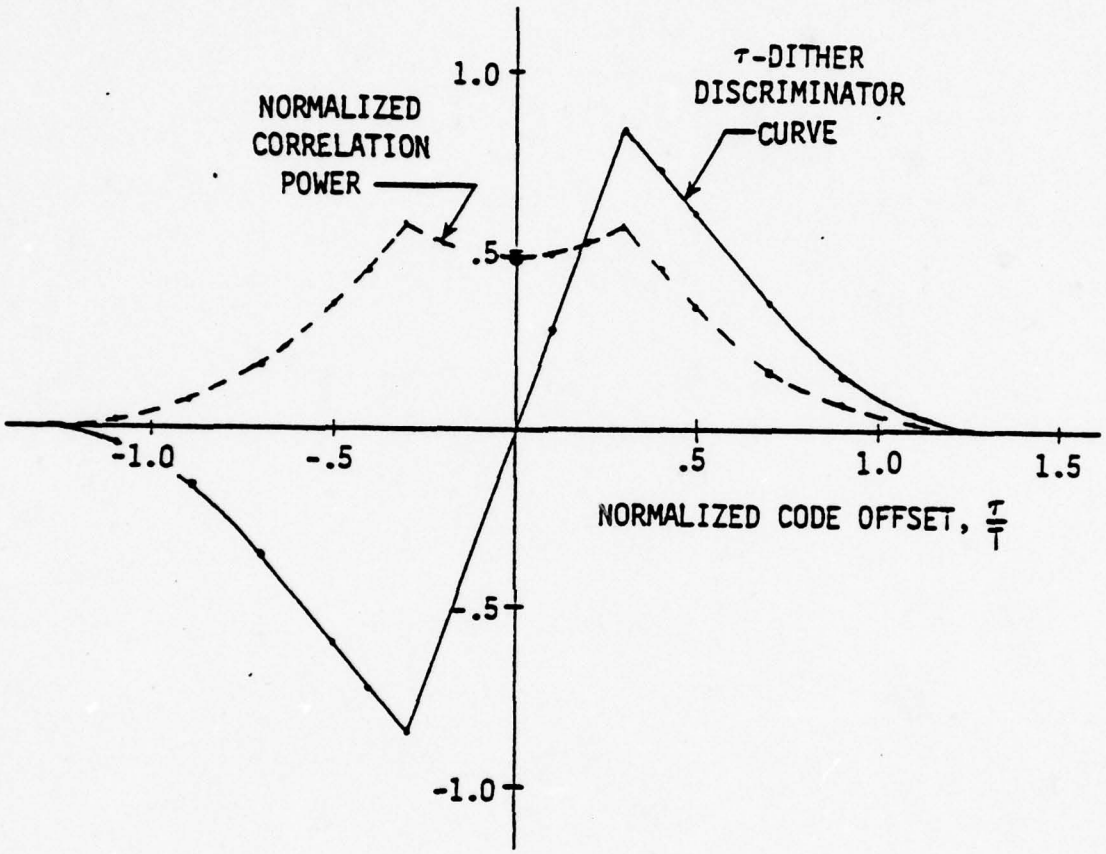

FIGURE A-8

τ-DITHER DISCRIMINATOR AND CORRELATION CURVE

One possible version of the code clock digital phase shifter is shown in Figure A-9. This is essentially a divide-by-70 counter which can be "lengthened" or "shortened" by one count, thus providing a phase shift of one-seventh of a code clock period. The counter also generates the advanced and delayed clocks for τ-dither operation.

A code tracking loop bandwidth of 55 Hz is recommended. The code loop parameters are summarized in Table A-1.

A.1.4.1.1 Code Acquisition

Initial code acquisition is performed as follows. The carrier VCXO is set to within $\pm$ 3 KHz of the incoming carrier frequency, which provides a code frequency estimate accurate to better than $\pm$ 2 Hz. The code loop is disabled and the code stepped in phase at a rate of 150 chips/sec until code presence is detected by the code lock detector. The loop is then closed and code tracking begins.

A.1.4.1.2 Code Loop Sequencing

The code loop is sequenced between satellites in the NAV mode with a dwell time of 200 ms per satellite. The code state number is stored at the end of each dwell period and is used to estimate the code state at the beginning of the dwell period when the receiver next returns to that satellite. This operation is implemented as shown in the block diagram of Figure A-10. Operation may be described briefly as follows. Each

TABLE A-1

CODE LOOP PARAMETERS

. SEARCH RATE	150 CHIPS/SEC
CORRELATION BANDWIDTH	6 KHz
CODE TRACKING LOOP BANDWIDTH (B_L)	55 Hz
τ-DITHER SPACING	$\pm$ .3 CHIPS
τ-DITHER RATE	1 kHz

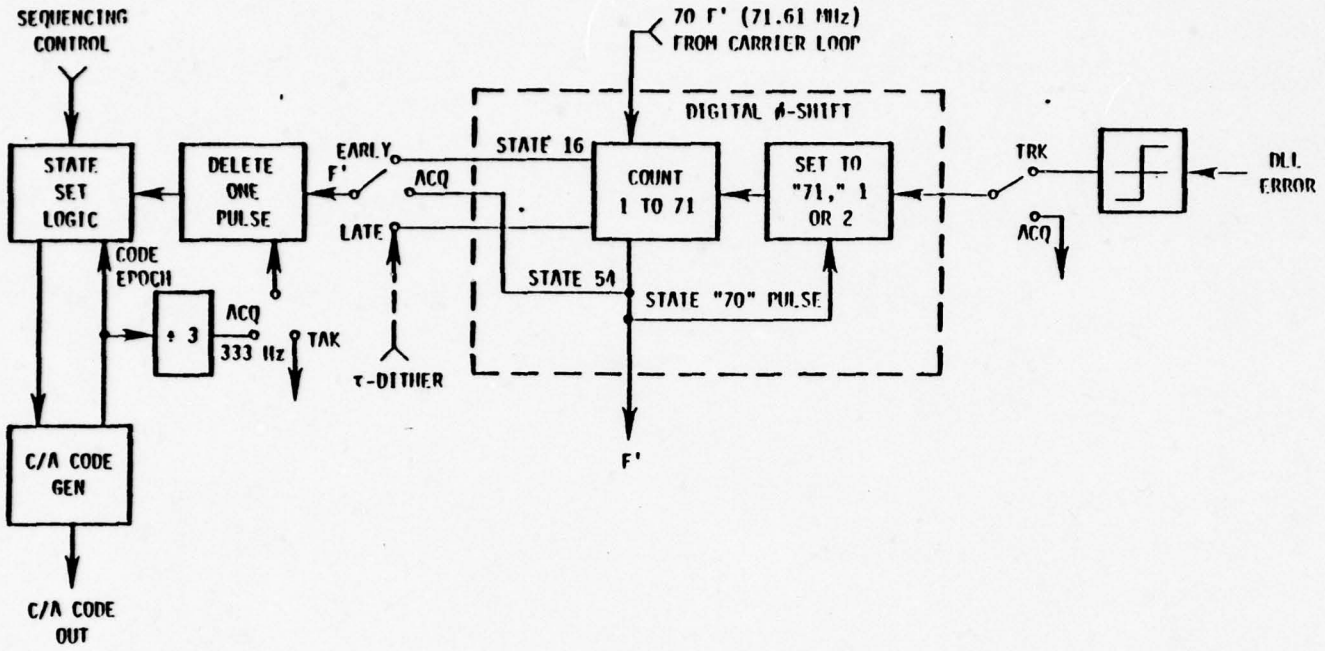

FIGURE A-9

CODE CLOCK PHASE-SHIFTER

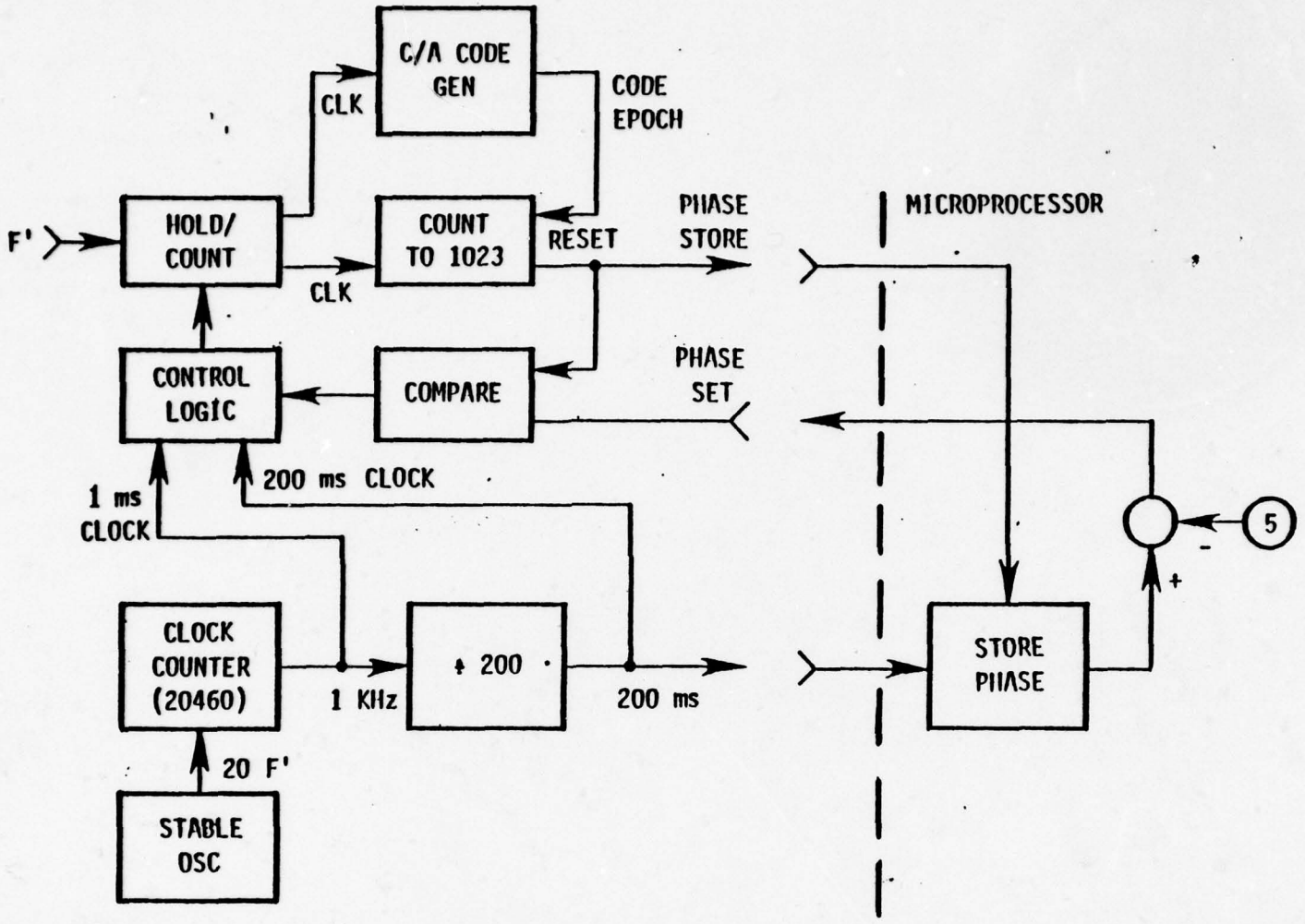

FIGURE A-10

CODE PHASE STORE

of the C/A code states is numbered from code epoch with a 1023 counter which is sampled at the end of the satellite dwell period. The stored code state is correct for any dwell time which is an integer multiple of 1 ms (the code period) except for differences between the received code clock and the stable oscillator due to doppler and drift.

Let us assume that the receiver is tracking five satellites and will return to the same satellite after 800 ms as measured with the receiver stable oscillator. The stored code position will be within 3 chips of the received code position for a given satellite including the effects of clock error, user doppler, and satellite doppler. The receiver code generation is therefore set 3 states early and a limited code search started over a 6 chip range when reacquiring a satellite. Note that code generator state setting is greatly facilitated by using code state numbers as opposed to storing the actual code state. A maximum of 1 ms is required to set the code generator to any code state.

An intermediate search range of $\pm$ 15 chips is used in the transition from the DATA to NAV modes as discussed in Section A.2.2.

A.1.4.2 Carrier Tracking Loop

The carrier tracking loop operates in either an AFC or Costas PLL configuration, depending on the receiver mode. Functional block diagrams of the carrier and code loops are shown in Figures A-6 and A-7. A simplified diagram is shown in Figure A-11 for illustrative purposes.

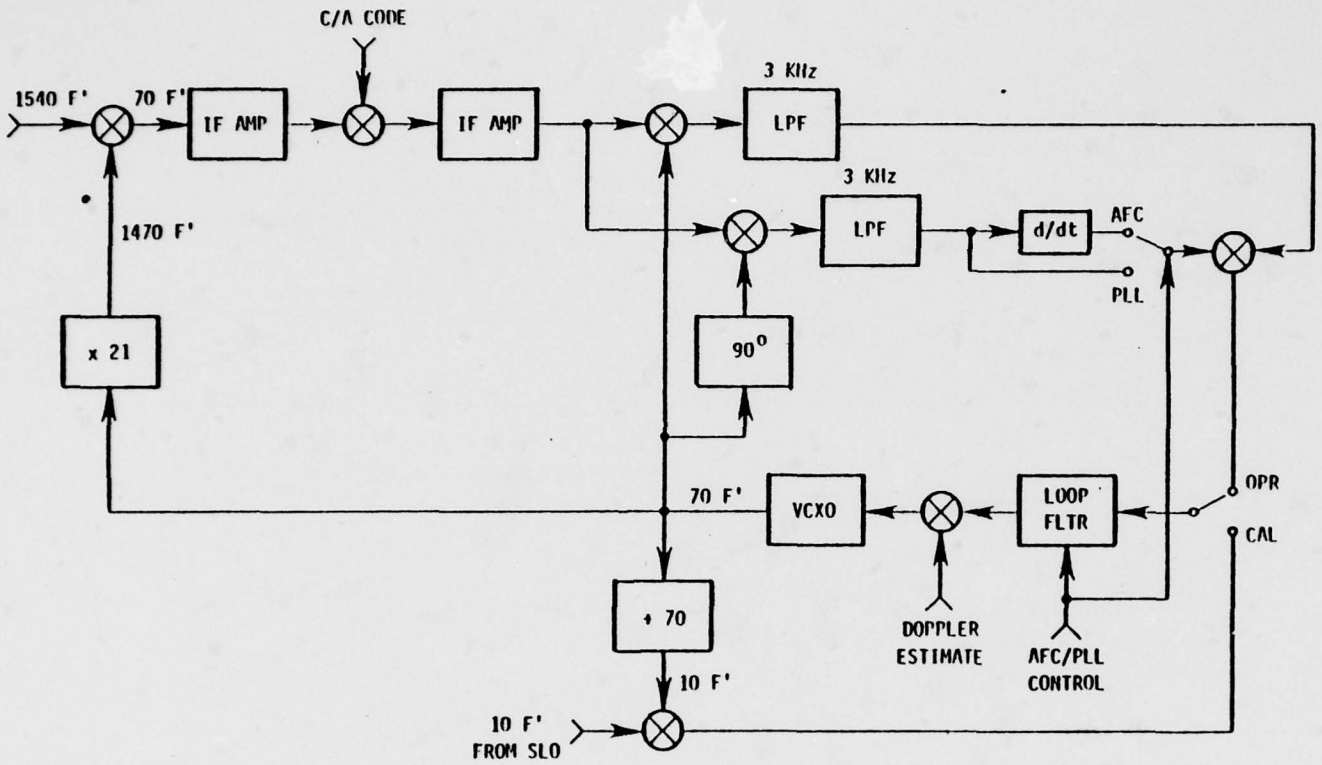

FIGURE A-11

CARRIER TRACKING LOOP

A "long loop" is employed which is coherent with the incoming signal at L-Band thus preserving carrier/code coherence. The first IF is normally 70 F' (71.61 MHz). The IF signal is multiplied directly by the C/A code after some amplification.

Note that leakage into the low level IF from the VCXO is spread by the C/A code, thus providing 20 to 25 dB of isolation. The despread IF signal is demodulated to baseband with I and Q mixers and passed through baseband correlation filters. Performing correlation filtering at baseband eliminates the need for a crystal filter at IF which represents a critical component. Further, double conversion is generally required when a crystal filter is employed, due to center frequency limitations.

The I-Q outputs are used to develop either a frequency or phase error voltage, depending on whether AFC or PLL operation is desired.

A block diagram of the loop filter is shown in Figure A-12. The filter has a transfer function of

$$F_{AFC}(s) = \frac{ka}{s}$$

$$F_{PLL}(s) = \frac{k\,(s + a)}{s}$$

This produces a first order AFC loop (which will track a constant doppler offset with no error) and a second order PLL. Loop bandwidths of

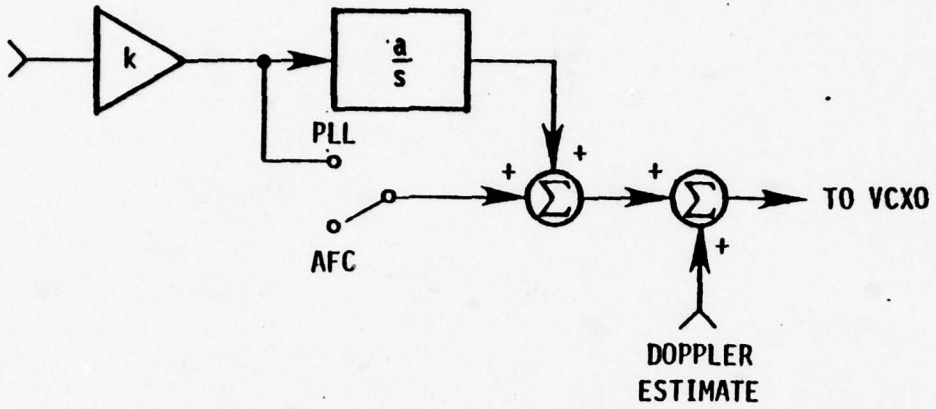

FIGURE A-12

CARRIER TRACKING LOOP FILTER

$$B_L(AFC) = 5 \text{ Hz}$$

and

$$B_L(COSTAS) = 120 \text{ Hz}$$

are recommended. The carrier loop parameters are summarized in Table A-2.

A.1.4.2.1 Carrier Acquisition

The carrier loop has a tracking range of $\pm$ 6 kHz which is sufficient to accommodate satellite doppler, user doppler, user oscillator drift, etc.

In order to acquire the carrier, the VCXO must be set to within $\pm$ 3 kHz of the received carrier frequency. This is accomplished by first locking the VCXO to the receiver standard at 10 F' for calibration purposes. The reference frequency is thus set to within 160 Hz (assuming 10^{-7} overall accuracy of the standard). The loop filter integrator stores the proper voltage to hold the VCXO at this frequency. A satellite doppler estimate accurate to $\pm$ 1 kHz is then added to the loop filter output to preset the VCXO (see Figure A-12) such that the received signal is within the correlation bandwidth of $\pm$ 3 kHz. The VCXO preset error contributions are summarized in Table A-3 and total a maximum of less than $\pm$ 2 kHz. This offset is acquired in the AFC mode which has a pull in range of $\pm$ 3 kHz. The loop may be switched into the Costas PLL configuration after AFC pull-in when phase-locked

TABLE A-2

CARRIER LOOP PARAMETERS

Acquisition Range	± 3 kHz
Tracking Range	± 6 kHz
B_L (COSTAS)	120 Hz
B_L (AFC)	5 Hz

TABLE A-3

VCXO PRESET ACCURACY

SAT Doppler Est	± 500 Hz
SAT Osc. Drift	< 1 Hz
User Doppler	± 500 Hz
User Osc Calibration (10^{-7})	± 158 Hz
VCXO Preset Accuracy	± 600 Hz
Total	± 1758 Hz

operation is required (for data demodulation).

A.1.4.2.2 Carrier Loop Sequencing

Satellite sequencing is performed in the NAV mode to obtain pseudo-range measurements. No data is taken in this mode of operation so the carrier loop operates in the AFC configuration only. A frequency memory is incorporated to reset the carrier frequency each time the loop returns to a particular satellite. This can be implemented as a simple analog sample and-hold with a demultiplexed output since a storage time of less than one second is required between updates.

A.1.5 Data Detection

The received data plus noise is available at the I channel output of the Costas loop. This is detected by the data detection filter in conjunction with the bit synchronizer of Figure A-13. Subframe sync is then accomplished as discussed below in the processor.

A.1.5.1 Bit Synchronization

The C/A code epochs which occur every 1 ms are synchronized with the data transitions. The process of bit synchronization is one of correctly resolving which of the 20 code epochs occuring within a data bit coincides with the data bit transition. A block diagram of the bit synchronizer is shown in Figure A-13. The noisy data stream is passed through a data detection filter

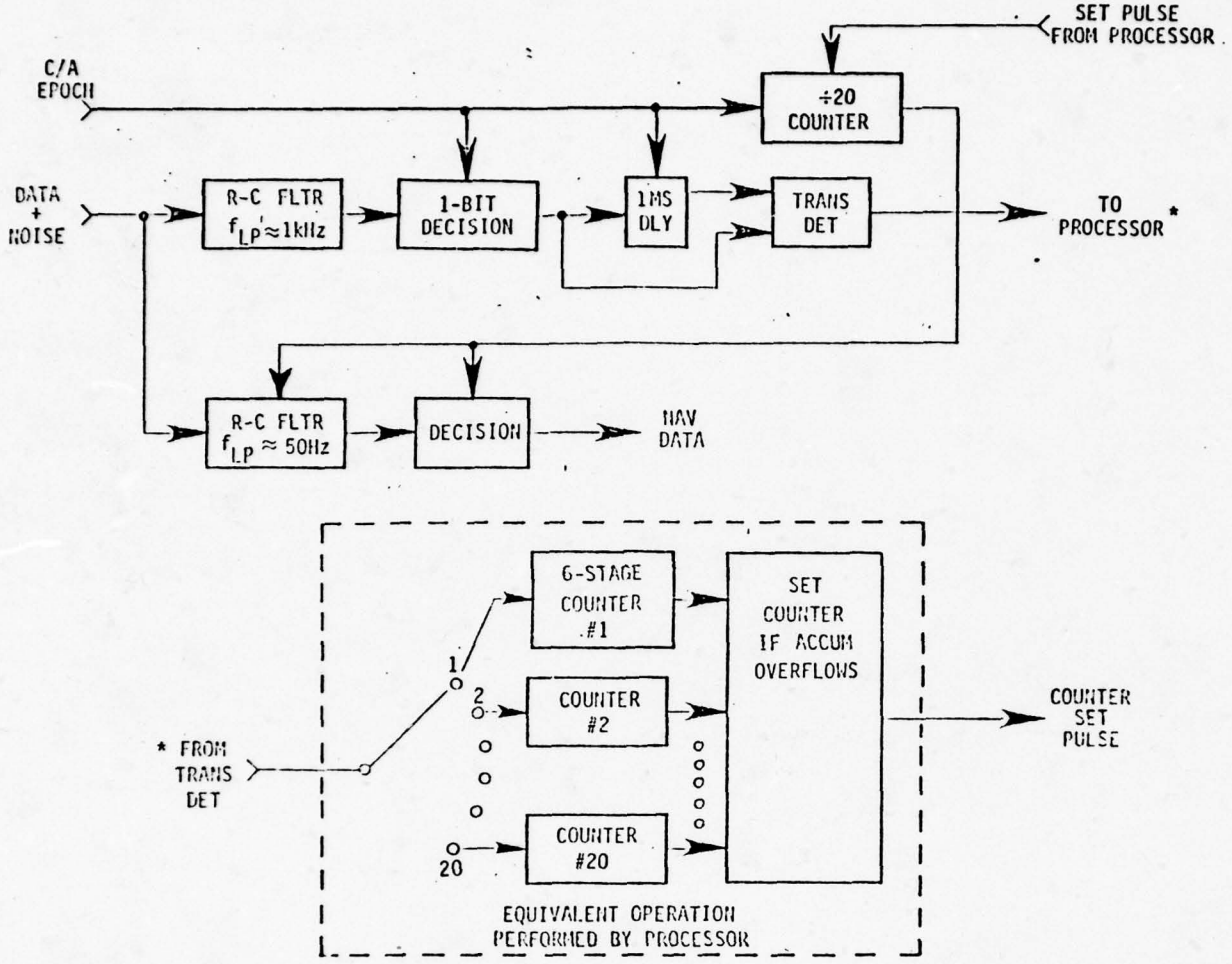

FIGURE A-13

BIT SYNCHRONIZER

and the output sampled every 1 ms. The output of the filter is checked for transitions, and the transitions counted at each of the 20 possible epoch phase positions. The first phase position to indicate 2^6 transitions, where 6 is the number of counter stages, is declared the proper sync position.

A.1.5.2 Subframe Sync

Subframe synchronization is achieved by recognition of an 8-bit preamble in the satellite NAV DATA stream. These data are acquired at a very low error rate due to the high SNR.

$$E_b/N_o \simeq 20 \text{ dB at } C/N_o = 37 \text{ dB-Hz}$$

Therefore the probability of missing the correct subframe sync word is small.

To avoid false subframe sync, it is required that the sync word appear in the proper place in two consecutive subframes and that the 4 least significant bits of the handover word (HOW) increment by 1 from the first subframe to the next before subframe sync is declared. During HOW increment check, ambiguity resulting from data inversion can be eliminated by re-inverting the data whenever an inverted preamble pattern is detected. The 90% time to acquire and check subframe sync is estimated to be 20 seconds.

A.1.6 System Time

System time is kept in the LCR primarily for use in the various navigation subroutines which compute satellite position, satellite clock error, etc. The receiver clock operates with 1 ms increments in the GPS time-of-week format and is implemented either partially or totally in the microprocessor. A simplefied block diagram of the time keeping operation is shown in Figure A-14.

The clock is set with the HOW at a six second subframe epoch, while the receiver is in the DATA mode. The clock correction for signal propagation time and satellite clock offset is then readily computed to within $\pm$ 1 ms assuming an operator user position estimate accurate to $\pm$ 150 nmi. A clock error of $\pm$ 1 ms represents a maximum computed satellite in-track position error of approximately $\pm$ 4 ft, which is more than adequate for present purposes. The clock correction is of course readily refined to accuracy on the order of 100 ns in the NAV mode.

A.1.7 Psuedo-Ranging

To obtain psuedo-range data in the NAV mode, the time-of-arrival of each satellite signal is measured with respect to the internal standard. This is accomplished as shown in Figure A-15. The time-of-arrival is measured relative to a 20.46 MHz (20 F') counter with a 1 ms period, driven by the receiver stable oscillator. The received code state number is multiplied by 20 and subtracted from the counter number to yield a psuedo-range with an approximate

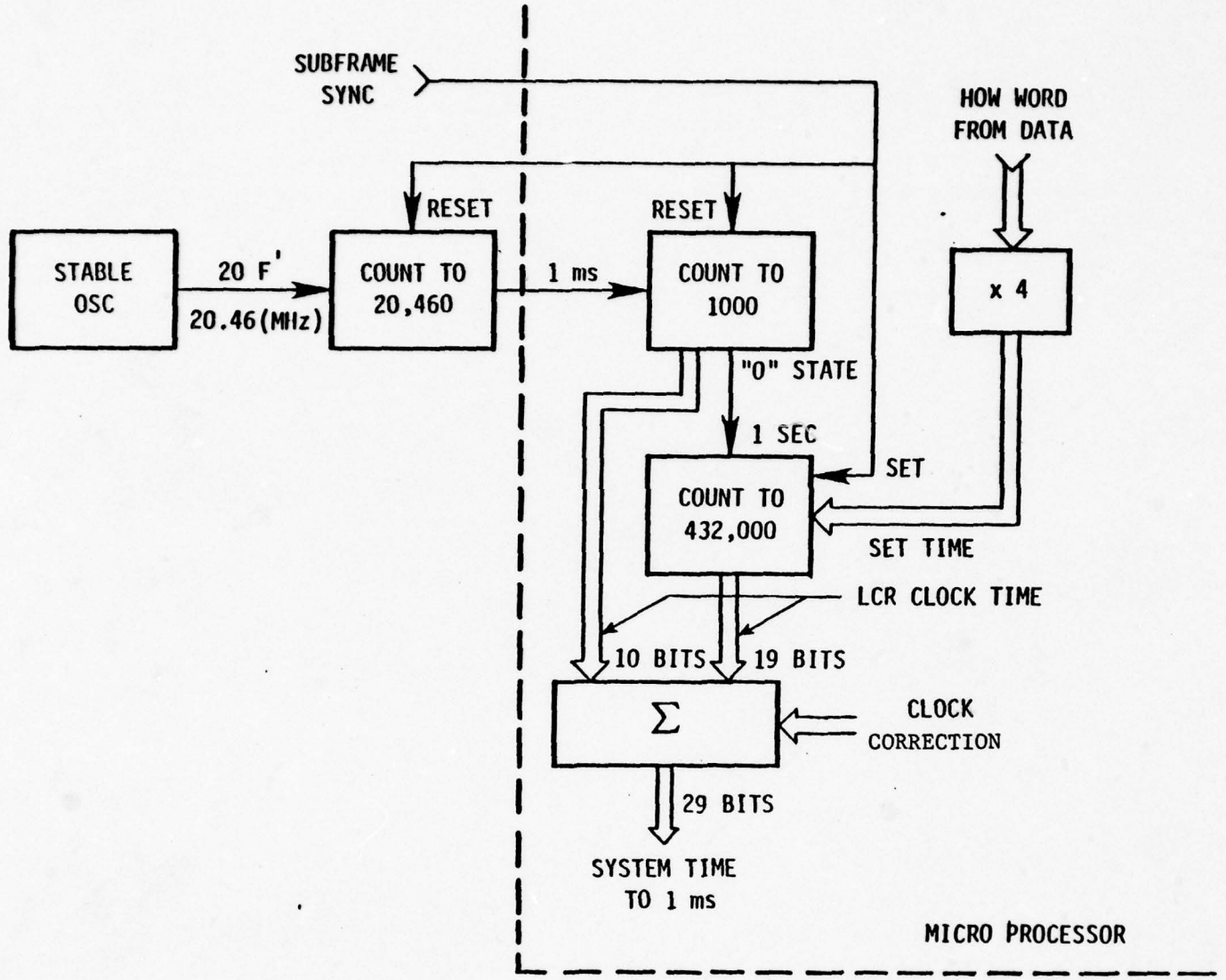

FIGURE A-14 SIMPLIFIED FUNCTIONAL DIAGRAM OF RECEIVER CLOCK

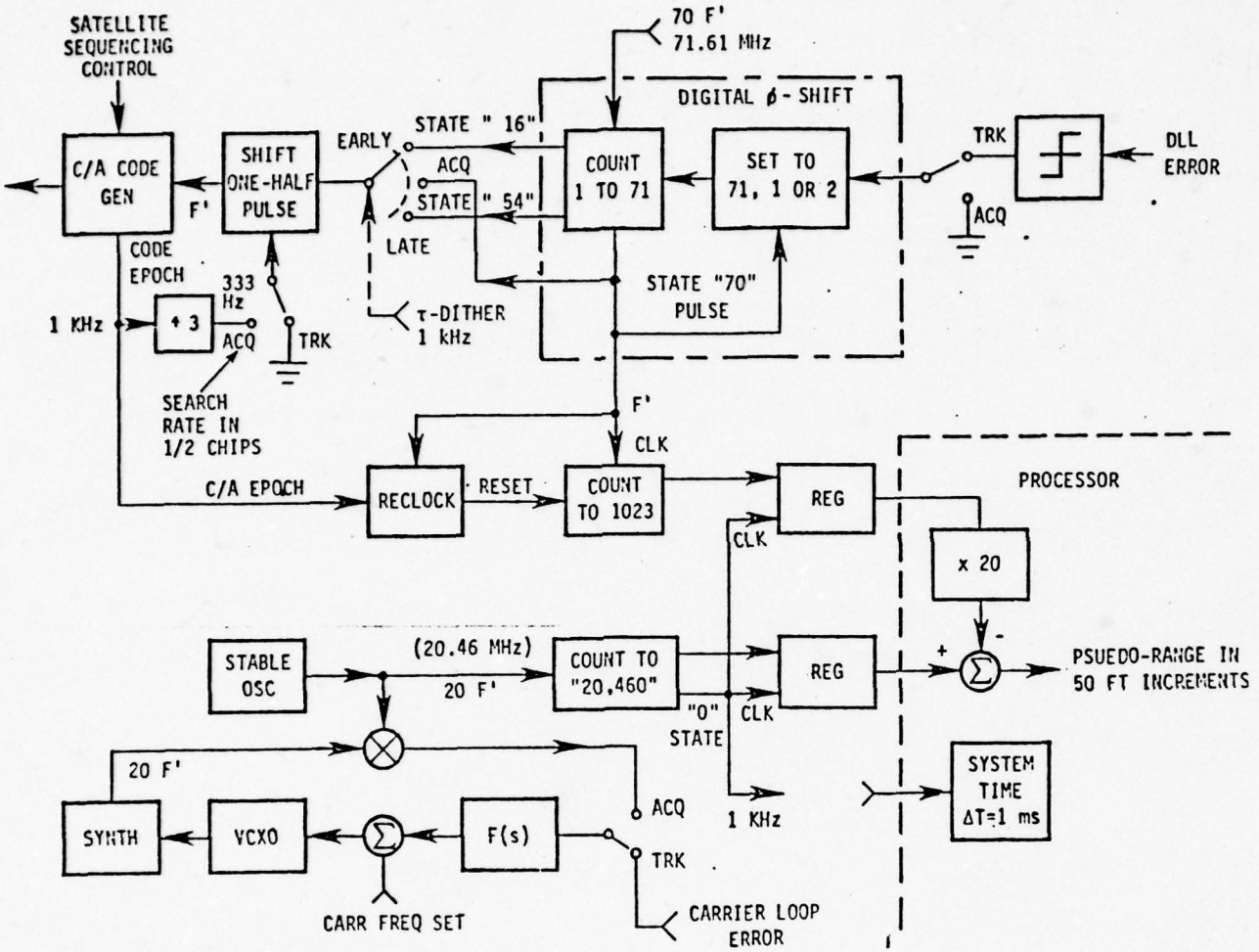

FIGURE A-15

SYSTEM TIME & RANGE MEASUREMENT

resolution of ± 50 ft.

A.1.8 Microprocessor

The LCR microprocessor is required to perform GPS navigation software functions and certain receiver functions as noted in Table A-4 and discussed above.

TABLE A-4

MICROPROCESSOR FUNCTIONS

- RECEIVER HARDWARE SUPPORT
  - SATELLITE SELECTION
  - SIGNAL CODE PHASE STORAGE & ESTIMATION (CODE SLIP)
  - CARRIER FREQUENCY STORAGE & ESTIMATION (DOPPLER PREDICTION)
  - BIT & FRAME SYNCHRONIZATION FOR DATA
  - CONTROL FUNCTIONS (AFC/PLL, SEARCH/TRACK)

- NAVIGATION COMPUTATIONS
  - SATELLITE EPHEMERIS UPDATE
  - NAV POSITIONING & TRACKING
    (POSITION & VELOCITY; CLOCK UPDATE)
  - DISPLAY DATA FORMATTING
    (DISTANCE-TO-GO & CROSS-TRACK DEVIATION;
    LATITUDE & LONGITUDE, ETC.)

A.2 RECEIVER OPERATION

Receiver operation is assumed to commence with the operator providing an approximate position (± 50 nmi. accuracy) and approximate system time (± 15 min accuracy). It is further assumed that almanac data is available in nonvolatile memory for satellite selection and acquisition, although such almanac data could also be an input. A typical time-line diagram of receiver operation is shown in Figure A-16. The receiver initially acquires and gathers data from up to five satellites chosen by the satellite selection subroutine. The receiver then switches to the NAV mode in which it continuously sequences over the selected satellites with a dwell time of 200 ms per satellite. A complete position and clock update would occur at a rate of once per second.

The NAV mode is occasionally interrupted for short intervals (1-5 min, every 0.5-2 hours) to re-enter the DATA mode. These interruptions are for the purpose of updating satellite data and/or changing satellites when required. The time of interruption, should not occur during a period critical to the user, such as during a landing approach. One possible means for interruption is to alert the operator of the need for new data by a light or alphanumeric display on the front panel. The operator can then push a button to initiate the interruption at his convenience.

A.2.1 Data Gathering (DATA Mode)

The various steps in the initial turn-on and data gathering phase of receiver operation are given in Table A-5.

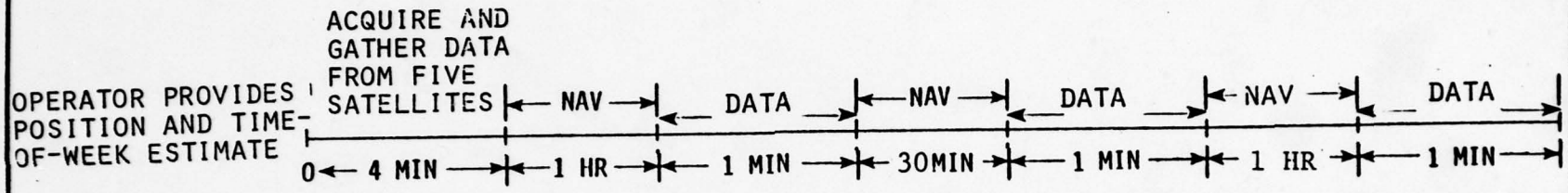

FIGURE A-16

TIME SEQUENCE OF RECEIVER OPERATION

TABLE A-5

OPERATING SEQUENCE FOR INITIAL DATA GATHERING

- INPUT APPROXIMATE POSITION AND TIME-OF-WEEK.
- ALMANAC ALGORITHM SELECTS SATELLITE CONFIGURATION, INPUTS PROPER SATELLITE ADDRESSES AND DOPPLER ESTIMATES.
- ACQUIRE EACH SATELLITE AND STORE DATA

  1) ACQUIRE C/A CODE (< 6.8 SEC WITH P = .9)
  2) ACQUIRE CARRIER FREQUENCY (<.2 SEC)
  3) ACQUIRE CARRIER PHASE (<.2 SEC)
  4) PERFORM BIT SYNC (< 5 SEC)
  5) PERFORM SUBFRAME SYNC AND CHECK (<20 SEC)
  6) STORE DATA (30 SEC)

- REACQUIRE SELECTED C/A CODES FOR SEQUENCING OPERATION

The almanac selects the satellite algorithm and indicates the proper satellite address and doppler to the C/A code generator and carrier loop VCXO respectively. The LCR then acquires the code, carrier, bit sync, frame sync and gathers data from each satellite in sequence. Details of the time required for each step of the acquisition process are given in Table A-6.

A.2.2 Satellite Sequencing for Psuedo-Ranging (NAV Mode)

The LCR sequences over the satellites of the chosen configuration with a dwell time of 200 ms per satellite. The relatively high sequencing rate is important in that it allows the use of a master oscillator with fairly low stability requirements. For example, consider that an oscillator with a normalized offset of 10^{-7} in its nominal center frequency would have a time drift of 100 ns/sec. Thus a maximum relative error of 80 ft. would occur in psuedo-ranges measured during the 800 ms required to sequence over four other satellites. Some of this systematic error can be removed by the NAV software.

In order to operate with a 200 ms dwell time, it is important to be able to reacquire the C/A code in a time much less than the dwell time. The receiver operates in the noncoherent mode during satellite sequencing and the AFC loop is updated during each dwell period as illustrated in Figure A-17. Code phase is stored to aid in reacquisition.

TABLE A-6

INITIAL ACQUISITION TIMES

ITEM		ACQ. TIME (WITH P_{ACQ} 90%)
C/A CODE SEARCH (MAX.)		6.8 SEC
FA CHECK		.2 SEC
CODE LOOP SETTLING		.02 SEC
AFC SETTLING		.15 SEC
PLL SETTLING		.2 SEC
BIT SYNC (MAX)		5.0 SEC
SUBFRAME SYNC (MAX)		20.0 SEC
	T_{ACQ}	32.4 SEC
RECEIVE FRAME OF DATA		30 SEC
	TOTAL	62.4 SEC

APPROXIMATELY 1 MIN. REQUIRED TO ACQUIRE AND COLLECT DATA FOR EACH SATELLITE.

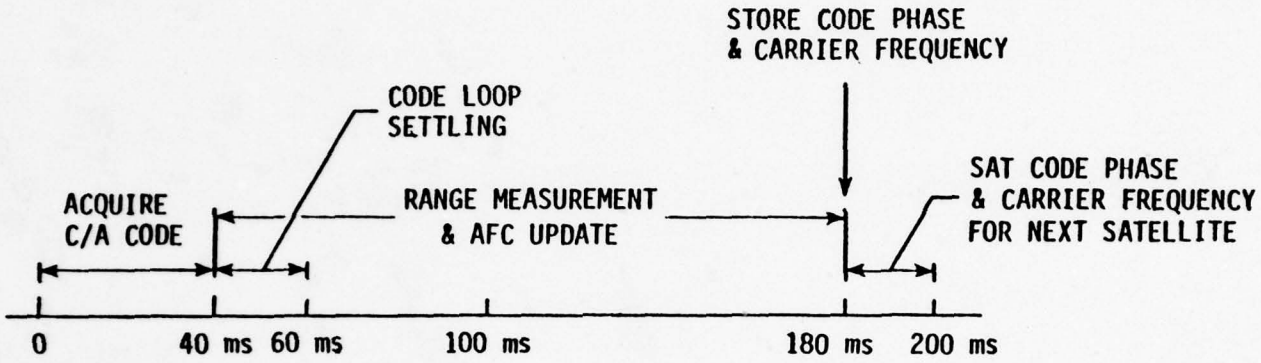

FIGURE A-17

SATELLITE SEQUENCE OPERATIONS

The transition from the Data mode to the NAV mode requires a transition region in which the search range for code acquisition is narrowed from a full code period to a 6 chip range. The codes are reacquired and the code phase uncertainty is reduced through intermediate search windows of 200 chips and 40 chips as discussed in Section A.3.9 and illustrated in Figure A-18 for a four satellite sequencing situation.

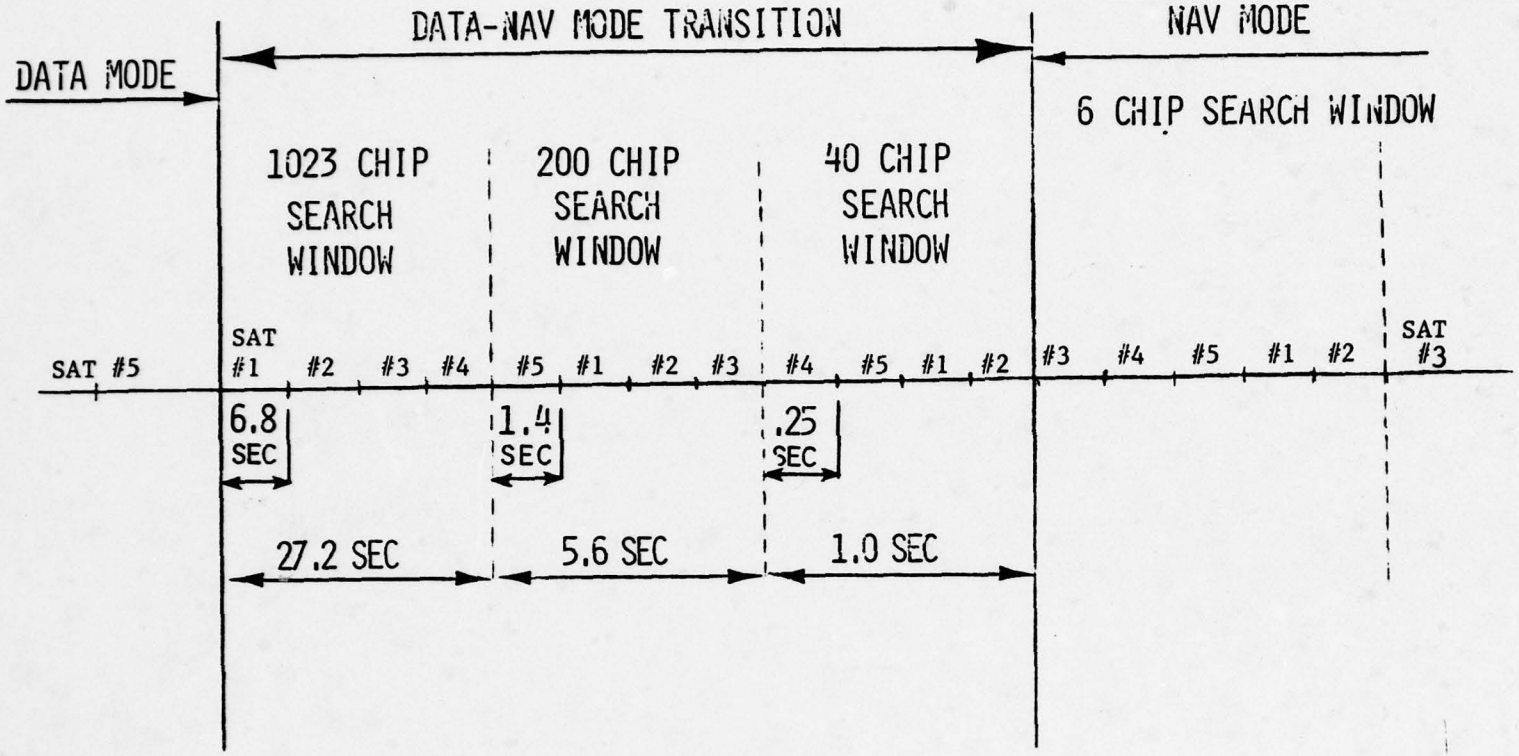

FIGURE A-18

DATA-NAV MODE TRANSITION

A.3 PARAMETER SELECTION AND PERFORMANCE ESTIMATES

This section presents a preliminary analysis to show concept feasibility and select the LCR parameters. A summary of the results is given in Table A-7.

A.3.1 IF Bandwidth

The effective IF bandwidth after correlation is twice the bandwidth of the low pass filters in the Costas loop. It is desirable to choose this bandwidth mode wide enough such that initial acquisition can be performed without a frequency sweep. The anticipated carrier frequency uncertainties are summarized in Table A-8 and have a maximum value of $\pm$ 1758 Hz. Thus a low pass filter with a noise bandwidth of $\pm$ 3 kHz, i.e. an effective IF bandwidth of

$$B_I = 6 \text{ kHz}$$

has been selected for design purposes.

A.3.2 Code Acquisition

The received C/A code is searched by stepping the LCR reference code in one-half chip increments. A noncoherent detector is used to detect code presence as shown in Figure A-19. Probability of detection results for this lock detector are computed in Ref. [8]. These results are shown in Figure A-20 for a probability of false-alarm, $P_{FA} = .01$. Let us assume:

TABLE A-7

RECEIVER PERFORMANCE SUMMARY

B_I (IF)	6 kHz
B_L(AFC)	5 Hz
B_L(PLL)	120 Hz
B_L(CODE LOOP)	55 Hz
C/A Code Search Rate	150 chips/sec
Data Acquisition Time	1 min/SAT
Dwell Time During NAV Mode	200 ms/SAT
Receiver Clock Accuracy	10^{-7}
Max. Pseudo-Range Error Due to Clock Offset	60 feet
Carrier Power to Noise Density (C/N_o)	40 dB-Hz
SNR_L(PLL)	14 dB
σ_τ(Code Loop Jitter)	50 ns
Received Signal Power for Normal Operation	-160 dBw
LCR Threshold in Data Mode	-162 dBw (due to PLL)
LCR Threshold in Nav Mode	-162 dBw (due to lock detector)

TABLE A-8

INITIAL CARRIER FREQUENCY UNCERTAINTY

ITEM	FREQUENCY UNCERTAINTY
LCR Local Oscillator (10^{-7} accuracy)	$\pm$ 158 Hz
Satellite Doppler Estimate	$\pm$ 500 Hz
User Doppler (200 mph)	$\pm$ 500 Hz
VCO Preset Accuracy ($\pm$ 5% of 12 kHz tracking range after calibration)	$\pm$ 600 Hz
TOTAL	$\pm$ 1758 Hz

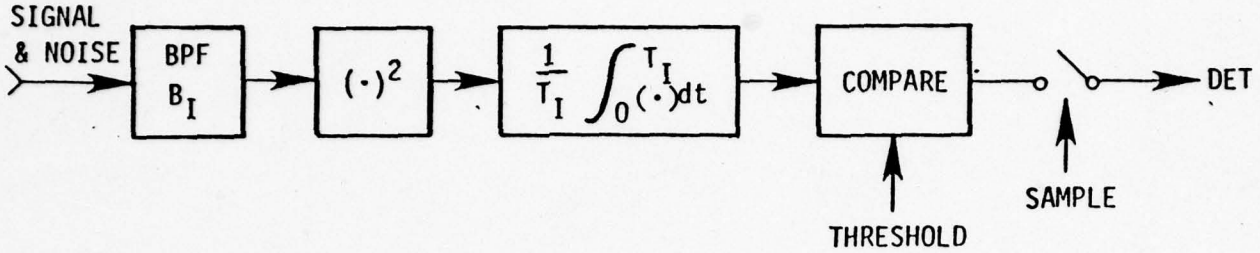

FIGURE A-19

MODEL OF SIGNAL PRESENCE DETECTOR

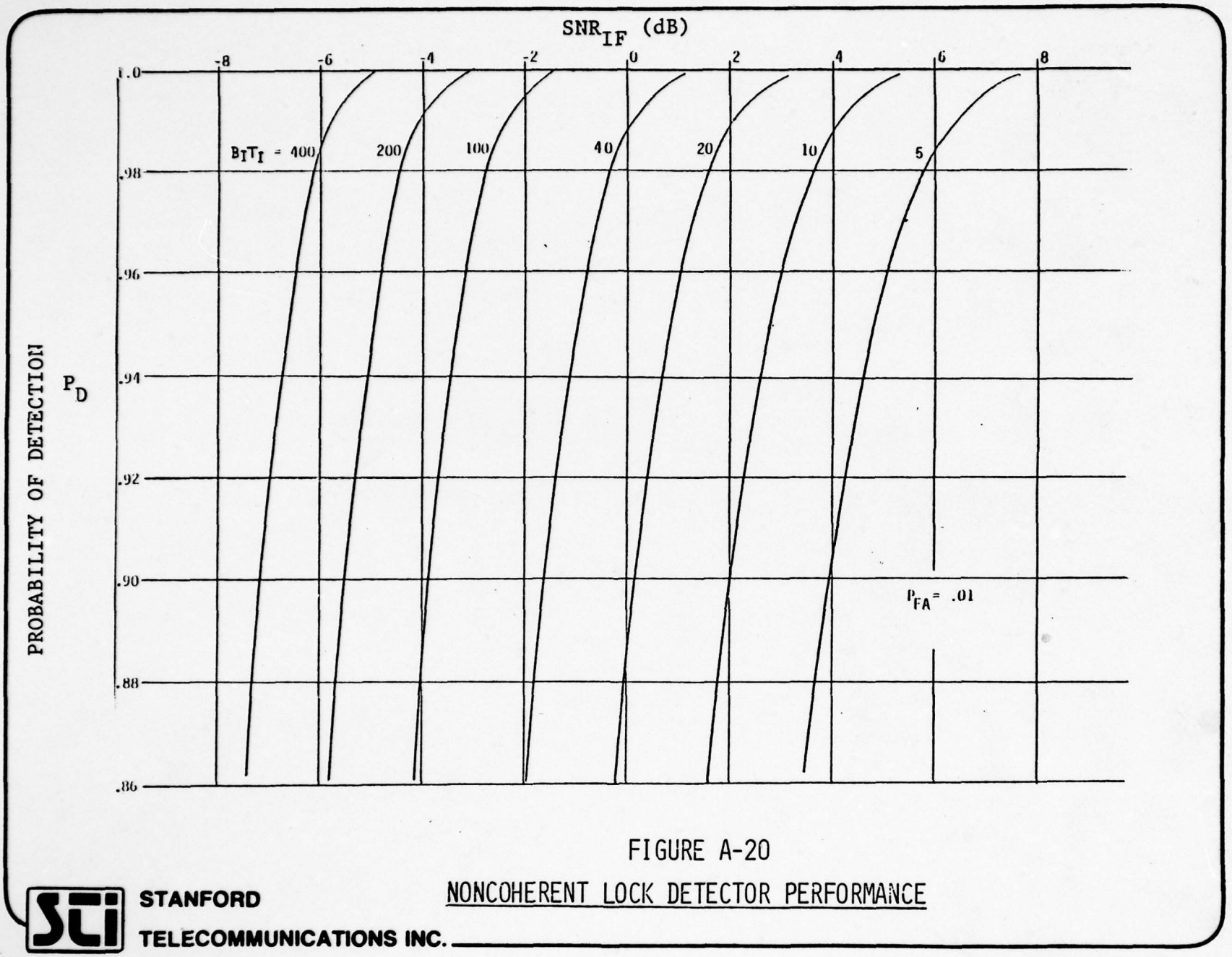

FIGURE A-20

NONCOHERENT LOCK DETECTOR PERFORMANCE

STANFORD TELECOMMUNICATIONS INC.

- Carrier-to-noise density ratio of C/N_o = 40 dB-Hz (based on P_S = -160 dBw and N_o = -200 dBw/Hz)
- 1 dB loss due to offset of the carrier in the IF filter.
- 1 dB average loss due to one-half chip code step increments.

Thus we have

$$SNR_I(dB) = C/N_o(dB) - B_I(dB)$$

$$= 40 \text{ dB} - 2 \text{ dB} - 37.8 \text{ dB}$$

$$= 0.2 \text{ dB}$$

for which $B_I T_I = 20$ for $P_D = .9$ and $P_{FA} = .01$.

A dwell of 2 T_I is required for each chip since the code is stepped in one-half chip increments. The permissable search rate is therefore

$$SR = \frac{1}{2T_I} = \frac{6000}{40} = 150 \text{ chips/sec}$$

The entire C/A code can thus be searched in 6.8 seconds.

False alarms are checked by stopping the code stepping and requiring that the next two out of three trials indicate detections in order for signal presence to be declared. This process takes 20 ms per false-alarm. A total time of about 0.2 sec will be

AD-A069 059 STANFORD TELECOMMUNICATIONS INC MCLEAN VA F/G 17/7
INVESTIGATION OF A PRELIMINARY GPS RECEIVER DESIGN FOR GENERAL --ETC(U)
JUL 78 B D ELROD, F D NATALI F04701-75-C-0239
UNCLASSIFIED STI/E-TR-8022 SAMSO-TR-79-34 NL

2 OF 2
AD
A069059

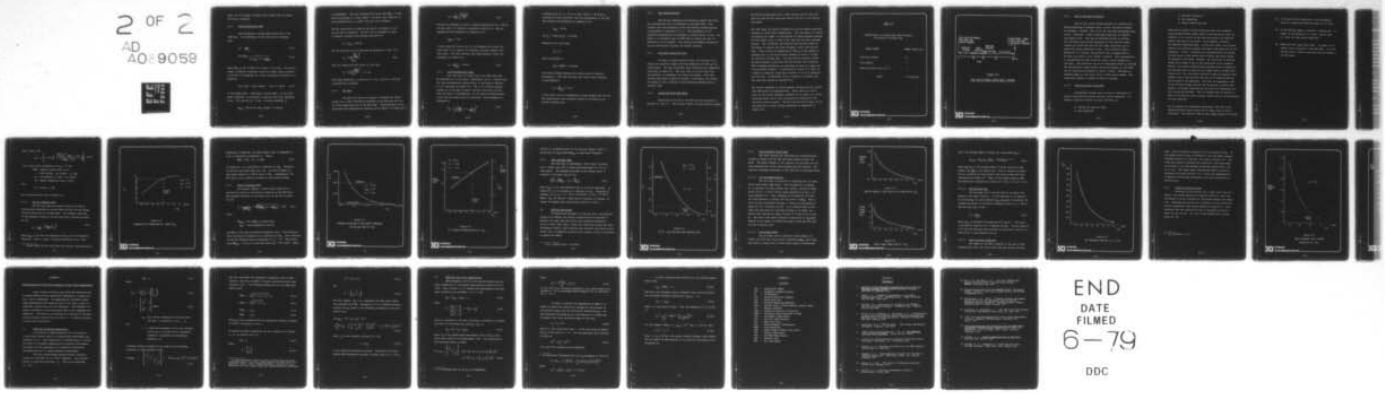

END
DATE
FILMED
6-79
DDC

spent, on the average, checking false alarms when the entire C/A code is searched.

A.3.3 Phase-Locked Loop (PLL)

The LCR employs a second order Costas PLL in the DATA mode. The performance of the loop may be evaluated from

$$\sigma_\phi^2 = \frac{1}{SNR_L} \tag{A-3}$$

$$\text{and } SNR_L = \frac{C}{N_o B_{PLL} \left(1 + \frac{1}{2SNR_I}\right)} \tag{A-4}$$

where SNR_I is the IF SNR at the input to the loop. The use of a single τ-dithered correlator causes the signal power available to the PLL to be degraded by 3 dB as discussed in Section 2.4.1. Therefore

$$C/N_o \text{ (eff)} = C/N_o \text{ (input)} - 3 \text{ dB} = 37 \text{ dB-Hz} \tag{A-5}$$

at the design point. Selecting a desired SNR_L = 14 dB (2 dB above threshold), we calculate a required loop noise bandwidth of B_L = 123.4 Hz for B_I = 6 kHz. A design bandwidth of

$$B_{PLL} = 120 \text{ Hz for } C/N_o \text{ (input)} = 40 \text{ dB-Hz}$$

is recommended. The loop threshold will occur when SNR_L = 12 dB, which corresponds to a C/N_o (input) = 38 dB-Hz (the reduction in loop bandwidth due to a lower C/N_o than this estimate).

The PLL acquisition is aided by AFC which is designed to preset the PLL in frequency. The AFC loop is designed to yield a frequency estimate with standard deviation of

$$\sigma_f = B_{PLL} = 120 \text{ Hz}$$

The PLL frequency pull-in time may be estimated as (Ref. [9])

$$T_F = \frac{4.16 \left(\frac{\Delta f}{B_{PLL}}\right)^2}{B_{PLL}} \qquad \text{(A-6)}$$

Thus the acquisition will occur in less than

$$T_f = \frac{4.16 \left(\frac{240}{120}\right)^2}{120} = .14 \text{ sec}$$

with high probability (a value of $\Delta f = 2\sigma_f$ = 240 Hz is used for a conservative estimate).

A.3.4 AFC Loop

The AFC loop serves the purpose of keeping the signal within the $\pm$ 3 kHz correlation bandwidth in the NAV mode and acts as a PLL acquisition aid in the DATA mode. The performance of the particular AFC configuration proposed can be shown to be expressed as

$$\sigma_f = \frac{2}{SNR_I} \sqrt{\frac{B_{AFC} B_I}{12}} \qquad \text{(A-7)}$$

The loop is designed to yield a standard deviation of σ_f = 120 Hz at C/N_o (eff) = 37 dB-Hz as discussed in Section 4.3, and the appropriate loop bandwidth is computed to be

$$B_{AFC} = 5 \text{ Hz}.$$

A first order AFC loop is felt to be adequate for present purposes since it is capable of tracking a constant doppler with zero error. The loop settling time (approximately three time constants) is taken to be

$$T_S = \frac{3}{4B_{AFC}} = 150 \text{ ms} \qquad \text{(A-8)}$$

A.3.5 Code Tracking Loop (DLL)

The code loop is a delay lock loop (DLL) which may be described as a first order, noncoherent, $\pm 0.3\Delta$, τ-dither loop. The loop discriminator characteristic is discussed in Section A.1.4.1 and shown in Figure A-8. The $\pm$ .3Δ τ-dither spacing results in a loop that is about 4 dB more efficient in noise than the usual 1Δ configuration, at the price of reduced acquisition and less time jitter at threshold. The performance is estimated by

$$\frac{\sigma_\tau}{\Delta} = \left[\frac{B_{DLL}}{5\ C/N_o} \left(1 + \frac{2}{SNR_I}\right) \right]^{\frac{1}{2}} \qquad \text{(A-9)}$$

A design point of σ_τ = 50 ns at C/N_o (input) = 40 dB-Hz is selected as being consistent with the requirements of the LCR. The required loop bandwidth is computed to be

$$B_{DLL} = 55 \text{ Hz}$$

for B_I = 6 kHz and $\frac{1}{\Delta}$ = 1.023 MHz.

Threshold will occur when

$$\frac{\sigma_\tau}{\Delta} = 0.1$$

which corresponds to

$$C/N_o \text{ (THRES)} = 36 \text{ dB-Hz}$$

(the above estimate neglects AGC effects and is therefore pessimistic.) The loop settling time (three time constants) is approximately

$$T_S = \frac{3}{4B_{DLL}} = 14 \text{ ms}$$

A first order loop is recommended as being adequate for the present application since frequency aiding is provided by the carrier tracking loop.

A.3.6 Data Synchronization

The LCR must demodulate the satellite signals and enter the received data into its processor in the DATA mode. This requires that the operations of bit and subframe synchronization be performed as discussed in 2.4.3. The performance of the proposed configurations is discussed in further detail in Ref. [10] where it is estimated that the 90% time to acquire bit sync is estimated to be 20 seconds. The results are probably pessimistic but are sufficiently accurate for present purposes.

A.3.7 Data Mode Acquisition Time

In order to gather satellite data, the LCR must first acquire the satellite signal and then demodulate the data as discussed above. The time to perform these operations was summarized previously in Table A-6. The total time to collect data from one satellite is estimated to be about one minute. This time could be shortened to about 40 seconds, if necessary, by storing 30 seconds of data (1500 bits) and performing subframe sync in non-real time.

A.3.8 Sequencing Times (NAV Mode)

Sequencing of the LCR in the NAV mode was discussed in Sections A.1 and A.2. The receiver "dwells on each satellite signal

for 200 ms during which time it must acquire the C/A code and both the code and AFC loops must settle (the PLL is not used in this mode).

The code phase and carrier frequency are stored between satellite accesses to allow rapid reacquisition. The code phase is "stored" by counting the number of code periods to elapse between accesses. The LCR stable clock is used as the time base for this counting process. The "estimated" and received code periods differ by the amount of doppler and clock frequency errors that are present. These errors are summarized in Table A-9 and indicate a maximum error in the stored phase estimate of about 3.6 chips per second of storage time. The time between accesses is 800 ms when tracking 5 satellites with 200 ms dwell per satellite. Thus a maximum uncertainty in code phase of about 2.9 chips can accrue between accesses. A reacquisition search of 6 chips ($\pm$ 3 chips) is employed, requiring a maximum of 40 ms to reacquire the C/A code. An addtional 10 ms is required to confirm lock. The code loop settles in another 18 ms.

The carrier frequency is stored between accesses and the carrier loop VCXO preset for reacquisition. There should be little error in the preset frequency, probably on the order of $\pm$ 100 Hz including offset due to user and satellite acceleration and oscillator reset accuracy. The AFC loop settles in about 150 ms. The time-line of events during sequencing is summarized in Figure A-21.

TABLE A-9

Maximum Error in Stored Code Phase Estimate
Per Second of Storage Time

ERROR SOURCE	ERROR (Chips/sec)
Satellite Doppler	3.2
User Doppler	.3
Receiver Clock Error (10^{-7})	.1
TOTAL	3.6 Chips/sec

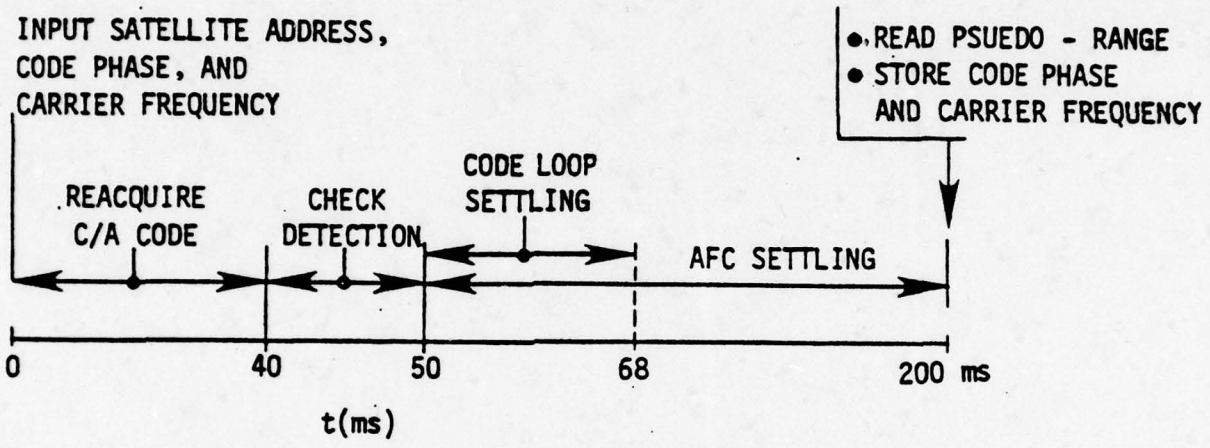

FIGURE A-21

TIME-LINE OF EVENTS DURING DWELL INTERVAL

A.3.9 DATA to NAV Mode Transition

The six chip search window employed for reacquisition during sequencing is adequate when a recent code phase estimate is available. However, this is not the case when sequencing first starts. Therefore, a DATA to NAV mode transition is required (see Figure A-18). This may be described briefly as follows. The code phase (and carrier frequency) of the satellite being tracked are stored and then the four other satellites are acquired and signal parameters stored. This operation takes a maximum of 27.2 seconds, during which time a maximum error of 98 chips can accrue in the "oldest" estimate. Thus reacquisition is accomplished for each satellite using a search window of $\pm$ 100 chips. The satellites can all be reacquired within 5.6 seconds. The reacquisition search window can now be reduced to $\pm$ 20 chips and all satellites reacquired in about 1 second. NAV mode sequencing begins at this point with a 6 chip search window. The transition requires a maximum of about 35 seconds.

A.3.10 Receiver Control Algorithms

Considerable thought must be given to permissible receiver states and the overall receiver control algorithm. For example, suppose we define the basic LCR modes as:

- Standby and Operator Input
- Data Gathering

- Data-Nav Transition
- Nav Sequencing
- Manual Control and Test

There may be several states within each mode with automatic transitioning between states based on the particular state the receiver is in, as well as the code and carrier lock detector outputs and time in that state. As an example, consider the DATA-NAV Transition mode. In the first state, the receiver acquires the satellite signals and stores code phase and carrier frequency. If four satellites are acquired within 28 seconds, the LCR can go to the second state in which the search window is narrowed to 200 chips. However, the transition to State #2 should not be made if one or more satellites is not acquired. Further, the fourth satellite phase estimate must be updated if the receiver stays in State #1 for longer than 28 seconds (See Figure A-18). If a particular satellite cannot be acquired after several tries a new satellite may have to be selected and the LCR returned to the DATA mode. This sort of reasoning is part of the receiver design and will not be pursued in detail here. However, an example algorithm will be given for sequencing control during the NAV Mode. This is intended only to serve as a basis for discussion about receiver control and is not necessarily the best approach.

Let us suppose that during NAV sequencing, code lock is not achieved during a dwell period due to signal fade or noise statistics. The receiver control logic might proceed as follows:

(1) If one-out-of-four satellites is not reacquired, allow two misses and widen the search to 40 chips.

(2) If the missing signal is detected, continue NAV. If signal is not detected in 3 trials, then go back to a full C/A code search (STOP NAV).

(3) Search the full code three times. If signal is detected, start transition to the NAV mode. If no detection occurs, choose a new satellite and return to the DATA mode.

input C/N_o by [8]

$$P_D = \tfrac{1}{2}\left[1 + \text{erf}\left\{\frac{\left(\frac{B_I T_I}{2}\right)^{\frac{1}{2}} SNR_I - 1.65}{(2SNR_I + 1)^{\frac{1}{2}}}\right\}\right] \quad \text{(B-1)}$$

for a false alarm probability of $P_{FA} = .01$ and

SNR_I = signal-to-noise ratio at IF

$= C/N_o$ (dB-Hz) - B_I (dB-Hz) - L_I (dB)

B_I = IF Bandwidth = 6 kHz = 37.8 dB-Hz

T_I = Signal Integration Time = $20/B_I$

and

L_I = Losses = 2 dB*

P_D is plotted versus C/N_o in Figure B-1.

B.1.2 Carrier Tracking (AFC)

The AFC loop keeps the signal within the 6 kHz IF (correlation) bandwidth in the NAV mode and aids the PLL during initial acquisition in the DATA mode. The standard deviation of the frequency output of the AFC loop after settling is given by [11]

$$\sigma_F = \frac{2}{SNR_I}\left(\frac{B_{AFC}\, B_I}{12}\right)^{\frac{1}{2}} \quad \text{(B-2)}$$

where B_{AFC} is the AFC loop bandwidth and B_I is the IF bandwidth (6000 Hz). Since a single τ-dithered correlator ($\pm$ 0.3 chip

*These losses do not occur after the initial code acquisition.

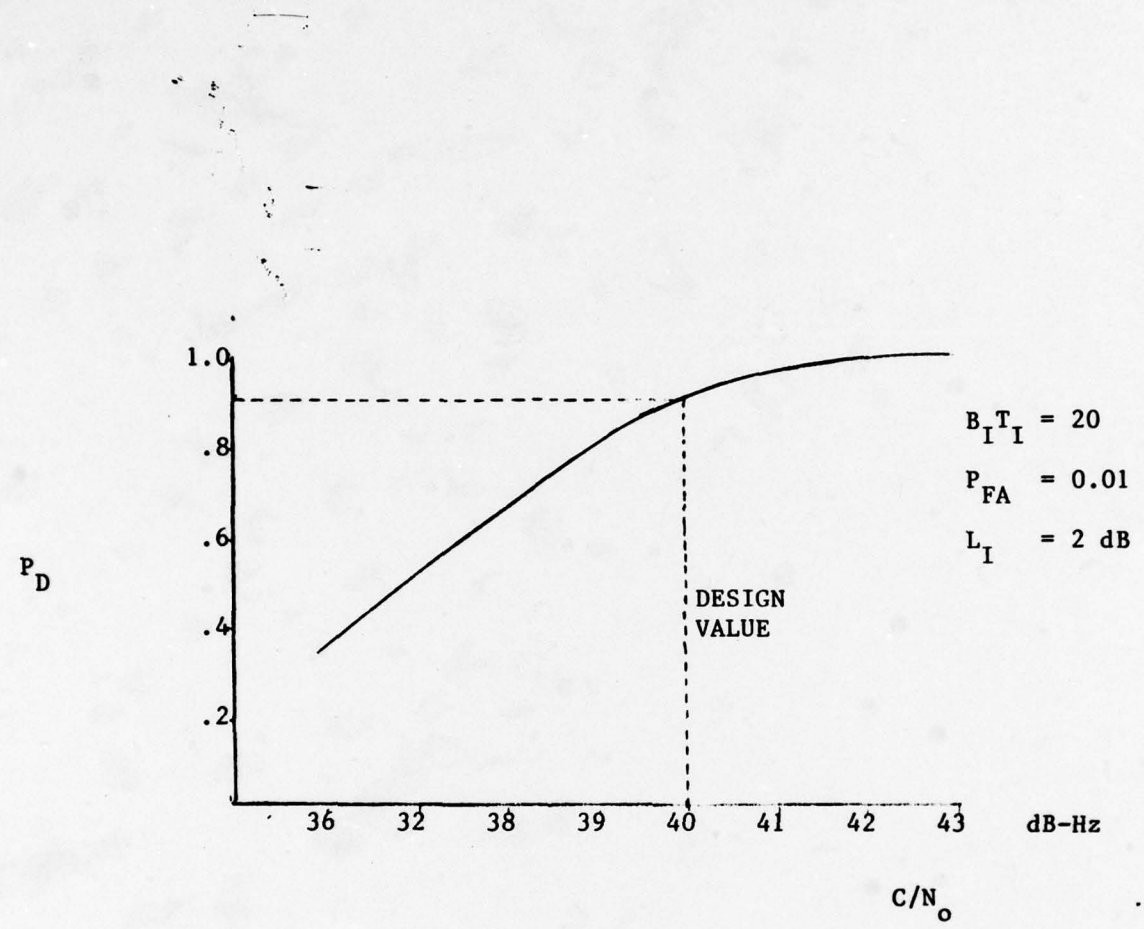

Figure B-1

PROBABILITY OF DETECTION VS. INPUT C/N_o

dithering) is employed, the input signal power is degraded by 3 dB, as discussed in Appendix A.1. Hence,

$$SNR_I = C/N_o - B_I - 3 \text{ (dB)} \qquad \text{(B-3)}$$

In Figure B-2, σ_F is plotted as a function of C/N_o. Threshold in the AFC loop occurs when $3\sigma_F = B_I$. In view of Figure B-2 this would require a 13 dB-Hz drop in C/N_o. Consequently, the AFC loop is not a sensitive element in the receiver design.

B.1.3 Carrier Tracking (PLL)

The receiver employs a second order Costas PLL to provide the necessary code/carrier coherence in the DATA mode. The standard deviation of the phase error in the PLL is given by [18]

$$\sigma_\phi = \frac{1}{\sqrt{SNR_{PLL}}} = \sqrt{\frac{B_{PLL}}{B_I SNR_I}\left(1 + \frac{1}{2SNR_I}\right)} \quad \text{(rad)} \qquad \text{(B-4)}$$

where

SNR_{PLL} = PLL signal-to-noise ratio

B_{PLL} = loop bandwidth of the PLL

and SNR_I is the same as defined in Equation (B-3). This relationship is plotted in Figure B-3 as a function of C/N_o. Also indicated is the PLL threshold which corresponds to $3\sigma_\phi = \pi/4$. This occurs when SNR_{PLL} = 12 dB or in this case when C/N_o = 38.5 dB-Hz. Hence,

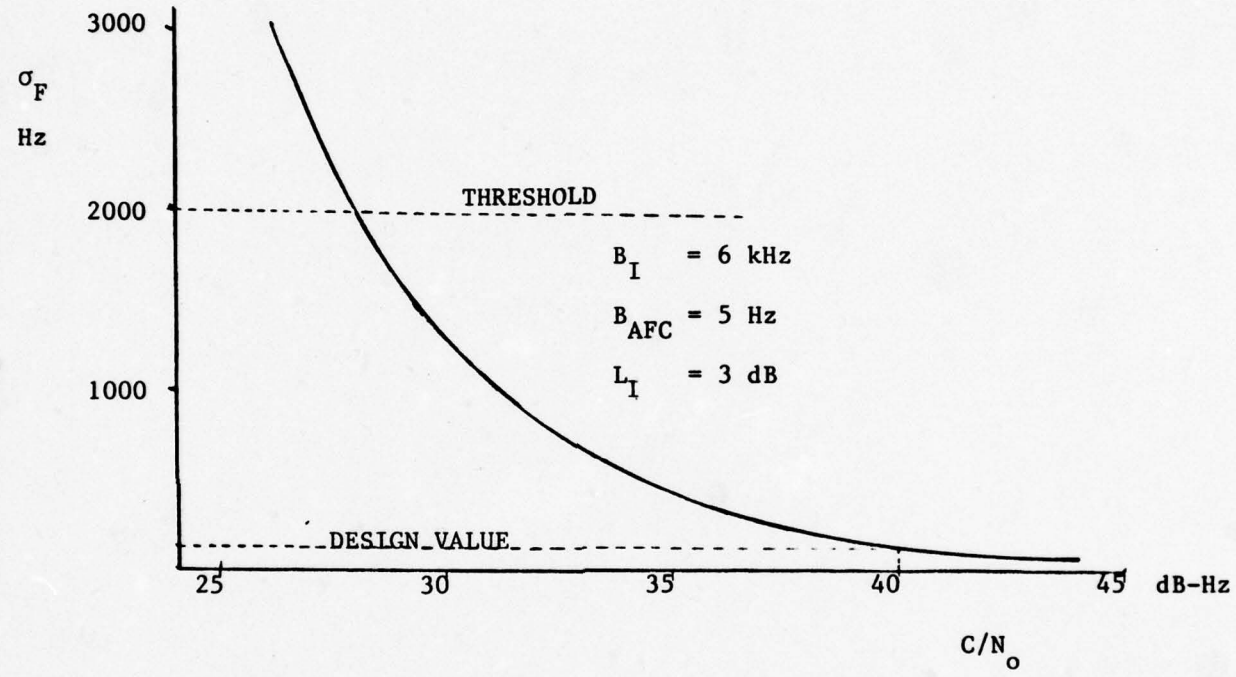

Figure B-2

STANDARD DEVIATION OF THE OUTPUT FREQUENCY

OF THE AFC LOOP VS C/N_o

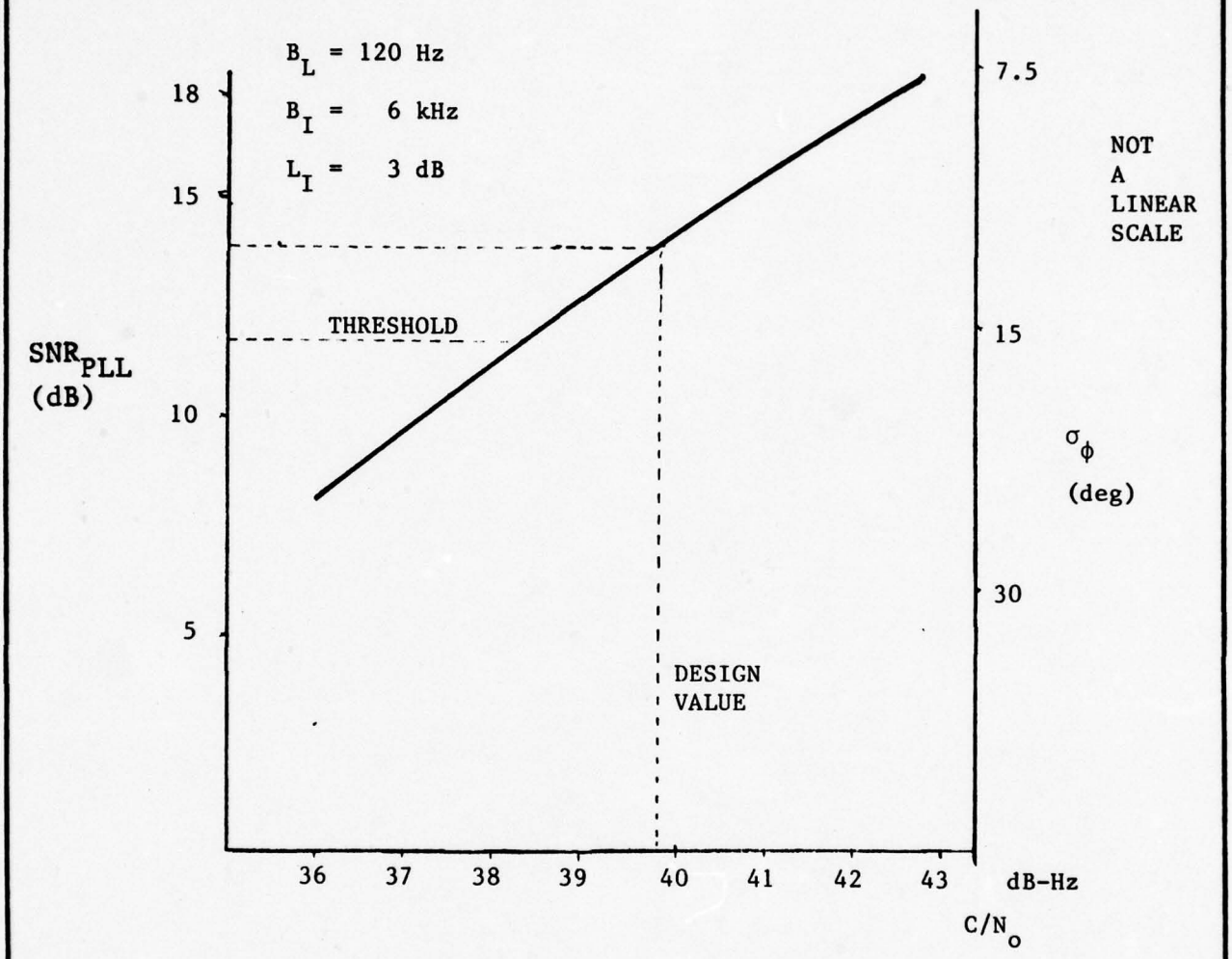

Figure B-3

PLL SIGNAL-TO-NOISE-RATIO VS. C/N_o

the PLL is a sensitive part of the receiver design, since a 2 dB-Hz drop in C/N_o causes SNR_{PLL} to drop below threshold.

B.1.4 Code Tracking (DLL)

The code loop is considered a first order, non-coherent τ-dither loop with a linear operating range of $\pm 0.3\Delta$ (Δ = chip width). The standard deviation of the timing jitter is related to the input C/N_o by [19]

$$\left(\frac{\sigma_\tau}{\Delta}\right)^2 = \frac{B_{DLL}}{5\ C/N_o}\left[1 + \frac{2B_I}{C/N_o}\right] \qquad \text{(B-5)}$$

where B_{DLL} is the loop bandwidth and B_I is the IF bandwidth. In Figure B-4 σ_τ/Δ is plotted as a function of C/N_o. Threshold is reached, if $(\sigma_\tau/\Delta) = 0.1$, which corresponds to $C/N_o = 36$ dB-Hz. Hence, C/N_o can drop by 4 dB-Hz before threshold is reached, although the timing error would double from 50 to 100 ns.

B.2 Modified LCR Design

If significant decreases in C/N_o can occur, the question arises as to whether the receiver design should be modified to maintain the same code and carrier loop tracking performance, but at a lower input C/N_o.* Since this would also affect two other performance aspects, dwell interval per satellite and initial acquisition time, a parametric analysis with respect to C/N_o is presented to assess the impact.

---

*e.g., nominal value = 36 dB-Hz.

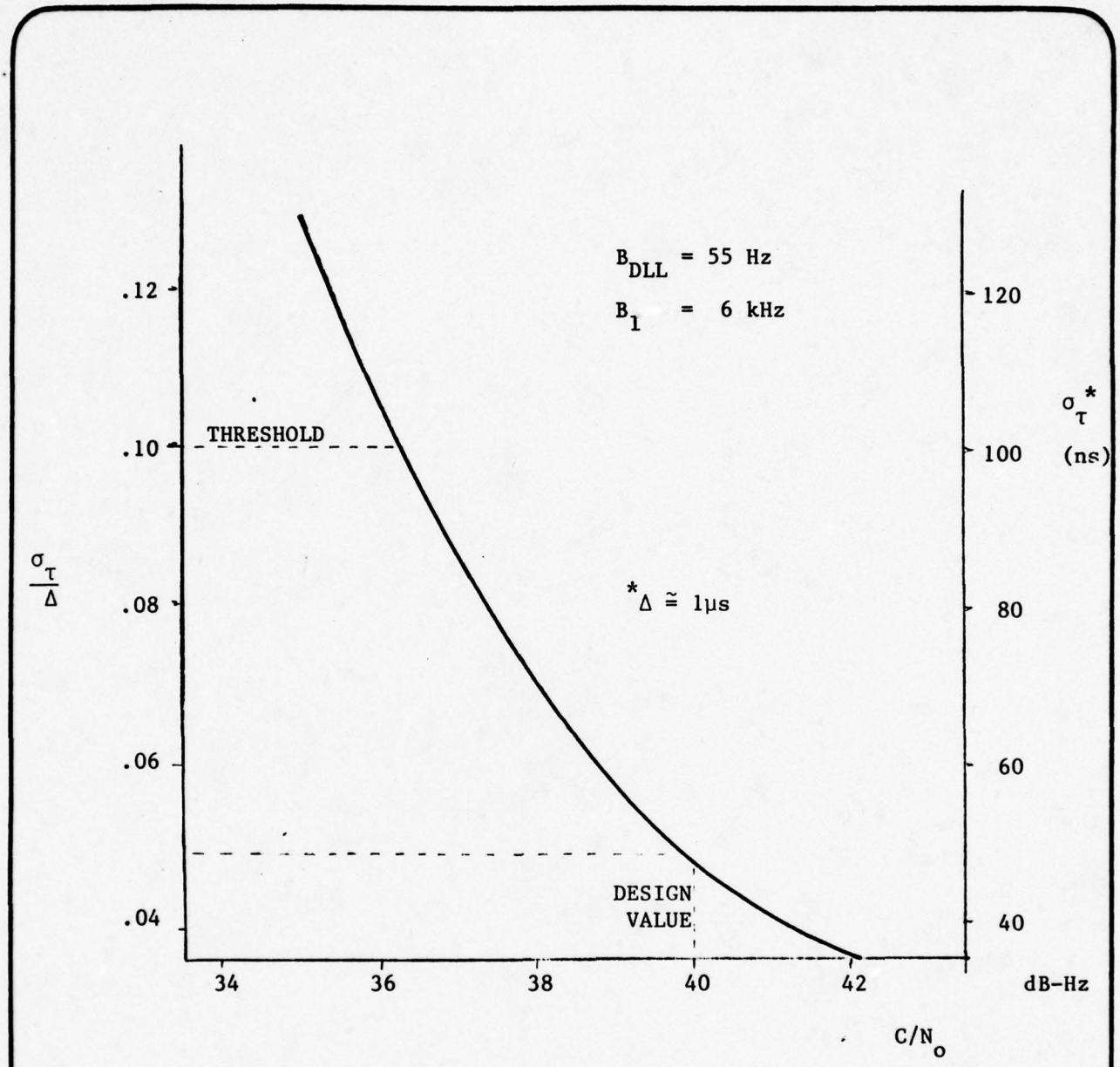

Figure B-4

$\frac{\sigma_\tau}{\Delta}$ VS. C/N_o FOR THE CODE TRACKING LOOP

B.2.1 Dwell Interval in NAV Mode

The dwell interval per satellite was illustrated previously in Figure A-20 for the LCR design based on C/N_o = 40 dB-Hz. The major elements of the interval are the times for C/A code reacquisition, false alarm checking and AFC settling. The receiver re-design pertaining to each function is discussed below.

B.2.1.1 C/A Code Reacquisition

The C/A code is reacquired by searching over an appropriate code window (N_{SW} chips). The procedure for re-design is to calculate the $B_I T_I$ product that yields a detection probability of P_D = .9 with a false alarm probability of P_{FA} = .01, using Equation B-1. Then, assuming an IF bandwidth of 6 kHz, the time necessary to search over the code is $2T_I N_{SW}$. The results of this calculation for N_{SW} = 6 chips are illustrated in Figure B-5 as a function of C/N_o. It is observed that as the input C/N_o decreases by 4 dB from 40 dB-Hz to 36 dB-Hz, the search time increases by about a factor of 5 from 38 ms to 190 ms. The search time would increase in proportion to N_{SW} which depends on the number of satellites being tracked and the code slip per tracking cycle.

B.1.2.2 False-Alarm Check

The procedure used to check for false alarms is to repeat each code step that yields a detection <u>three</u> more times and reject it unless two of these trials result in detections.

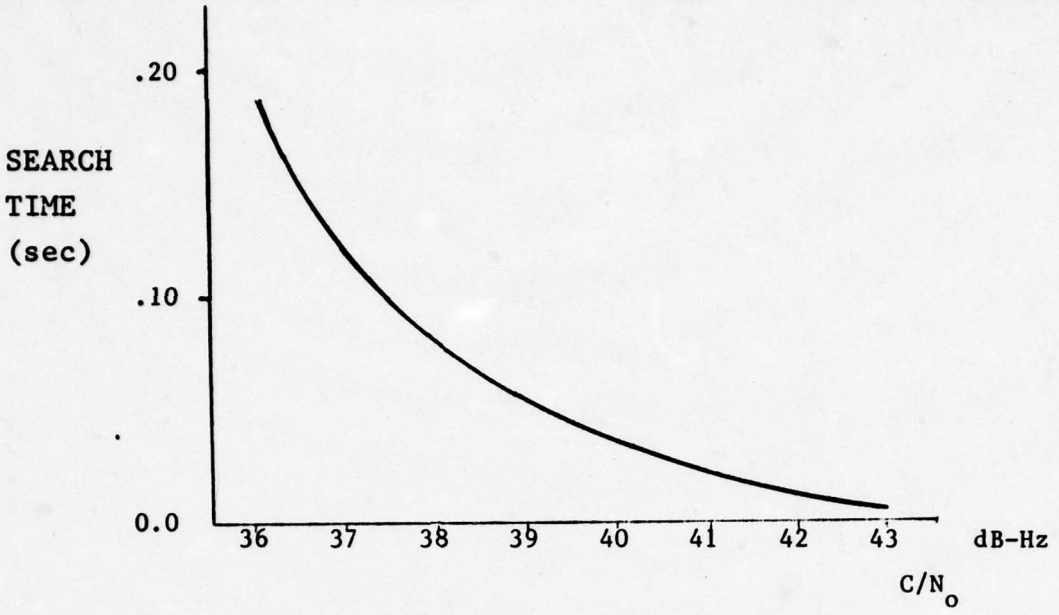

Figure B-5

TIME TO SEARCH 6 CODE CHIPS AS A FUNCTION OF C/N_o

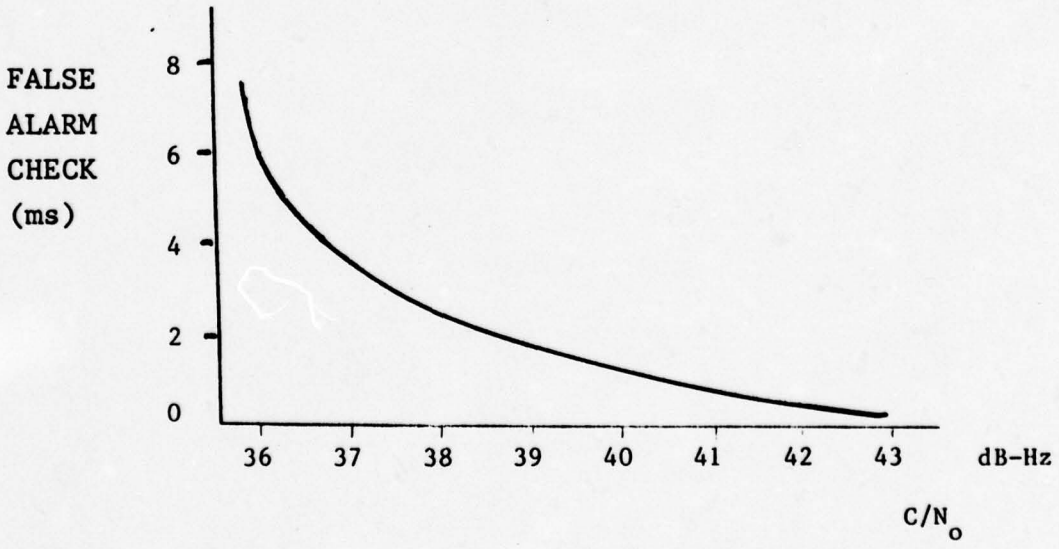

Figure B-6

FALSE ALARM CHECK TIME VS. C/N_o

Thus, the average number of checks per code window N_{SW} is

$$T_{total} = N_{SW} P_{FA} \frac{4}{1/2T_I} = (2T_I N_{SW} P_{FA}) \times 4 \qquad \text{(B-6)}$$

where $N_{SW} P_{FA}$ is the average number of false alarms per code window, and $\frac{1}{2T_I}$ is the search rate. This is plotted in Figure B-6 as a function of C/N_o based on the search times that were illustrated in Figure B-5. Here, if the signal drops by 4dB, the check time increases by a factor of 5 from 1.5 ms to 7.6 ms.

B.2.1.3 AFC Settling Time

The settling time of the AFC loop is the major component of the dwell interval. For the NAV mode it is computed by calculating the loop bandwidth B_{AFC} necessary to maintain the standard deviation of the output frequency error at σ_F = 120 Hz. The settling time is then

$$T_S = \frac{3}{4B_{AFC}} \qquad \text{(B-7)}$$

where B_{AFC} is obtained from Equations B-2 and B-3. The result is plotted in Figure B-7 as a function of C/N_o. If C/N_o drops by 4 dB, the AFC settling time increases by more than a factor of 4, from 150 ms to approximately 942 ms.

B.2.1.4 Dwell Interval Evaluation

The length of the dwell interval is the sum of code reacquisition time, the false alarm time and the AFC settling

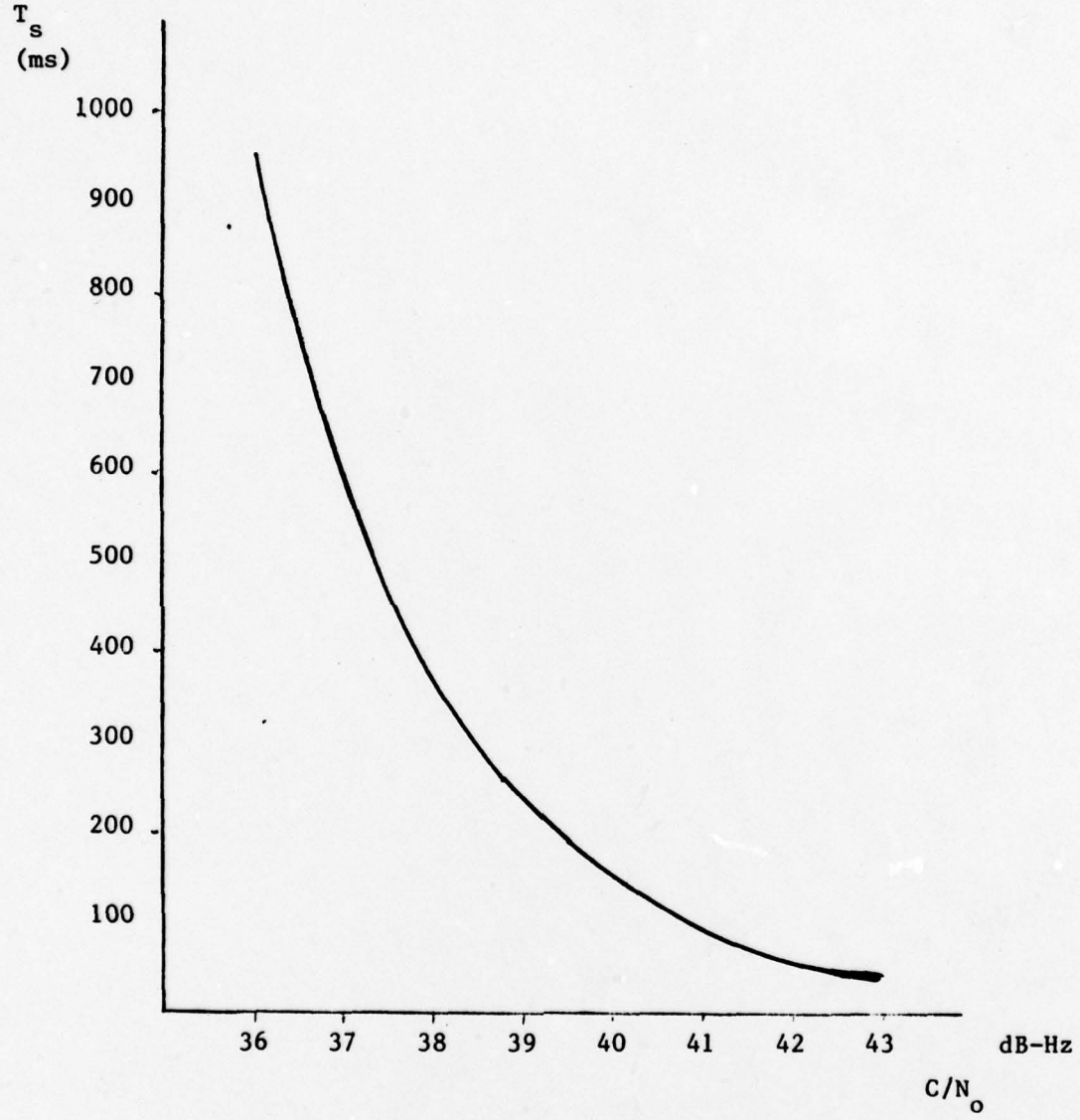

Figure B-7

AFC SETTLING TIME FOR σ_F = 120 Hz

time. This is plotted in Figure B-8 as a function of C/N_o. If the design value of C/N_o is reduced by 4 dB, the dwell interval increases form 0.2 to 1-10 sec, or by over a factor of 5. For a NAV mode based on tracking five satellites, this would mean an increase in the time between navigation updates from 1 sec to 5.5 sec. The larger dwell interval may lead to iterative updating of aircraft position (i.e., after each measurement)* to maintain positioning performance even with availability of velocity data.

B.2.2 Initial Acquisition Time

Re-design of the receiver for a lower input C/N_o also impacts the initial acquisition time per satellite, which was calculated to be 62.4 seconds for the present design (see Table A-6). Repeating this process as a function of C/N_o yields the initial acquisition time results plotted in Figure B-9. This indicates that the acquisition time is increased by nearly a factor of two (62 sec - 117 sec) if the design value of C/N_o drops by 4 dB.

---

* See footnote, p. 2-7

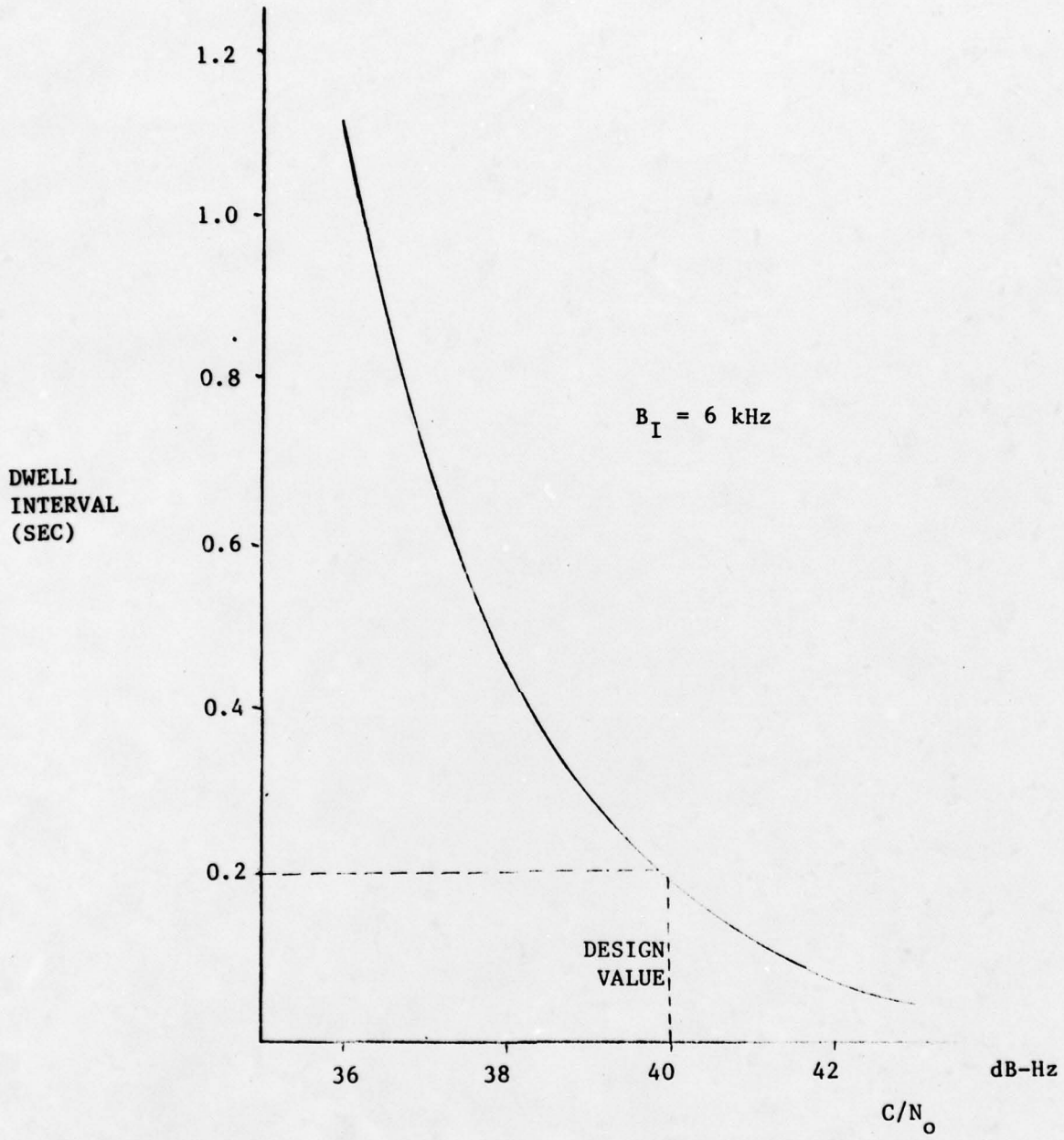

Figure B-8

DWELL INTERVAL FOR A SINGLE

SATELLITE VS. C/N_o

APPENDIX C

GDOP Evaluation for GPS with Altimeter or User Clock Augmentation

Under certain conditions only three GPS satellites may be usable because of poor geometrical deployment or signal loss (e.g., due to shadowing). By augmenting the available pseudo-range measurements with altimetry data or the user's clock, an acceptable solution may still be achievable. This Appendix considers a derivation of the equivalent GDOP in the augmented configuration. The results are presented as a function of the additional parameter involved in each case (i.e., altimeter accuracy or clock bias uncertainty).

C.1 GDOP With Altimeter Augmentation

A derivation of GDOP parameters for a 3D position + clock bias solution based on n pseudo-range measurements was presented in [2]. That formulation is extended here to include the effect of altimeter augmentation on geometric performance. The result is also applicable to a hyperbolic positioning technique based on n-1 range-difference measurements.

The basic pseudo-range solution process involves a system of n equations ($n \geq 4$) with 4 unknowns: user position vector, $\underline{r}_u$ and user clock bias, b_u. This can be expressed as: [2]

$$G\underline{X}_u = \underline{\rho} \qquad \text{(C-1)}$$

where

$$\underline{X}_u \equiv \begin{pmatrix} \underline{r}_u \\ b_u \end{pmatrix} = \begin{pmatrix} x \\ y \\ z \\ b_u \end{pmatrix} \qquad \text{(C-2)}$$

$$G \equiv \begin{bmatrix} \underline{e}_1^T & -1 \\ \vdots & \vdots \\ \underline{e}_n^T & -1 \end{bmatrix} \quad (nx4) \qquad \text{(C-3)}$$

$\underline{e}_i \equiv$ unit vector defining the direction from the user to satellite i (i=1,...,n)

and

$\underline{\rho} \equiv$ a derived measurement vector that includes errors due to receiver noise; multipath; ephemeris, ionosphere and troposphere modeling, etc.

A minimum variance estimate for $\underline{X}_u$ leads to the following covariance of the estimation error

$$\text{cov}(\delta\underline{X}_u) = \begin{bmatrix} \sigma_x^2 & - & - & - \\ - & \sigma_y^2 & - & - \\ - & - & \sigma_z^2 & - \\ - & - & - & \sigma_t^2 \end{bmatrix} = [G^T(\text{cov}\ \delta\underline{\rho})^{-1}G]^{-1} = \sigma_\rho^2(G^TG)^{-1} \qquad \text{(C-4)}$$

The last step makes the fundamental assumption used in GDOP analyses, that the n elements of $\delta\underline{\rho}$ are uncorrelated with equal variances (σ_ρ^2). The following definitions for the GDOP parameters apply:

$$\text{PDOP} = \sqrt{\sigma_x^2 + \sigma_y^2 + \sigma_z^2}/\sigma_\rho \qquad \text{(C-5)}$$

$$\text{HDOP} = \sqrt{\sigma_x^2 + \sigma_y^2}/\sigma_\rho \qquad \text{(C-6)}$$

$$\text{VDOP} = \sigma_z/\sigma_\rho \qquad \text{(C-7)}$$

$$\text{TDOP} \quad \sigma_t/\sigma_\rho \qquad \text{(C-8)}$$

These are then evaluated from the appropriate diagonal elements of $(G^TG)^{-1}$ according to (C-4).*

To extend the above formulation for the altimeter case (where $n \geq 3$), we rewrite (C-1) as

$$G\underline{X}_u = \underline{\hat{\rho}} \qquad \text{(C-9)}$$

where

$$G \equiv \begin{bmatrix} G \\ \underline{\ell}^T \end{bmatrix} \qquad \text{(C-10)}$$

* A range-difference solution process would produce an error covariance matrix, cov ($\delta\underline{r}_u$), which equals the upper left, 3x3 portion of (C-4). Hence, GDOP parameters, (C-5)-(C-7), are equivalent for both pseudo-range and range-difference techniques.

$$\underline{\ell}^T \equiv (0\ 0\ 1\ 0) \tag{C-11}$$

and

$$\hat{\underline{\rho}} \equiv \begin{pmatrix} \underline{\rho} \\ R_e + h \end{pmatrix} \tag{C-12}$$

The last element, $(R_e + h)$, represents the mean earth radius plus measured altitude. Analogous to (C-4) a minimum variance estimate for $\underline{X}_u$ leads to the following covariance of the estimation error,

$$\text{cov}(\delta \underline{X}_u) = [G^T\ (\text{cov}\ \delta\hat{\underline{\rho}})^{-1}\ G]^{-1}$$

$$= \left(\begin{bmatrix} G^T \\ \underline{\ell} \end{bmatrix} \begin{bmatrix} \text{cov}\ \delta\underline{\rho} & \underline{0} \\ \underline{0}^T & \sigma_h^2 \end{bmatrix}^{-1} \begin{bmatrix} G \\ \underline{\ell}^T \end{bmatrix} \right)^{-1} = \sigma_\rho^2\ (G^T G + \frac{1}{\mu^2}\underline{\ell}\underline{\ell}^T)^{-1} \tag{C-13}$$

where σ_h is the altimeter accuracy (1σ) and

$$\mu \equiv \sigma_h/\sigma_p \tag{C-14}$$

is the normalized altimeter accuracy. Evaluation of corresponding GDOP parameters proceeds as before from (C-5) - (C-8).

C.2 GDOP with User Clock Augmentation

GDOP parameters for this case can be derived from the basic formulation of the pseudo-range equations given in (C-1)-(C-3). Here, however, it is assumed that measurements from only three satellites are available, so n = 3 and

$$G\underline{X}_u = H_3\underline{r}_u + \underline{1}_3 b_u = \underline{\rho} \qquad \text{(C-15)}$$

where

$$G = \left[\begin{array}{c|c} \underline{e}_1^T & -1 \\ \underline{e}_2^T & -1 \\ \underline{e}_3^T & -1 \end{array}\right] = \left[H_3 \;\vdots\; -\underline{1}_3\right] \qquad \text{(C-16)}$$

Since an estimate for the user clock bias is assumed to be known, the error in estimating user position ($\underline{r}_u$) is

$$\delta\underline{r}_u = H_3^{-1}\,(\delta\underline{\rho} + \underline{1}_3\tilde{b}_u) \qquad \text{(C-17)}$$

where $\delta\underline{\rho}$ is the pseudo-range measurement error and $\tilde{b}_u$ is the clock error (bias) at the measurement time. The covariance of the estimation error is then*

$$\text{cov}\;\delta\underline{r}_u = \begin{bmatrix} \sigma_x^2 & - & - \\ - & \sigma_y^2 & - \\ - & - & \sigma_z^2 \end{bmatrix} = H_3^{-1}\,(\text{cov}\;\delta\underline{\rho} + \underline{1}_3\;\text{cov}\;\tilde{b}_u\,\underline{1}_3^T)\;H_3^{-T}$$

$$= \sigma_\rho^2\,H_3^{-1}\,(I_3 + k_c^2\,\underline{1}_3\,\underline{1}_3^T)\,H_3^{-T} \qquad \text{(C-18)}$$

---

* It is assumed that $\delta\underline{\rho}$ and $\tilde{b}_u$ are independent.

where

$$k_c^2 \equiv \frac{\text{cov } \tilde{b}_u}{\sigma_\rho^2} = \sigma_b^2/\sigma_\rho^2 \qquad \text{(C-19)}$$

is the clock error variance normalized to the pseudo-range error variance.* The corresponding GDOP parameters are as defined in (C-5) - (C-7).

In order to evaluate the degradation in GDOP it is useful to relate the clock error variance to the accuracy of the previous update and the clock drift characteristics. For time intervals extending up to a few minutes it is sufficient to assume a two term clock error model of the form

$$b_u = b_o + \dot{b}\tau \qquad \text{(C-20)}$$

where $\dot{b}$ is the clock drift rate, τ is the time since an update and b_o is the error at $\tau = 0$. The corresponding error variance is given by

$$\sigma_b^2 = \sigma_{b_o}^2 + \sigma_{\dot{b}}^2\tau^2 \qquad \text{(C-21)}$$

if b_o and $\dot{b}$ are assumed to be independent.

---

* An equivalent formulation for cov $\delta\underline{r}_u$ analogous to (C-13) is

$$\text{cov } \delta\underline{r}_u = \sigma_\rho^2 \left[H_3^T H_3 - \frac{1}{\mu_c^2}\left(H_3^T \underline{1}_3\right)\left(H_3^T \underline{1}_3\right)^T\right]^{-1}$$

where

$$\mu_c^2 = \underline{1}_3^T \underline{1}_3 + 1/k_c^2 = 3 + 1/k_c^2$$

A fully satellite-based solution at the previous update would yield

$$\sigma_{b_o} = TDOP_o \cdot \sigma_\rho \qquad \text{(C-22)}$$

The drift rate parameter ($\sigma_b^{\cdot}$) is related to the clock's oscillator fractional frequency uncertainty $\left(\sigma_{\Delta f/f}\right)$, i.e.

$$\sigma_b^{\cdot} = c\ \sigma_{\Delta f/f} \qquad \text{(C-23)}$$

where c is the speed of light. Thus the parameter k_c^2 in (C-19) is

$$k_c^2 = \frac{\sigma_b^2}{\sigma_\rho^2} = TDOP_o^2 + \left(\frac{c\ \sigma_{\Delta f/f}}{\sigma_\rho}\right)^2 \tau^2 \qquad \text{(C-24)}$$

If, for example, $TDOP_o = 2$, $\sigma_{\Delta f/f} = 10^{-7}$ and $\sigma_\rho = 100$ ft, then

$$k_c^2 = 4 + \tau^2 \qquad \text{(C-25)}$$

Thus, $2 \leq k_c \leq 60$ for a one minute interval between clock updates. The net impact on GDOP depends on the satellite deployment which determines H_3.

APPENDIX D

GLOSSARY

ACQ - Acquisition (Mode)
AFC - Automatic Frequency Control
B_I - IF Bandwidth
C/A - Coarse Acquisition (Signal)
DLL - Delay-Lock Loop
DME - Distance Measuring Equipment
C/N_o - Carrier Power to Noise Spectral Density Ratio
GA - General Aviation
GDOP - Geometric Dilution of Precision
HDOP - Horizontal Plane Component of GDOP
IFR - Instrument Flight Rules
LCR - Low Cost (GPS) Receiver
PLL - Phase-Lock Loop
RFI - Radio Frequency Interference
RNAV - Area Navigation
SNR - Signal-Power-to-Noise Power Ratio
VFR - Visual Flight Rules
VOR - VHF Omni-Range System
HOW - Handover word
RSS - Root Sum Square

Appendix E

REFERENCES

1. Approval of Area Navigation Systems for Use in the U.S. National Airspace System, DOT/FAA Advisory Circular AC90-45A; 21 February 1975.

2. Bogen, A. H., "Geometric Performance of the Global Positioning System," AEROSPACE Corp., SAMSO TR-74-169 (AD 783 210), June 1974.

3. Edwards, T. L., Application of the GPS to the AEROSAT Test and Evaluation Program," AEROSPACE Corp., FAA-RD-76-142, May 1976.

4. Elrod, B. D., Weinberg, A., and Sinha, L. P., "Investigation of Some Satellite-Aided ATC System Concepts Employing the NAVSTAR Global Positioning System," The Mitre Corporation, MTR 7688, January 1978.

5. Parkinson, B. W., "GPS Overview", 34th Annual ION Meeting, Arlington, Virginia, June 1978.

6. "Radio Noise and Interference," Ch. 29, ITT REFERENCE DATA FOR RADIO ENGINEERS, Sixth Edition (1977).

7. Antenna Gain Characteristics measured by Microwave Specialty Corp., San Diego, CA., 18 October 1976.

8. Natali, F. T., "Coherent Lock Detectors for BPSK Signals," STI-TM-6008, 23 June 1976.

9. Hummels, D. R., "Some Simulation Results for the Time to Indicate Phase Lock," IEEE Trans. Comm., Vol. COM-20, February 1972.

10. Chang, H., et.al. "GPS Receiver Performance Analysis," STI-TR-7033, December 1977.

11. Natali, F. T., "AFC Loop Performance in Noise," STI-TM-8806, 28 July 1978.

12. Noe, P. R. and Rhyne, V.T., "Low Cost NAVSTAR GPS Receiver/Microprocessor Floating Point Design", NAECON '78 Record, May 1978.

13. System Specification for the NAVSTAR Global Postioning System - Phase II, GPS Joint Program Office, SS-GPS-200, 1 September 1977.

14. Breitwieser, G.F. (Ed.), "Computer Program Development Specification for the GPS Master Control Station Ephemeris Computer Programs," General Dynamics, Report CP-CS-304 Part I (12436), October 1977.

15. Lorenzini, D. and Soulia, J., "The GPS Field Test Program", 33rd Annual ION Meeting, Costa Mesa, CA, June 1977.

16. "ATS-5 Multipath/Ranging/Digital Data L-Band Experimental Program", (Summary) DOT/FAA Report, RAA-RD-73-57, April, 1973.

17. ATC Experimentation and Evaluation with the NASA ATS-6 Satellite", DOT/FAA Report, FAA-RD-75-173, (Vol. I) August 1977, (Vol.II) April 1976, (Vols. III-VII) September 1976.

18. Spilker, J. J., Digital Communications by Satellite, Prentice Hall (N.J.), 1977.

19. Hartman, H. P., "Analysis of a Dithering Loop for a PN Code Tracking", IEEE Trans. AES, January 1974.